

BERICHTE

aus dem Fachbereich Geowissenschaften
der Universität Bremen

Nr. 51

Bleil, U., M. Breitzke, K. Däumler, L. Dittert, J. Ewert,
K. Gohl, B. Heesemann, W.-D. Heinitz, P. Helmke, H. Keil,
T. Merkel, B. Pioch, F. Pototzki, U. Rosiak, R. Schneider,
T. Schwenk, V. Spieß, G. Uenzelmann-Neben

BERICHT UND ERSTE ERGEBNISSE DER SONNE-FAHRT SO 86

BUENOS AIRES - KAPSTADT, 22.4.1993 - 31.5.1993

REPORT AND PRELIMINARY RESULTS OF SONNE CRUISE SO 86

BUENOS AIRES - CAPETOWN, 22.4.1993 - 31.5.1993

Berichte, Fachbereich Geowissenschaften, Universität Bremen, Nr. 51,
116 S., 58 Abb., 7 Tab., Bremen 1994.

ISSN 0931-0800



Die "Berichte aus dem Fachbereich Geowissenschaften" werden in unregelmäßigen Abständen vom Fachbereich 5, Universität Bremen, herausgegeben. Sie dienen der Veröffentlichung von Forschungsarbeiten, Doktorarbeiten und wissenschaftlichen Beiträgen, die im Fachbereich angefertigt wurden.

Die Berichte können beim:

Fachbereich 5 Geowissenschaften

Universität Bremen

Klagenfurterstr.

28334 BREMEN

Telefon: (0421) 218-4124

Telefax: (0421) 218-3116

angefordert werden.

Zitat:

Bleil, U., M. Breitzke, K. Däumler, L. Dittert, J. Ewert,
K. Gohl, B. Heesemann, W.-D. Heinitz, P. Helmke, H. Keil,
T. Merkel, B. Pioch, F. Pototzki, U. Rosiak, R. Schneider,
T. Schwenk, V. Spieß, G. Uenzelmann-Neben

Bericht und erste Ergebnisse der SONNE-Fahrt SO 86, Buenos Aires - Kapstadt, 22.4.1993 - 31.5.1993.

Report and Preliminary Results of SONNE Cruise SO 86, Buenos Aires - Capetown, 22.4.1993 - 31.5.1993.

Bremen, Nr. 51, 116 S., 58 Abb., 7 Tab., Bremen 1995.

Table of Contents

	Page
1 Participants	3
2 Research Program	4
3 Narrative of the Cruise	5
4 Underway Geophysics	9
4.1 Data Acquisition	9
4.2 On Board Data Processing	9
4.3 Congo Fan Area	15
4.3.1 Introduction	15
4.3.2 Strategy of Site Survey	16
4.3.3 Bathymetry	16
4.3.4 Seismostratigraphy	19
4.3.5 PARASOUND Acoustostratigraphy	23
4.3.6 Proposed Drill Sites in the Congo Fan Area	26
4.4 Angola Diapir Field at 12°S	35
4.4.1 Introduction	35
4.4.2 Strategy of Site Survey	36
4.4.3 Bathymetry	36
4.4.4 Seismostratigraphy	36
4.4.5 PARASOUND Acoustostratigraphy	42
4.4.6 Proposed Drill Sites	42
4.5 Namibia - Angola Upwelling at 17°S	52
4.5.1 Introduction	52
4.5.2 Strategy of Site Survey	52
4.5.3 Bathymetry	52

4.5.4	PARASOUND Acoustostratigraphy	55
4.5.5	Seismostratigraphy and Proposed Drill Sites	55
4.6	Additional Seismic Surveys	60
5	Sediment Sampling	63
5.1	Multicorer	63
5.2	Gravity Corer	66
5.3	Sediment Pattern	66
5.4	Physical Properties Studies	82
5.4.1	Introduction	82
5.4.2	Physical Background and Experimental Techniques	82
5.4.2	Shipboard Results	87
5.5	Accelerator Monitored Coring	104
5.5.1	Introduction	104
5.5.2	Measuring System	105
5.5.3	Shipboard Results	105
6	Hydroacoustic System Development with the SEL-90 Echosounder	108
7	Plankton Sampling	110
8	References	113
9	Acknowledgements	116

1 Participants

Name	Discipline	Institution
Bleil, Ulrich, Prof. Dr. (Chief Scientist)	Geophysics	GeoB
Breitzke, Monika, Dr.	Geophysics	GeoB
Däumler, Katharina, Student	Geophysics	GeoB
Dittert, Lars, Student	Geology	GeoB
Ewert, Jörn, Dipl.-Ing.	Geoacoustics	INIR
Gohl, Karsten, Dr.	Geophysics	AWI
Heesemann, Bernd, Dipl.-Ing.	Marine Technology	GeoB
Heinitz, Wolf-Dieter, Dr.	Geoacoustics	INIR
Helmke, Peer, Student	Geology	GeoB
Keil, Hanno, Student	Geophysics	GeoB
Merkel, Tobias, Student	Geoacoustics	INIR
Pioch, Bernd, Technician	Geophysics	GeoB
Pototzki, Frank, Technician	Geophysics	GeoB
Rosiak, Uwe, Technician	Geophysics	GeoB
Schneider, Ralph, Dr.	Geology	GeoB
Schwenk, Tilmann, Student	Geophysics	GeoB
Spieß, Volkhard, Dr.	Geophysics	GeoB
Uenzelmann-Neben, Gabriele, Dr.	Geophysics	AWI

AWI Alfred-Wegener-Institut für Polar- und Meeresforschung
Columbus Straße, 27568 Bremerhaven / FRG

GeoB Fachbereich Geowissenschaften
Universität Bremen
Klagenfurter Straße, 28359 Bremen / FRG

INIR Institut für Nachrichtentechnik und Informationselektronik
Universität Rostock
Richard Wagner Straße, 18119 Warnemünde / FRG

2 Research Program

The eastern South Atlantic is still poorly covered by Deep Sea Drilling Project (DSDP) and Ocean Drilling Program (ODP) drill holes at present. Only DSDP Sites 364 and 365 on the southwest African continental margin off Angola and several sites in the Walvis Ridge area have been studied in greater detail. High resolution information remains sparse however for the Cenozoic and in particular the Neogene sedimentation history of the region. Modern high quality coring techniques have not yet been applied and data sets relevant to analyse the development and variability of the Benguela Current System since Miocene times remain fragmentary.

The pre-site survey cruise SO 86 with R/V SONNE was primarily projected to collect seismic and echographic data from three different areas which have been identified as adequate drilling targets for a paleoceanographic reconstruction of the Benguela Current and Upwelling Systems.

The first area is located between 4 and 7°S off the mouth of the Congo River which is the second largest river of the world with respect to water discharge. The depositional regime is characterized by a significant sediment influx from the continent most of which finds its way through the unique Congo Canyon directly into the deep sea. The canyon opens already several kilometers inshore and guides almost all of the coarser grained sedimentary components into a narrow and in some sections more than 1000 m deep channel which opens into the Congo Cone in water depths greater than 2500 m. There, typical fan deposits and channel/levee systems associated with more or less chaotic sedimentary structures are found.

The hemipelagic input mainly originates from river transported, fine grained suspended material and a related high biologic productivity. The latter results in a significant flux of organic matter to the sea floor. Calcareous microfossils are only a minor constituent, while the biosiliceous fraction is of the same order as the terrigenous clay sedimentation. The Benguela Current System in combination with upwelling processes caused by the regional wind pattern controls the distribution and accumulation of the pelagic components which therefore are useful indicators for the development and intensity of the current system.

The second working area in the Angola Diapir Field at about 12°S represents the typical depositional regime at a continental margin with a normal terrigenous input and minor coastal upwelling, but relatively high oceanic productivity influenced by the Benguela Current. Available evidence from several gravity cores indicates a better preservation of organic matter than in the more southern Namibia Upwelling System contributing to relatively high late Quaternary sedimentation rates of up to 4 cm/kyr. The regional basement structure is characterized by a rift basin which developed during the early opening phase of the South Atlantic and filled with Aptian and Albian

evaporites of several hundred meters thickness. Since then, vertical movement of the salt and associated tectonism has featured the regional morphology and largely influenced the sedimentation pattern.

The third area is located between the Angola Diapir Field and the Walvis Ridge at 17°S. Any relict of a rift basin is absent here and the continental margin rather narrow, therefore. Due to an intense current activity on the shelf and the steepness of the continental slope, gravitational sediment transport by slides, debris flows and turbidity currents to a large extent dominates the sedimentary regime. Although the rate of pelagic sedimentation is rather high in this northernmost part of the Angola/Namibia Upwelling Cell, only a few places could be identified with an undisturbed sediment pattern. The morphology is further complicated by sediment tectonism and giant sediment slides.

Complementary to a recording of the sediment structures with high resolution seismic techniques, a second objective of SONNE Cruise 86 was to recover sediment samples from the sea floor in the different working areas with a multicorer and a gravity corer. After preliminary analyses and measurements on board, their detailed micropaleontological, geochemical, geophysical and isotopic characteristics will be determined subsequently to the cruise in shore based laboratories. These materials are also to supplement the core collection of the long-term project Sonderforschungsbereich 261 at Bremen University aimed at reconstructing the mass budget and current systems of the South Atlantic during the late Quaternary.

3 Narrative of the Cruise

The German Research Vessel SONNE departed Buenos Aires, Argentina, according to schedule on Thursday, 22 April 1993 at 11 a.m. local time beginning its 86th cruise. The scientific crew on board included 12 geophysicists and 3 geologists from the Geoscience Department of Bremen University and the Alfred-Wegener-Institute for Polar and Marine Research, Bremerhaven. It was completed by 3 colleagues from the Institute for Telecommunication Engineering and Information Electronics at Rostock University. The planned participation of a guest scientist from the Republic of Congo was ultimately cancelled.

Financial support for cruise SO 86 was provided by the German Federal Ministry for Research and Technology (Bundesministerium für Forschung und Technologie, BMFT) under contract "PROBOSWA" (PROjektstudie für eine geplante Bohrkampagne des Ocean Drilling Program (ODP) vor SüdWestAfrika). Main objective was a pre-site survey for the Ocean Drilling Program (ODP) to define a series of suitable deep drill sites at the southwest African continental margin on basis of high resolution seismic and echographic measurements as well as the sampling of the sedimentary deposits.

These scientific activities are closely related to a long-term interdisciplinary research program of the Geoscience Department at Bremen University aimed at reconstructing the late Quaternary mass budget and current systems of the South Atlantic (Sonderforschungsbereich 261 sponsored by the German Research Foundation, DFG).

Several German and American groups have been involved in the original planning of a scientific deep drilling project off southwest Africa. Their joint interests focus on the climatic evolution during Neogene and Quaternary times. Its detailed reconstruction from ocean floor sediments is achieved with a wide variety of modern analytical methods. The western South Atlantic and in particular the African continental margin are key regions for this purpose. First of all, it documents the variations of a mainly north - south directed water mass and heat energy transport system which is of global importance as it links both hemispheres. The second feature of direct climatic relevance are nearshore upwelling and high productivity zones sustained by the prevailing regional wind systems and an upwelling cell induced by the Congo River whose fluvial sediment load additionally reflects changes in vegetation on the African continent.

After leaving the Argentinian waters at the La Plata River mouth, R/V SONNE headed northeastward along the South American coast (Fig. 1) to enter the harbor of Vitória/Brazil on 26 April. During the five hours visit a container with the entire geophysical laboratory equipment was taken on board which had not been delivered to Buenos Aires in time. Thanks to a most efficient support by the German Ambassies at Brasilia and Buenos Aires it was possible to obtain the landing permission to Vitória at very short notice. With course to the first working area, the Congo Sediment Fan, we afterwards crossed the South Atlantic enjoying good to excellent weather and sea conditions. A seminar of several days served to prepare for the research activities during this journey.

Beginning at the Brazilian 200 mile zone boundary, a continuous, round-the-clock survey with the two shipboard echographic systems PARASOUND and HYDROSWEEP was established which ended only after almost 11.500 km just before reaching the final destination of the cruise, Cape Town, South Africa. Both devices proved to be extremely reliable and only a few short failures occurred. Also along most of the cruise track a large number of samples were taken from the surface waters for plankton analyses.

The seismic survey in the northern part of the Congo Sediment Fan began in the afternoon of 8 May with the launching of the streamer und the airgun. The initial program at about 5°S comprised a series of profiles of about 300 nm total length. A preliminary shipboard evaluation of the data, which are supplemented by a set of high quality echographic records, suggests various options to define suitable drill sites despite widespread intensive salt tectonism. To finish the work in this area, the gravity corer was used three times in water depths of around 1400, 1800 and 2500 m.

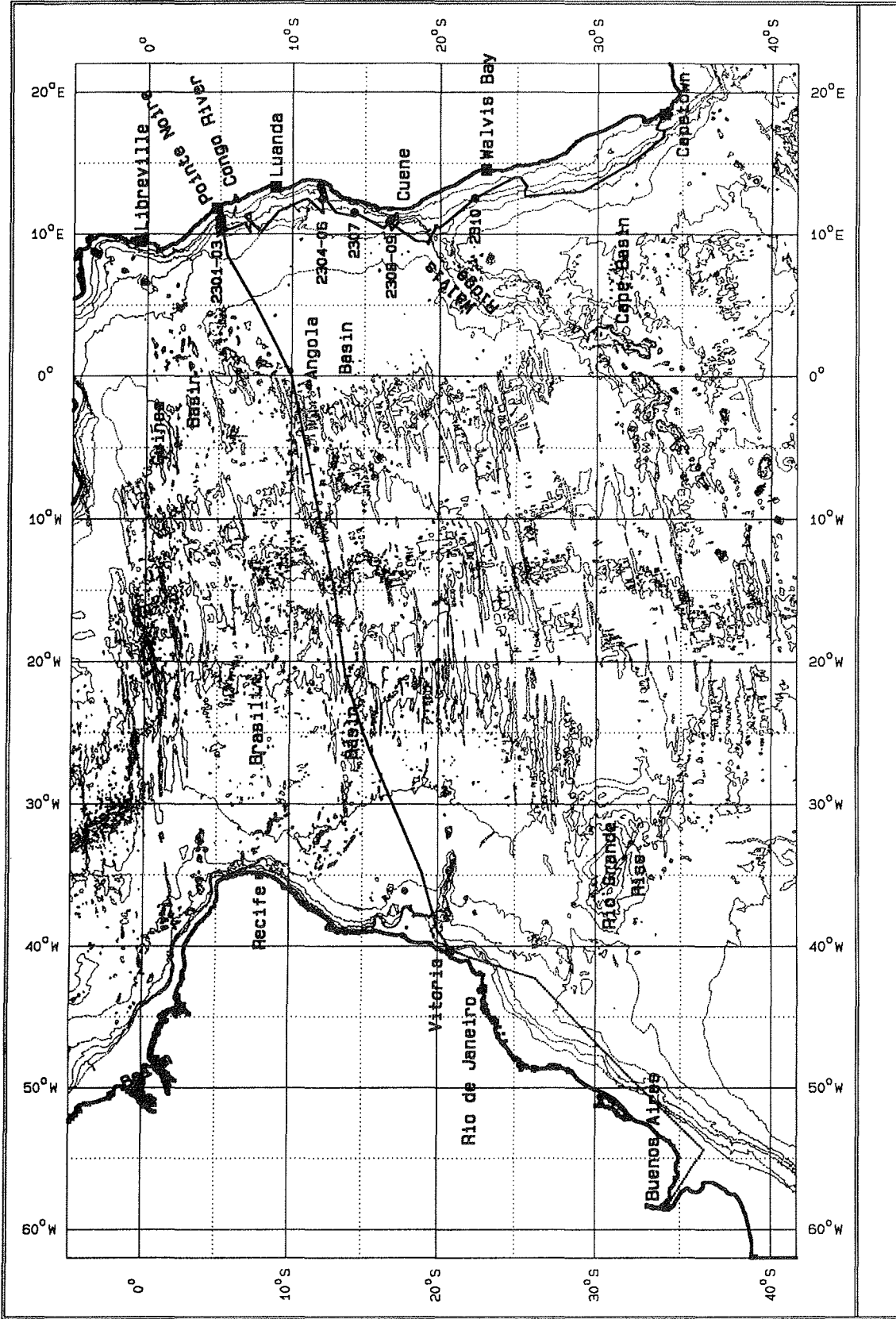


Figure 1 Ship's track and sampling stations of SONNE Cruise 86.

Recoveries ranging from 14 to 18 m were higher than expected. The multicorer, which was employed at all stations, also yielded excellent results. During the night of 13 May the activities were then transferred to about 7°S, south of the Congo Canyon. A less extended seismic profiling than in the northern area indicated a much more complex depositional regime offering almost no appropriate drilling locations, though. For this reason, the originally planned sediment sampling was cancelled.

From 16 to 21 May an extensive seismic and echographic survey was performed in the large field of salt diapirism at about 12°S off the coast of Angola. In spite of once more very pronounced salt tectonics, a selection of ODP drill sites should be possible here without major problems. As before, the scientists from Rostock University successfully used their own echosounding system in this region along most of the cruise track for a detailed recording of the uppermost sediment structures. For the first time during the seismic measurements a sonobuoy was successfully launched following persistent efforts to repair the receiving unit. On 18 and 19 May the profiling program was interrupted three times for station work. In most cases optimum results were obtained with the multicorer. Although the recoveries of the gravity corer did not reach the record lengths of the northern Congo Sediment Fan, no real failures were experienced. A new sensor system, which directly monitors the coring process *in situ*, again operated absolutely perfect and apparently provided most interesting data sets.

On transit to the last major working area of Cruise SO 86 additional sediments were sampled at about 14,5°S in around 3000 m water depth. Seismic profiles across the African continental margin at 17°S off Namibia were begun in the early morning of 22 May. Although this area has not been affected by salt tectonism, the sediment sequences appear to be largely disturbed due to very steep slopes and related mass movements. Suitable drilling locations could thus only be identified in water depths between about 1900 und 2700 m, where sediments were recovered at two stations with the multicorer and gravity corer. A further intensive search for alternative drill sites both in shallower and deeper waters unfortunately had no striking success.

After 25 May seismic profiles were positioned over Sites 530 and 532 in the Walvis Ridge area which have been occupied 1980 by the former Deep Sea Drilling Project (DSDP). The results obtained from these holes should provide important clues for a quantitative acoustostratigraphic interpretation of the present seismic data sets. Station work of the cruise was terminated in the night of 27 May at close to 22°S in about 1000 m water depth. Final seismic profiling near 25°S had to be abandoned because of rapidly deteriorating weather and sea states in the afternoon of 28 May. R/V SONNE took course towards Cape Town, South Africa, reaching port and safely ending Cruise SO 86 in the early morning of 31 May, 1993.

4 Underway Geophysics

V. Spieß, U. Bleil, M. Breitzke, K. Gohl, B. Heesemann, H. Keil, B. Pioch, F. Pototzki, U. Rosiak, T. Schwenk, G. Uenzelmann-Neben

4.1 Data Acquisition

The seismic equipment used during Cruise SO 86 consisted of a streamer of 600 m active length with 24 channels and a group spacing of 25 meters. The source was a GI-GUN of 150 in³ total volume with a generator volume of 45 in³. It produces a signal of broad spectral bandwidth with maximum frequencies around and above 500 Hz. The low frequency bubble signal is suppressed by injection of air from a second chamber. The resulting short wavelet was optimized for highest resolution of the upper few hundred meters of the sedimentary column. The multichannel data were recorded with a GEOMETRICS ES-2420 at a sampling rate of 0.5 ms and an anti-alias filter of 720 Hz. The recording length varied from 2 to 8 seconds depending on the water depth. The shot distance was 10 seconds at a ship's speed of 4.9 knots, providing a shot distance of 25 meters and a CMP distance of 12.5 meters.

Digital data were also recorded with the PARASOUND echosounder system of R/V SONNE which was routinely run with a signal of 4 kHz and 250 μ s total length. A sound generation based on the parametric acoustic effect restricts the main lobe to an angle of 4°. The resulting normal incidence seismograms were sampled at a rate of 25 μ s over a length of 266 ms. The shot interval is discontinuous and depends on the water depth. After emission of a series of pulses at 400 ms intervals, the burst is received by the echosounder before the next sequence is sent forth. On average, a seismogram is recorded every 1 - 2 seconds providing a spatial resolution on the order of a few meters on the seismic profiles.

Table 1 summarizes navigation data, length, start and end time of all seismic lines GeoB 93-001 to 93-045. The technical and storage parameters for each profile are given in Table 2.

4.2 On Board Data Processing

For an immediate quality control, the data were provisionally processed with a PC based system on board. After demultiplexing from the original SEG-D tape, the data were sorted in CMPs of 12.5 m distance according to a shot interval of 10 seconds and a ship's speed of 4.9 knots. To circumvent a velocity analysis at present, a brute stack of the first 4 traces of each CMP was made to reduce the noise and to enhance in particular the deeper reflectors. Before stacking, the data were filtered with a band pass filter from 30 to 700 Hz with a slope of 24 db/octave. Although a significant noise level is observed at the power line frequency of 50 Hz and all multiples, no sharp notch filters were applied at this stage.

Table 1 Navigation data, length, start and end time of seismic lines GeoB 93-001 to 93-045.

Profile GeoB	Start of Profile		End of Profile		Length [nm]	Date Start	Time Start	Date End	Time End
	Latitude	Longitude	Latitude	Longitude					
93-000	17° 50,7' S	32° 05,0' W	17° 45,0' S	31° 51,1' W	15,6	29.04.1993	15:37	29.04.1993	18:56
93-001	05° 29,4' S	08° 33,3' E	05° 00,9' S	11° 24,9' E	173,2	08.05.1993	14:59	10.05.1993	02:25
93-002	04° 41,6' S	11° 09,2' E	04° 48,0' S	09° 50,0' E	79,2	10.05.1993	06:32	10.05.1993	22:44
93-003	04° 48,0' S	09° 49,9' E	05° 07,0' S	10° 22,0' E	37,2	10.05.1993	23:22	11.05.1993	06:57
93-004	05° 07,0' S	10° 22,0' E	05° 15,0' S	10° 22,0' E	8,0	11.05.1993	06:57	11.05.1993	08:33
93-005	05° 15,0' S	10° 22,0' E	05° 15,0' S	10° 25,8' E	3,8	11.05.1993	08:33	11.05.1993	09:22
93-006	05° 15,0' S	10° 25,8' E	04° 42,4' S	10° 25,3' E	32,6	11.05.1993	09:22	11.05.1993	16:00
93-007	04° 42,4' S	10° 25,3' E	05° 11,9' S	10° 56,4' E	42,8	11.05.1993	16:00	12.05.1993	00:48
93-008	05° 11,9' S	10° 56,4' E	05° 09,0' S	11° 06,2' E	10,2	12.05.1993	00:48	12.05.1993	02:55
93-009	05° 09,0' S	11° 06,2' E	05° 00,0' S	11° 06,4' E	9,0	12.05.1993	02:45	12.05.1993	04:45
93-010	06° 42,2' S	10° 45,6' E	07° 05,0' S	10° 10,0' E	42,1	13.05.1993	10:13	13.05.1993	18:46
93-011	07° 05,0' S	10° 10,0' E	07° 05,0' S	11° 30,0' E	79,4	13.05.1993	19:10	14.05.1993	11:23
93-012	07° 05,0' S	11° 30,0' E	06° 40,0' S	11° 15,0' E	29,1	14.05.1993	11:47	14.05.1993	17:41
93-013	06° 40,0' S	11° 15,0' E	07° 50,0' S	10° 10,0' E	95,2	14.05.1993	18:04	15.05.1993	13:27
93-014	11° 01,8' S	12° 28,3' E	12° 07,3' S	11° 27,4' E	88,6	16.05.1993	10:38	17.05.1993	04:42
93-015	12° 07,3' S	11° 27,4' E	11° 54,6' S	13° 30,0' E	120,6	17.05.1993	04:42	18.05.1993	05:28
93-016	11° 54,6' S	13° 30,0' E	12° 06,4' S	13° 24,8' E	12,8	18.05.1993	06:00	18.05.1993	08:34
93-017	12° 06,4' S	13° 24,8' E	12° 22,3' S	12° 30,0' E	55,9	18.05.1993	08:34	18.05.1993	20:18
93-018	11° 51,6' S	13° 21,8' E	12° 01,5' S	13° 21,8' E	9,9	19.05.1993	13:01	19.05.1993	15:02
93-019	12° 01,5' S	13° 22,4' E	12° 01,5' S	13° 19,0' E	3,3	19.05.1993	16:08	19.05.1993	16:47
93-020	12° 01,5' S	13° 19,0' E	11° 51,8' S	13° 19,0' E	9,7	19.05.1993	16:47	19.05.1993	18:44
93-021	11° 51,8' S	13° 19,0' E	11° 52,9' S	13° 07,0' E	11,8	19.05.1993	18:44	19.05.1993	21:09
93-022	11° 52,9' S	13° 07,0' E	12° 02,8' S	13° 07,0' E	9,9	19.05.1993	21:09	19.05.1993	23:10
93-023	12° 02,8' S	13° 07,0' E	12° 02,8' S	13° 02,0' E	4,9	19.05.1993	23:10	20.05.1993	00:15
93-024	12° 02,8' S	13° 02,0' E	11° 51,5' S	13° 02,0' E	11,3	20.05.1993	00:15	20.05.1993	02:34

Table 1 continued

Profile GeoB	Start of Profile		End of profile		Length [nm]	Date Start	Time Start	Date End	Time End
	Latitude	Longitude	Latitude	Longitude					
93-025	11° 51,5' S	13° 02,0' E	11° 52,0' S	12° 56,7' E	5,2	20.05.1993	02:34	20.05.1993	03:41
93-026	11° 52,0' S	12° 56,7' E	12° 03,9' S	12° 56,3' E	11,9	20.05.1993	03:41	20.05.1993	06:10
93-027	12° 03,9' S	12° 56,3' E	12° 03,9' S	12° 53,2' E	3,0	20.05.1993	06:10	20.05.1993	06:47
93-028	12° 03,9' S	12° 53,2' E	11° 54,4' S	12° 53,1' E	9,5	20.05.1993	06:47	20.05.1993	08:45
93-029	11° 54,4' S	12° 53,1' E	13° 00,0' S	11° 30,0' E	104,3	20.05.1993	09:28	21.05.1993	06:43
93-030	16° 15,5' S	10° 26,0' E	17° 03,2' S	11° 27,4' E	75,4	22.05.1993	06:28	22.05.1993	21:52
93-031	17° 06,5' S	11° 27,3' E	17° 11,8' S	10° 51,1' E	35,0	22.05.1993	22:34	23.05.1993	05:40
93-032	17° 11,7' S	10° 50,5' E	16° 45,1' S	10° 15,1' E	43,1	23.05.1993	05:48	23.05.1993	14:35
93-033	16° 45,1' S	10° 15,1' E	16° 31,6' S	10° 55,9' E	41,4	23.05.1993	14:35	23.05.1993	23:06
93-034	16° 31,6' S	10° 55,9' E	16° 45,9' S	10° 56,0' E	14,3	23.05.1993	23:06	24.05.1993	02:03
93-035	16° 45,9' S	10° 56,0' E	16° 55,0' S	11° 07,0' E	13,9	24.05.1993	02:03	24.05.1993	04:53
93-036	19° 05,1' S	09° 25,9' E	19° 15,9' S	09° 21,0' E	11,7	25.05.1993	06:12	25.05.1993	08:34
93-037	19° 15,9' S	09° 21,0' E	19° 13,4' S	09° 15,1' E	6,1	25.05.1993	08:34	25.05.1993	09:50
93-038	19° 13,4' S	09° 15,1' E	19° 08,9' S	09° 17,9' E	5,2	25.05.1993	09:50	25.05.1993	10:54
93-039	19° 08,9' S	09° 17,9' E	19° 47,4' S	10° 36,6' E	83,6	25.05.1993	10:54	26.05.1993	04:03
93-040	19° 47,4' S	10° 36,6' E	19° 42,3' S	10° 39,7' E	5,9	26.05.1993	04:03	26.05.1993	05:15
93-041	19° 42,3' S	10° 39,7' E	19° 39,1' S	10° 33,3' E	6,8	26.05.1993	05:15	26.05.1993	06:40
93-042	19° 39,1' S	10° 33,3' E	19° 56,9' S	10° 26,5' E	18,9	26.05.1993	06:40	26.05.1993	10:32
93-043	24° 49,8' S	13° 59,9' E	25° 09,9' S	14° 00,0' E	20,1	27.05.1993	20:58	28.05.1993	01:04
93-044	25° 09,9' S	14° 00,0' E	25° 37,0' S	13° 21,0' E	44,4	28.05.1993	01:04	28.05.1993	10:05
93-045	25° 37,0' S	13° 21,0' E	25° 27,5' S	13° 03,5' E	18,4	28.05.1993	10:05	28.05.1993	13:50

Table 2 Technical and storage parameters of seismic reflection profiles GeoB 93-000 (AWI 93010) to 93-045 (AWI 93082).

Profile GeoB	Profile AWI	Lead-in [m]	Channel	Group [m]	Record Length [s]	Sample Rate [ms]	Shot Interval [s]	Delay [s]	Field-Tape No.	Remarks
93-000	93010		24+3	25	6	0,25	12	0	001-008	streamer test
93-001	93021	194	24+3	25	8	0,5	10	0	009-092	
		194	24+3	25	6	0,5	10	0	092-107	
		194	24+3	25	4	0,5	10	0	107-112	
93-002	93022	194	24+3	25	4	0,5	10	0	113-117	
		194	24+3	25	6	0,5	10	0	118-126	
		194	24+3	25	8	0,5	10	0	127-157	
									158	full turn
93-003	93023	194	24+3	25	8	0,5	10	0	159-183	
93-004	93024	194	24+3	25	8	0,5	10	0	183-188	185: crossing 1
93-005	93025	194	24+3	25	8	0,5	10	0	188-191	
93-006	93026	194	24+3	25	8	0,5	10	0	191-212	194: crossing 2
93-007	93027	194	24+3	25	8	0,5	10	0	212-219	
		194	24+3	25	6	0,5	10	0	220-236	
93-008	93028	194	24+3	25	6	0,5	10	0	236-241	
93-009	93029	194	24+3	25	6	0,5	10	0	241-243	243: crossing 6
		194	24+3	25	4	0,5	10	0	244-245	
93-010	93030	194	24+3	25	6	0,5	10	0	246-251	
		194	24+3	25	8	0,5	10	0	252-271	272: full turn
93-011	93031	194	24+3	25	8	0,5	10	0	273-299	
		194	24+3	25	6	0,5	10	0	300-313	
		194	24+3	25	4	0,5	10	0	314-317	
93-012	93032	194	24+3	25	4	0,5	10	0	318-328	
93-013	93033	194	24+3	25	4	0,5	10	0	329-332	
		194	24+3	25	6	0,5	10	0	333-347	
		194	24+3	25	8	0,5	10	0	348-383	
93-014	93040	194	24+3	25	6	0,5	10	0	384-393	
		194	24+3	25	8	0,5	10	0	394-438	
93-015	93041	194	24+3	25	8	0,5	10	0	438-459	change of profile on tape
		194	24+3	25	6	0,5	10	0	460-491	
		194	24+3	25	4	0,5	10	0	492-501	502: full turn

Table 2 continued

Profile GeoB	Profile AWI	Lead-in [m]	Channel	Group [m]	Record Length [s]	Sample Rate [ms]	Shot Interval [s]	Delay [s]	Field-Tape No.	Remarks
93-016	93042	194	24+3	25	4	0,5	10	0	502-506	
93-017	93043	198	24+3	25	4	0,5	10	0	506-517	
		198	24+3	25	6	0,5	10	0	518-529	
93-018	93044	198	24+3	25	4	0,5	10	0	530-533	
93-019	93045	198	24+3	25	4	0,5	10	0	533-534	
93-020	93046	198	24+3	25	4	0,5	10	0	534-537	
93-021	93047	198	24+3	25	4	0,5	10	0	538-541	
93-022	93048	198	24+3	25	4	0,5	10	0	542-545	
93-023	93049	198	24+3	25	4	0,5	10	0	545-547	
93-024	93050	198	24+3	25	4	0,5	10	0	547-551	
93-025	93051	198	24+3	25	4	0,5	10	0	551-552	
		198	24+3	25	6	0,5	10	0	553	
93-026	93052	198	24+3	25	6	0,5	10	0	553-558	
93-027	93053	198	24+3	25	6	0,5	10	0	558-559	557: change airgun array
93-028	93054	198	24+3	25	6	0,5	10	0	560-564	565: change to airgun array
93-029	93055	209	24+3	25	6	0,5	10	0	565-584	566-581: sonobuoy aux#3
		209	24+3	25	8	0,5	10	0	585-628	
93-030	93060	220	24+3	25	8	0,5	10	0	629-658	
		220	24+3	25	6	0,5	10	0	659-665	
		220	24+3	25	4	0,5	10	0	666-671	
93-031	93061	220	24+3	25	4	0,5	10	0	672-680	
		220	24+3	25	6	0,5	10	0	681-683	
		220	24+3	25	8	0,5	10	0	684-687	
93-032	93062	220	24+3	25	8	0,5	10	0	688-714	
93-033	93063	220	24+3	25	8	0,5	10	0	715-742	737: crossing 1
93-034	93064	220	24+3	25	8	0,5	10	0	742-751	
93-035	93065	220	24+3	25	8	0,5	10	0	752-760	
93-036	93070	215	24+3	25	8	0,5	10	0	761-768	765: DSDP 530
93-037	93071	215	24+3	25	8	0,5	10	0	768-772	
93-038	93072	215	24+3	25	8	0,5	10	0	772-775	

Table 2 continued

Profile GeoB	Profile AWI	Lead-in [m]	Channel	Group [m]	Record Length [s]	Sample Rate [ms]	Shot Interval [s]	Delay [s]	Field-Tape No.	Remarks
93-039	93073	215	24+3	25	8	0,5	10	0	775-790	779: DSDP 530
		195	24+3	25	"	0,5	10	0	791-801	
		195	24+3	25	6	0,5	10	0	802-803	
		195	24+3	25	4	0,5	10	0	804-806	
		195	24+3	25	6	0,5	10	0	807-823	820: DSDP 532
93-040	93074	195	24+3	25	6	0,5	10	0	823-825	
93-041	93075	195	24+3	25	6	0,5	10	0	826-829	
93-042	93076	195	24+3	25	6	0,5	10	0	829-839	832: DSDP 532
93-043	93080	219	24+3	25	4	0,5	10	0	840-846	843: NCB 1
93-044	93081	219	24+3	25	4	0,5	10	0	846-862	
93-045	93082	219	24+3	25	4	0,5	10	0	862-867	
		219	24+3	25	6	0,5	10	0	868	868: NCB 2

It was not possible to process the complete data set. The shipboard processing focussed on a first evaluation of data quality, the signal penetration and resolution as well as the local sedimentary and basement structures at the selected drill sites. A standard processing of all relevant seismic lines will be carried out after the cruise at the Alfred-Wegener-Institute, Bremerhaven.

The seismic data presented here shall primarily illustrate that the sedimentation is continuous at the proposed drill sites and the sedimentary structures do not give indications for mass movements. A preliminary stratigraphic assignment was attempted, but will require further detailed analyses.

The digital PARASOUND data were immediately processed with the PARADIGMA data acquisition system using a band pass filter from 10 to 100 kHz which preserves the total bandwidth of 10 kHz of the source signal. The data were plotted online in 8 colors. A constant normalization factor was chosen to achieve maximum penetration and to image at least the upper 50 to 100 meters of the sediment cover. In all plots the two-way travelttime has been converted to an "echogram depth" using a constant velocity of 1500 m/s which should be a reasonable approximation for surface sediments.

4.3 The Congo Fan Area

4.3.1 Introduction

Delta and fan deposits are typically found at the mouth of large river systems with considerable sediment discharge. Delta facies develop in shallow waters by consecutively moving the shelf break towards the open sea. At the edge of the delta, slides, slumps, debris flows and turbidity currents are initiated and represent the predominant downslope transport and depositional mechanisms. The entire continental margin from shallow water to the deep sea is affected and overprinted by this type of river activity.

In contrast, the Congo River is associated with a deep incision into the continental margin, the Congo Canyon (HEEZEN et al., 1964; SHEPARD & EMERY, 1973). The canyon extends far into the lower stretches of the river with water depths of several hundred meters already inshore. The sediment is guided through the shelf and accumulates in small basins. From time to time these materials are released and move down the canyon (PETERS, 1978) which in places has steep flanks of more than 1000 meters. Within the deep-sea fan, the sediment is transported further downslope through numerous distributary channels to the topographic lows. Where considerable portions of fine material are included, channel/levee systems have developed and layered sediments are produced on the flanks by local spill over. In the working area

typical fan deposits are found only below ~2500 meters water depth after the canyon has opened into the channel system.

Available geologic and oceanographic data indicate significant differences between the southern and northern part of the Congo Fan. Surface currents cause a seasonal north - south migration of the river plume, but the regional circulation pattern leads to a northward shift of the suspended sediment discharge near the coast (EISMA & VAN BENNEKOM, 1978). On the other hand, there are indications that the recent fan sedimentation by turbidity currents was generally directed southwestward (VAN WEERING & VAN IPEREN, 1984; JANSEN et al., 1984).

4.3.2 Strategy of Site Survey

Major scientific targets on the northernmost drilling transect projected at 5°S are related to the interdependence of the Benguela Current with local upwelling and productivity which should result in a characteristic sedimentary record. Changes in the Benguela Current System will have a direct impact on the sediment composition and accumulation rates. Due to the general northward shift of the river plume relative to the Congo Canyon, the main effort was to define adequate drilling sites on the northern flank of the Congo Cone. The southern flank was covered only with a few seismic lines and generally found to be much more complex in morphology and sedimentary structures. This part will be excluded from a further discussion at present.

The original selection of drill sites oriented along the seismic line #62 of EMERY et al. (1975b). The published data are insufficient, however, to identify fine scale sedimentary structures, in particular disturbances. Prime objective, therefore, was to survey the area in greater detail and with a higher resolution. Those localities on the initial line GeoB 93-001 which were identified as potential drill sites from the online seismic records were crossed by additional profiles (Fig. 2).

4.3.3 Bathymetry

The bathymetric data collected with the HYDROSWEEP swath sounder system along all seismic and PARASOUND lines are compiled in Figure 3. The general morphology of the working area is rather smooth. The lower Congo Cone is disrupted however by numerous small and a few larger distributary channels. Upslope, the general character of the sea floor changes at around 2500 m water depth from a rough, diffracting surface to a continuous layering with numerous parallel internal reflectors. No indications of channels, downslope transport or slumping were found in the surface sediments above 2500 m of water depth.

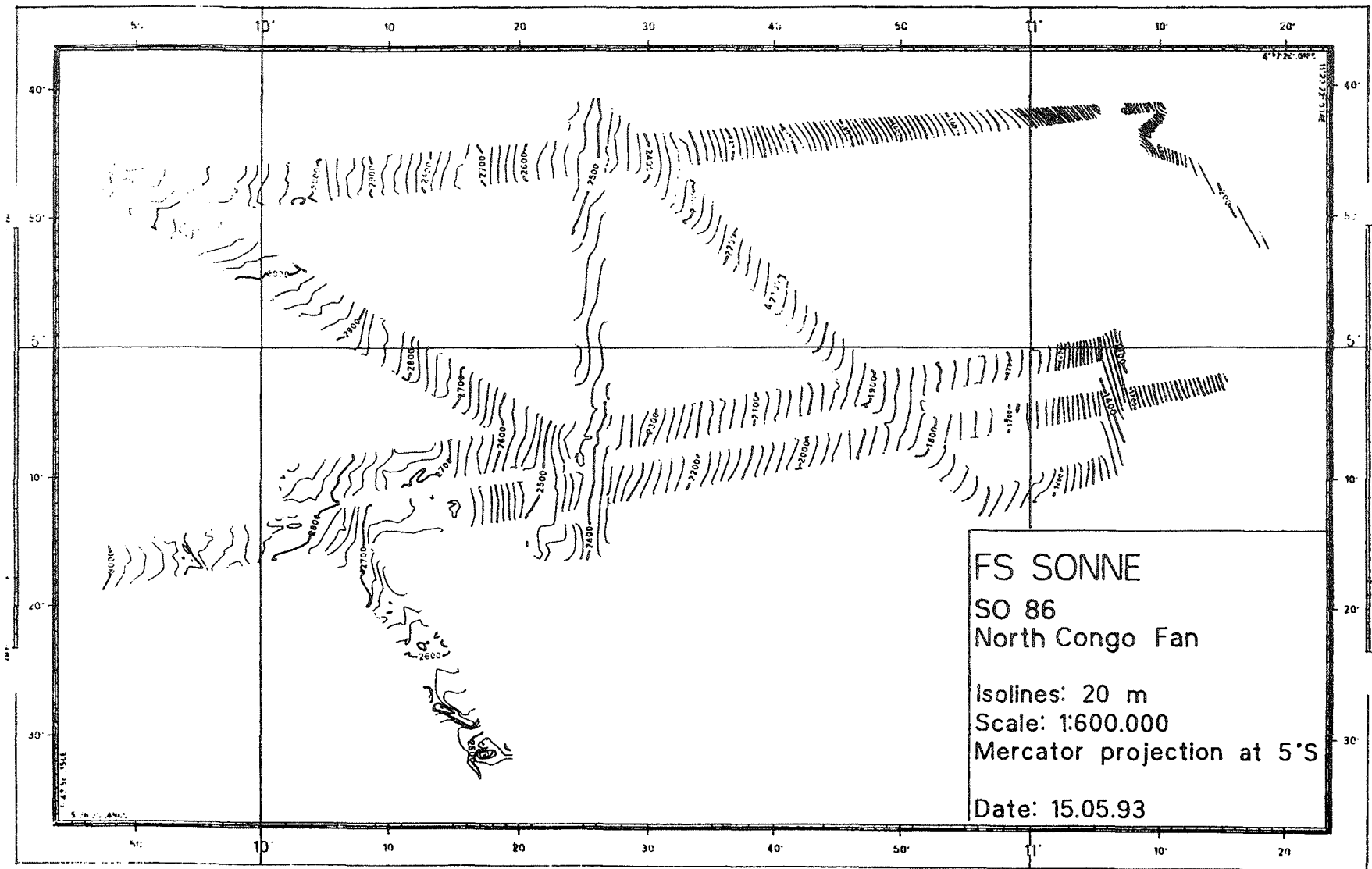


Figure 3 Bathymetry in the northern Congo Sediment Fan area.

4.3.4 Seismostratigraphy

Altogether 9 seismic lines were recorded in the northern Congo Fan area with 6 crossings at potential drill sites in water depths between 1400 and 3000 m (Fig. 2). Connecting profiles will later allow a detailed regional seismic correlation. The first profile (GeoB 93-001) started at 8°30'E / 5°30'S to cover the depositional environment of the fan and in particular its change to a predominantly (hemi-) pelagic sedimentation at the continental slope.

The area of the seismic survey generally shows similar overall acoustic characteristics, but a few significant differences exist. The southern profile GeoB 93-001 has basically recorded the same features as line #62 of EMERY et al. (1975b). The basement near the continent is deeply buried and no salt diapirs are observed close to the surface. Deep reflectors are undulating, however, indicating minor deformation of deeper layers by salt movement or an early tectonism. These undulations are smoothed out towards the surface and do not control the ocean floor morphology. Already on profile GeoB 93-002, which is about 25 nm further to the north, intense salt diapirism is apparent and numerous disturbed sequences are observed near the surface. For this reason, the crossing lines were concentrated on those sections of lines GeoB 93-001 and 93-002, where penetration was high and a distinct layering observable.

For paleoceanographic drilling objectives only sites with longer intervals of undisturbed, continuous sedimentation are of major interest. The early phase of the initially developing current system may well have been associated with increased terrigenous input and considerable downslope transport, though.

Figure 4 shows a typical example of fan deposits dominated by diffractions from subsurface structures. They represent the chaotic fan deposition regime with turbidity currents, slumps and debris flows and a variable paleosurface morphology. Frequently the diffractions appear to mask lower, more regularly deposited sequences. The upper unit of more distinctly layered sediments is about 100 ms thick.

Above a water depth of ~2250 meters the characteristic pattern of fan deposits has completely disappeared in the upper sedimentary column. It is replaced by a series of seismostratigraphic units (Fig. 5) which will subsequently be used as a type sequence for the working area. These seismostratigraphic units are described as follows:

Unit I Acoustically transparent layers with a few weak, parallel internal reflectors. The thickness of the unit fluctuates between 80 and 120 ms. Its base is easily identified by a relatively strong reflector which is present on all profiles in the study area. Another interbedded reflector at ~30 to 50 ms can be traced along several lines. The interval between these two reflectors mostly contains only low and incoherent seismic energy.

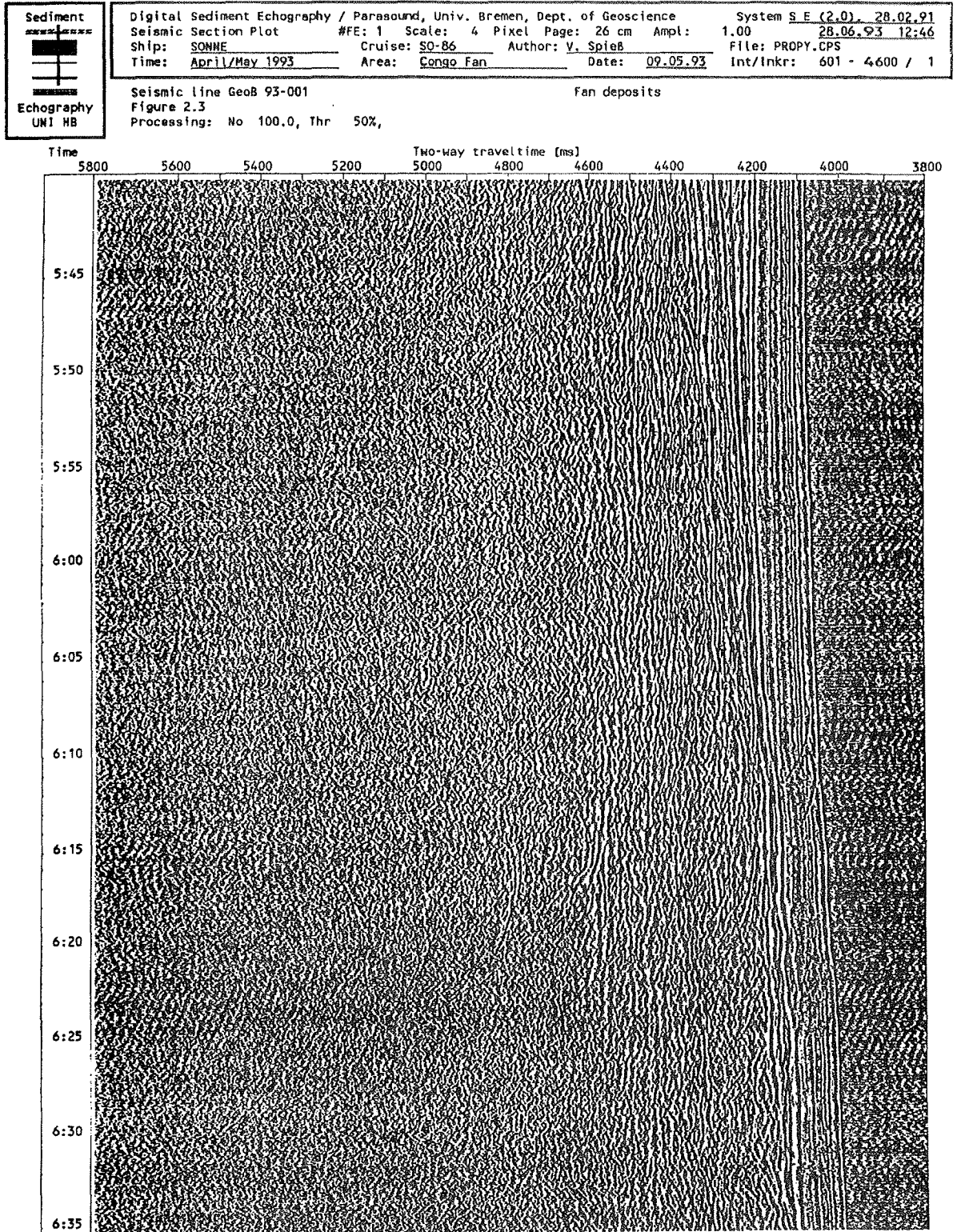


Figure 4

Seismic record of Congo Fan deposits (line GeoB 93-001, ~09°47'E).

	Digital Sediment Echography / Parasound, Univ. Bremen, Dept. of Geoscience		System S.E. (2.0), 28.02.91		
	Seismic Section Plot	#FE: 1	Scale: 6 Pixel	Page: 28 cm	Ampl: 1.00
	Ship: SONNE	Cruise: 90-86	Author: V. Spiess	File: PROPO01B.CPS	
	Time: April/May 1993	Area: Congo Fan	Date: 09.05.93	Int/Inkr: 401 - 4400 / 1	

Seismic line GeoB 93-001
 Figure 2.4
 Processing: No 150.0, Thr 50%,
 Undisturbed slope sediments

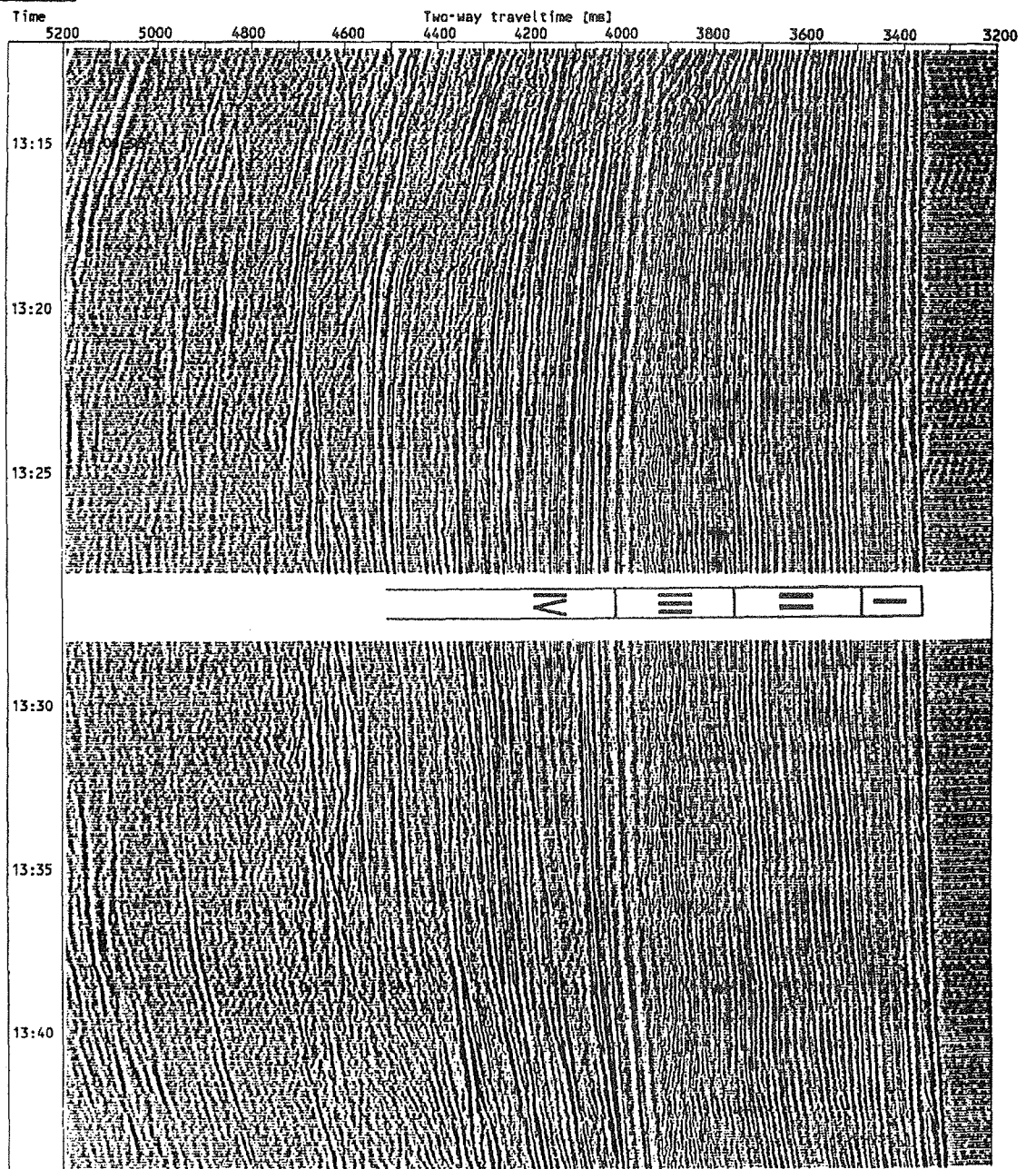


Figure 5
 Seismic record of slope deposits in the Congo Fan area (line GeoB 93-001, ~10°22'E) with a preliminary seismostratigraphic classification.

Unit II This unit shows a large number of reflectors of significantly higher amplitude than in Unit I. Its thickness varies between 180 and 300 ms. The reflectors are slightly undulating, but parallel. In some intervals onlap structures seem to occur, however the identification of these fine scale features is yet uncertain. It cannot completely be excluded that the top of Unit II is an unconformity. Unit II is subdivided into two subunits by a zone of high reflection amplitudes at ~150 ms TWT. The general reflection pattern does not change across this interface.

Unit III The transition between Units II and III is marked by a change in reflection pattern, not a distinct reflector. While continuous reflectors are found above, disrupted reflectors and diffractions prevail below and the reflection amplitudes are significantly lower. The number of diffracting elements is rather high, their lateral extent generally not as wide as in the fan deposits. In some intervals, where the width of hyperbolae increases considerably, they dominate the section.

The thickness of Unit III varies between 100 and 200 ms. Its base is identified as the most prominent reflector in the region which most likely corresponds to the "lost" Horizon A of EMERY et al. (1975b), who were unable to trace this feature in the Congo Cone area. In greater water depth indications of a chaotic deposition and, in places, buried channel/levee systems are seen.

The top of Unit III is sometimes observed in PARASOUND records as the "acoustic basement" with a rough subsurface.

Unit IV A penetration of the seismic signal of more than 3 seconds below Horizon A is repeatedly observed along line GeoB 93-001 and on other profiles. Some reflectors seem to be continuous, but a final evaluation of these strata, which are probably of Paleocene and Cretaceous age, has to be postponed until further data processing.

Because of the predominant Neogene drilling objectives, an interpretation of seismostratigraphic Unit IV was not attempted at present.

In order to define suitable Neogene drill sites on the seismic lines, a chronostratigraphic concept was developed and tentatively applied to the seismostratigraphic units. It was derived from different published sources, primarily from the scientific results obtained at DSDP Sites 364/365 and several other drill holes in the Walvis Ridge area (EMERY et al., 1975b; JANSEN, 1985; BRICE et al., 1982; BOLLI, RYAN et al., 1978).

Gravity core material from the Congo Fan was found to contain very high contents of organic matter (SCHNEIDER, 1991). Partly because of a considerable biosiliceous component, the water content is also very high in the surface sediments. Both findings are indicative of high sedimentation rates caused by upwelling and an associated increased productivity. The resulting sediment composition is rather homogenous and

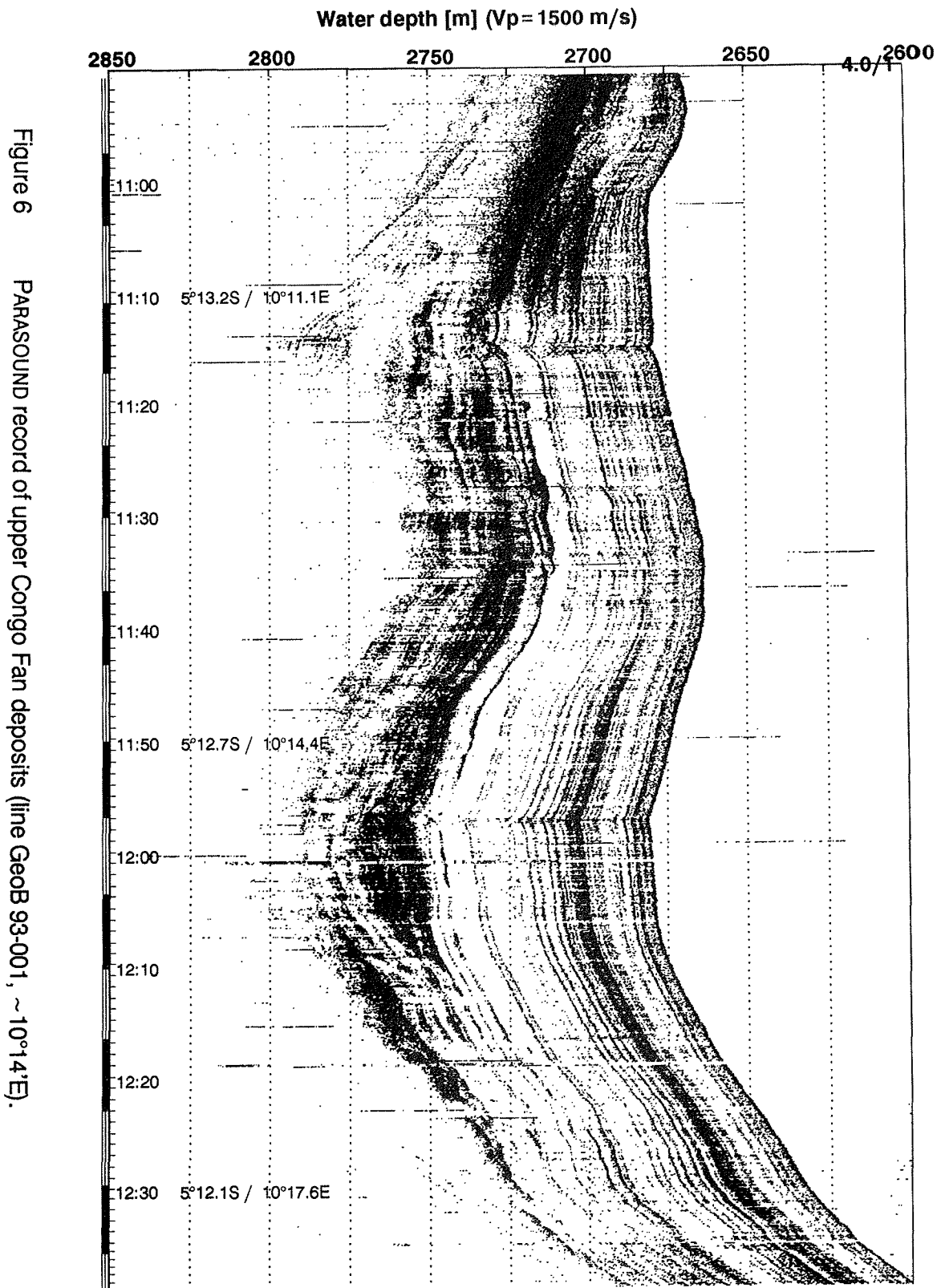
therefore shows a trend to be acoustically transparent. Seismostratigraphic Unit I is assigned to the typical upwelling situation which was probably most intense during Pleistocene, when current activity was at a maximum. The TWT of 80 to 120 ms corresponds to a thickness of around 80 to 120 meters for this unit. Sedimentation rates of 5 to 8 cm/kyr observed in gravity cores covering the last 200,000 years (SCHNEIDER, 1991) are well within the range.

Due to a less intense global circulation, upwelling may have been reduced in the area during Pliocene (the regional paleoceanographic history is poorly known, however). At DSDP Site 364 Pliocene sediments have higher carbonate contents than those of Pleistocene age, an indication for a limited coastal upwelling and relatively low productivity. The large number of high amplitude reflectors characterizing seismostratigraphic Unit II are thus interpreted as representing a highly variable carbonate deposition associated with pronounced acoustic impedance contrasts. Unit II most likely reflects rapid and numerous changes in location and/or intensity of both the Benguela Current and the local upwelling system during Pliocene and late Miocene times.

Seismostratigraphic Unit III documents a distinct shift in depositional environment from a more pelagic sedimentation to processes which produce rough, scattering surfaces. The different widths of the diffraction hyperbolae suggest variations in the microtopography between short sediment waves and a chaotic distribution of diffraction elements. This unit is interpreted as representing fan deposits (see Fig. 4) or at least an intense downslope sediment transport by slumping or turbidity currents. It may be associated with the tectonically driven development of the Congo River drainage system in early/middle Miocene (EMERY & UCHUPI, 1984) which should have significantly increased the influx of terrigenous material. At the same time, a major transgression due to global warming may have initiated erosional activity on the shelf and at the coast (KENNETT, 1982; EMERY & UCHUPI, 1984). The onset of an intensified terrigenous sedimentation can possibly be related to the termination of a major global hiatus at the Eocene/Oligocene boundary which was identified in the working area as the Horizon A reflector (EMERY et al., 1975b; EMERY & UCHUPI, 1984; BOLLI, RYAN et al., 1978).

4.3.5 PARASOUND Acoustostratigraphy

As the processing of digital PARASOUND echosounder data had only second priority during this cruise, a final evaluation has to await further processing ashore. To optimize for penetration, a variable scaling factor was applied to the online recordings. Nevertheless, there are still substantial deficiencies in the graphical output which complicate an immediate detailed interpretation. The processing of the digital data set will particularly result in a significant improvement of the acoustostratigraphic resolution of sedimentary structures. Although the length of the echosounder signal



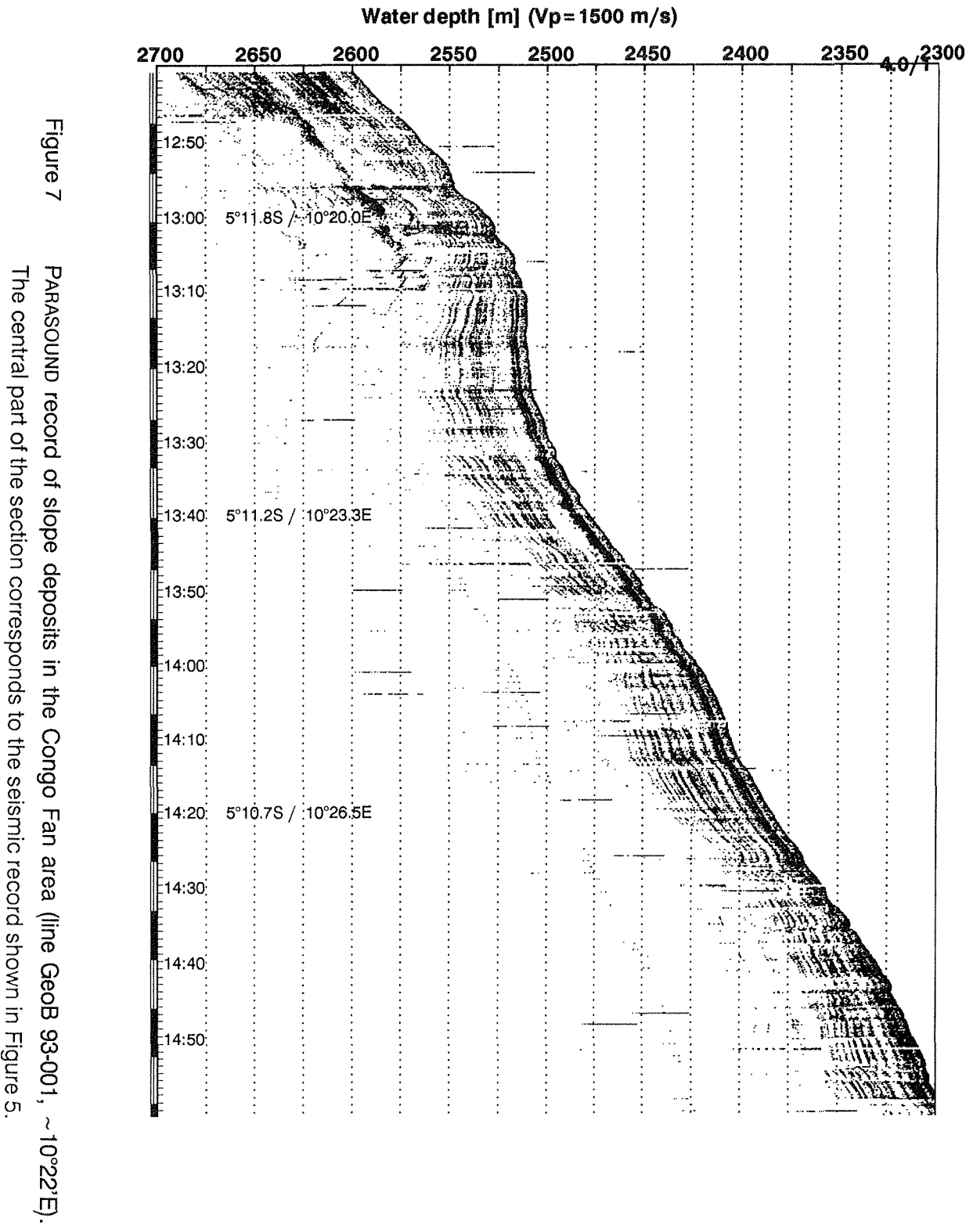


Figure 7 PARASOUND record of slope deposits in the Congo Fan area (line GeOB 93-001, $\sim 10^{\circ}22'E$). The central part of the section corresponds to the seismic record shown in Figure 5.

was extraordinarily short (250 μ s), a penetration of 70 to 150 meters could generally be reached.

In the Congo Fan area the upper sedimentary unit shows a very low acoustic reflectivity with only a few pronounced reflectors. To a first approximation, the upper ~70 meters can be described as acoustically transparent. Only one prominent reflector is found at ~20 m sub-bottom depth which was also identified in the seismic records. This acoustic unit is easily correlated to seismostratigraphic Unit I.

Below ~70 m sub-bottom depth a clear change in reflectivity occurs on Line GeoB 93-001. In water depths below 2600 m an about 30 - 40 m thick band with numerous reflectors is observed (Fig. 6). In places, there is evidence for fan deposition with disturbed sedimentation and rough subsurfaces. The band disappears in waters shallower than 2600 m (Fig. 7). Upslope, the rough subsurface, which is usually related to a marked contrast in grain size and wet bulk density, is replaced in the seismic record by a more regular reflection pattern. The impedance contrasts are apparently subdued and cannot be imaged with the PARASOUND system any further. Therefore, seismostratigraphic Units I and II can no longer be distinguished in the online processed echographic data. Exceptions are a few intervals at ~1550 and 1750 water depth, where again a rough subsurface with high reflection amplitudes was encountered.

Nowhere in the working area a slumping of surface sediments was observed. On the other hand, the microtopography shows a large number of furrows or holes, producing overlapping hyperbolic reflections. They may partly result from threedimensional features. The wavy surface morphology with an amplitude of a few meters extends to greater sub-bottom depth presumably indicating a long-term low intensity current activity. As the reflection amplitudes in the upper acoustostratigraphic unit are generally low, an enrichment of coarse grained material by current activity can probably be excluded. A possible explanation for the observed furrows could be slow creep processes in the upper sediment cover which is known to have very high water contents. The echosounder data clearly show, however, that the sedimentary sequences have not been significantly disturbed.

4.3.6 Proposed Drill Sites in the Congo Fan Area

Seven potential drill sites have been identified in the upper Congo Fan area north of the Congo Canyon in water depths between 1400 and 3000 meters (Table 3). They all represent basically the same depositional environment in varying distance to the shelf break, varying water depth and at different positions with respect to the Congo River plume. For 6 sites, CF-1 to CF-6, cross profiles are available. In all cases the sites are unaffected by sediment slumping or local threedimensional basement structures.

Table 3 Proposed drill sites in the northern Congo Fan area. For each site the geographical coordinates and seismic line numbers as well as the date, time and water depth at crossings are listed.

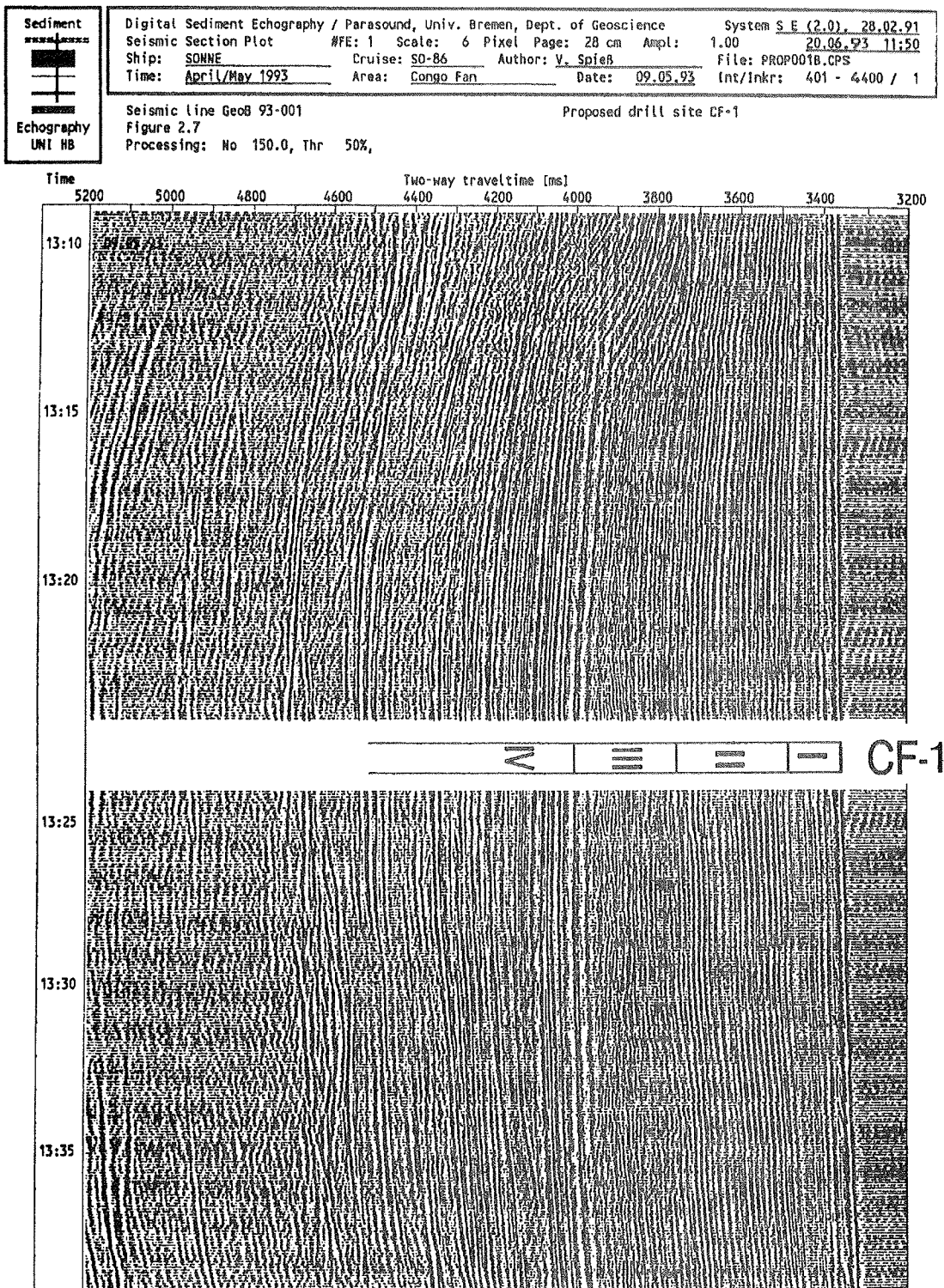
Site	Geographic		Seismic Line	Date	Time	Water Depth (m)
	Latitude	Longitude				
CF-1	5°11.4'S	10°22.0'E	GeoB 93-001	09.05.93	13:24	2506
			GeoB 93-004	11.05.93	7:50	2506
CF-2	5°10.8'S	10°25.9'E	GeoB 93-001	09.05.93	14:12	2403
			GeoB 93-006	11.05.93	10:14	2400
CF-3	4°45.3'S	10°25.3'E	GeoB 93-002	10.05.93	15:30	2522
			GeoB 93-006	11.05.93	15:24	2522
CF-4	4°45.0'S	10°29.3'E	GeoB 93-001	10.05.93	14:40	2430
			GeoB 93-007	11.05.93	17:04	2432
CF-5	5° 6.6'S	10°51.1'E	GeoB 93-001	09.05.93	19:25	1832
			GeoB 93-007	11.05.93	23:18	1826
CF-6	5° 4.1'S	11° 6.4'E	GeoB 93-001	09.05.93	22:34	1397
			GeoB 93-009	12.05.93	3:54	1397
CF-7	4°47.1'S	10° 4.6'E	GeoB 93-002	10.05.93	19:48	3001

Sites CF-1 and CF-2 (Figs. 8, 9) are located in water depths of 2400 to 2500 m. The seismic records do not show any apparent basement structures. Horizon A is clearly identified at 650 and 550 ms TWT, respectively. Sites CF-3 and CF-4 (Figs. 10, 11) are located on the northern Line GeoB 93-002 in water depths between 2430 and 2520 m. Compared to Sites CF-1 and CF-2 no major differences are observed but slight changes in thickness of the seismostratigraphic units. The diffractions in Unit III are less pronounced here which may be related to the greater distance of these sites to the Congo River mouth.

The proposed Sites CF-5 and CF-6 (Figs. 12, 13) are closer to the shelf break in water depths of 1830 and 1400 m, respectively. At Site CF-5, the acoustic transparency of Unit I is very pronounced, perhaps indicating a higher accumulation rate. The internal microtopography of Unit II is somewhat enhanced, but still seems to reflect a mostly regular sedimentation pattern. In several short intervals the site may already be affected by downslope transport and thin interbedded turbidites or slumps. In Unit III

Figure 8

Seismic record at the proposed drilling location CF-1 (see Table 3 for details).



	Digital Sediment Echography / Parasound, Univ. Bremen, Dept. of Geoscience		System S E (2.0), 28.02.91	
	Seismic Section Plot #FE: 1 Scale: 6 Pixel Page: 28 cm Ampl: 1.00		20.06.93 11:54	
	Ship: SONNE	Cruise: SO-86	Author: V. Spieß	File: PROPO01B.CPS
	Time: April/May 1993	Area: Corcha fan	Date: 09.05.93	Int/Inkr: 1 - 4000 / 1
Seismic line GeoB 93-001		Proposed drill site CF-2		
Figure 2.8				
Processing: No 150.0, Thr 50%,				

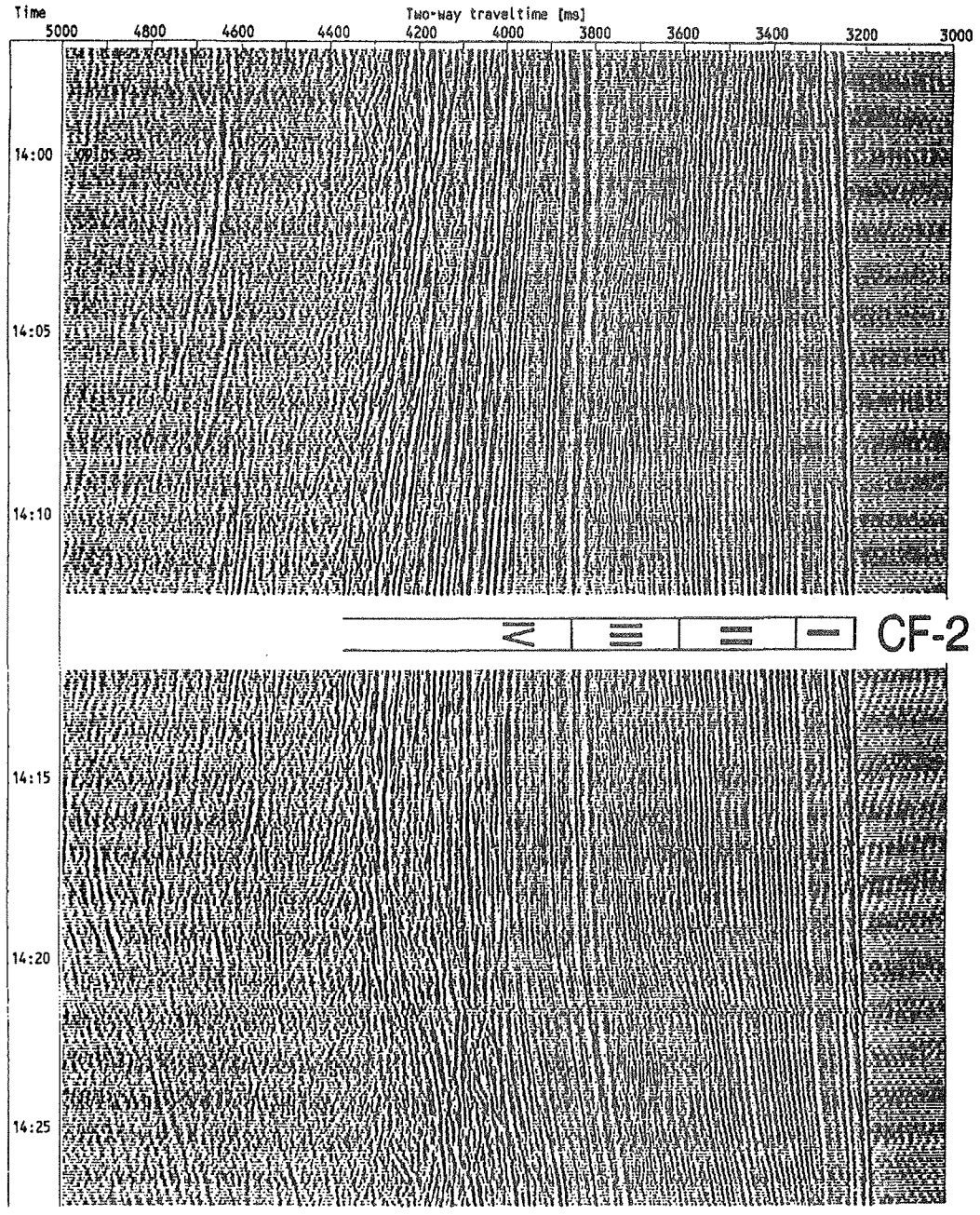


Figure 9

Seismic record at the proposed drilling location CF-2 (see Table 3 for details).

Figure 10

Seismic record at the proposed drilling location CF-3 (see Table 3 for details).

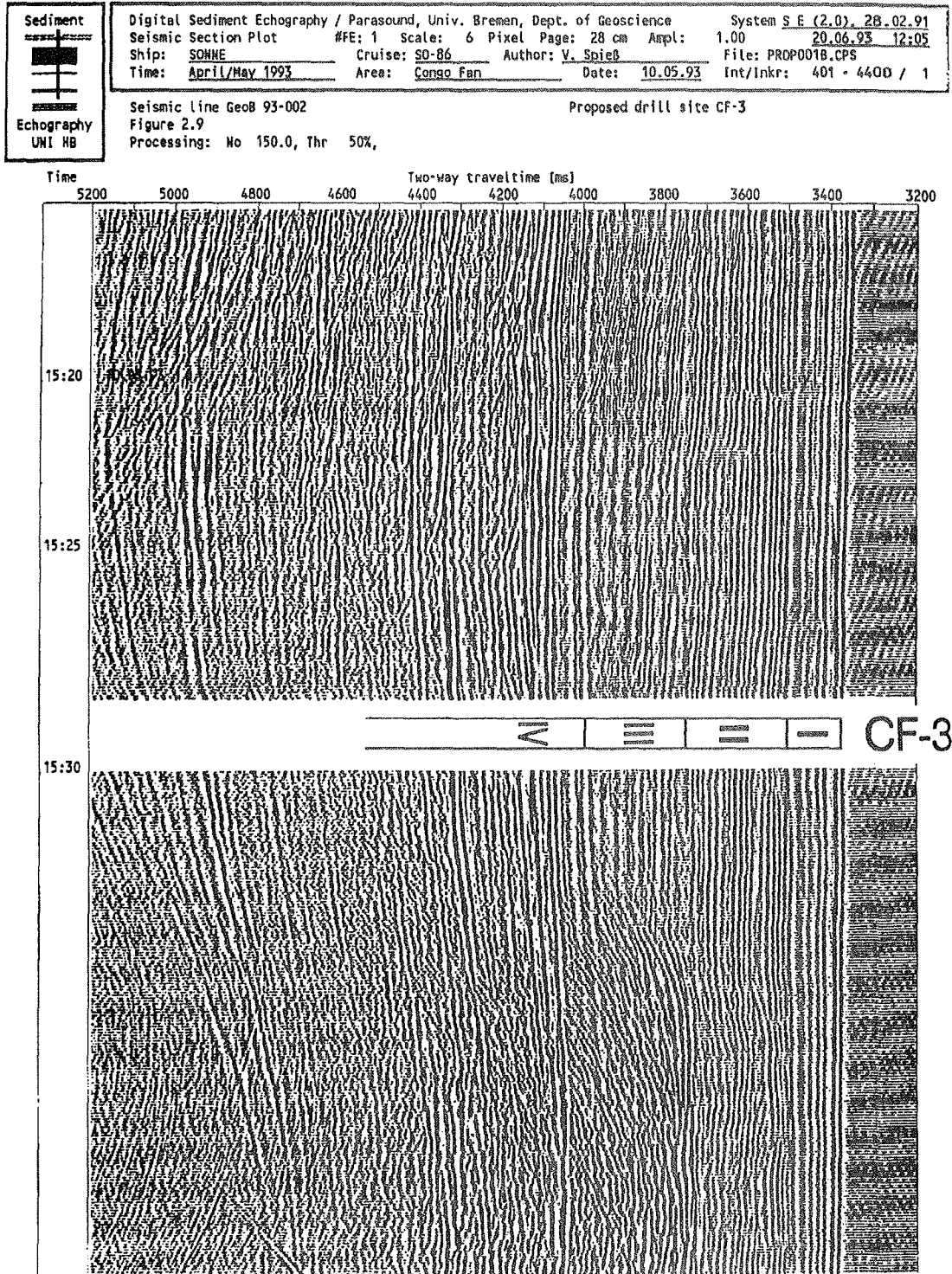


Figure 11

Seismic record at the proposed drilling location CF-4 (see Table 3 for details).

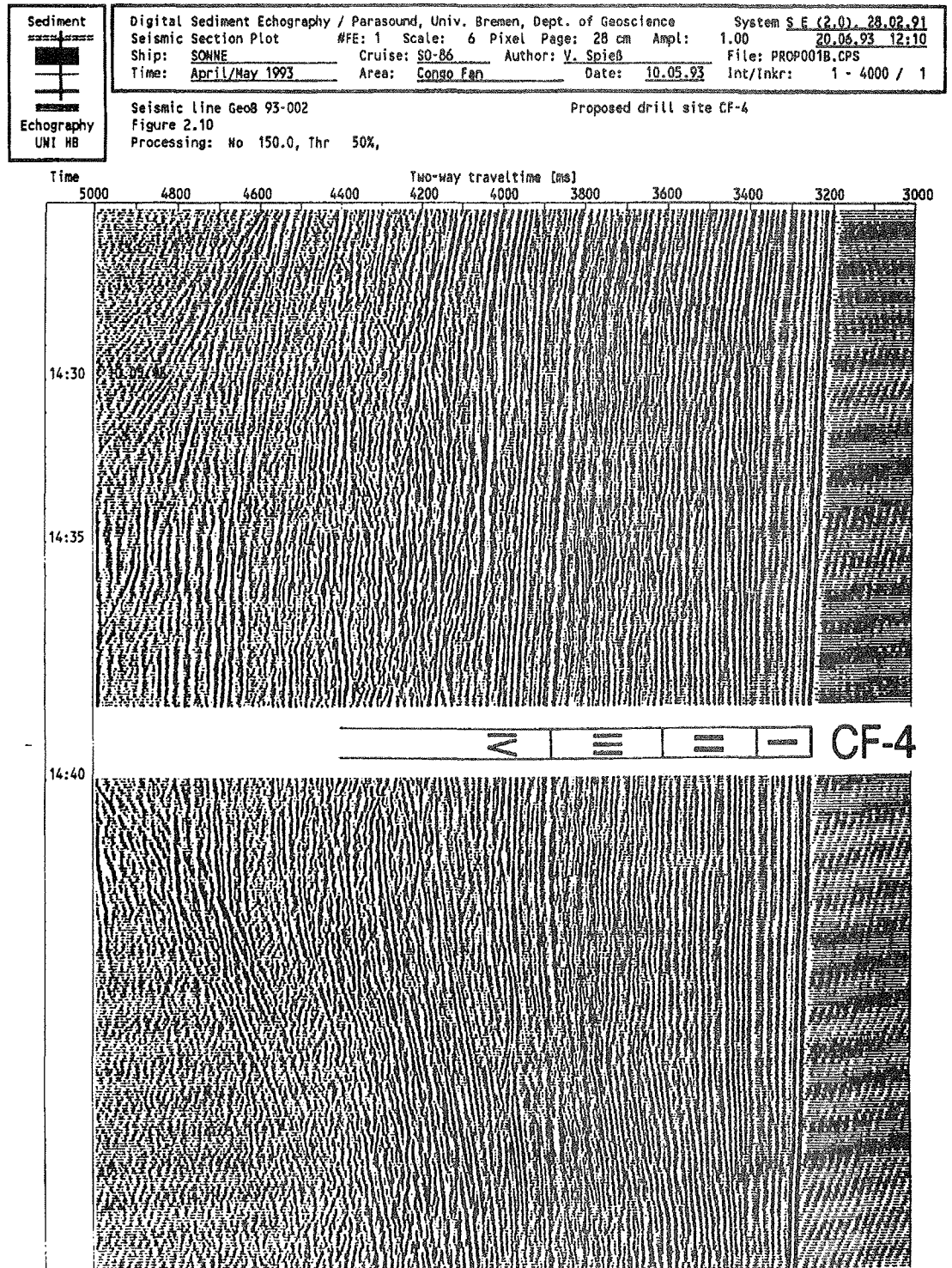


Figure 12

Seismic record at the proposed drilling location CF-5 (see Table 3 for details).

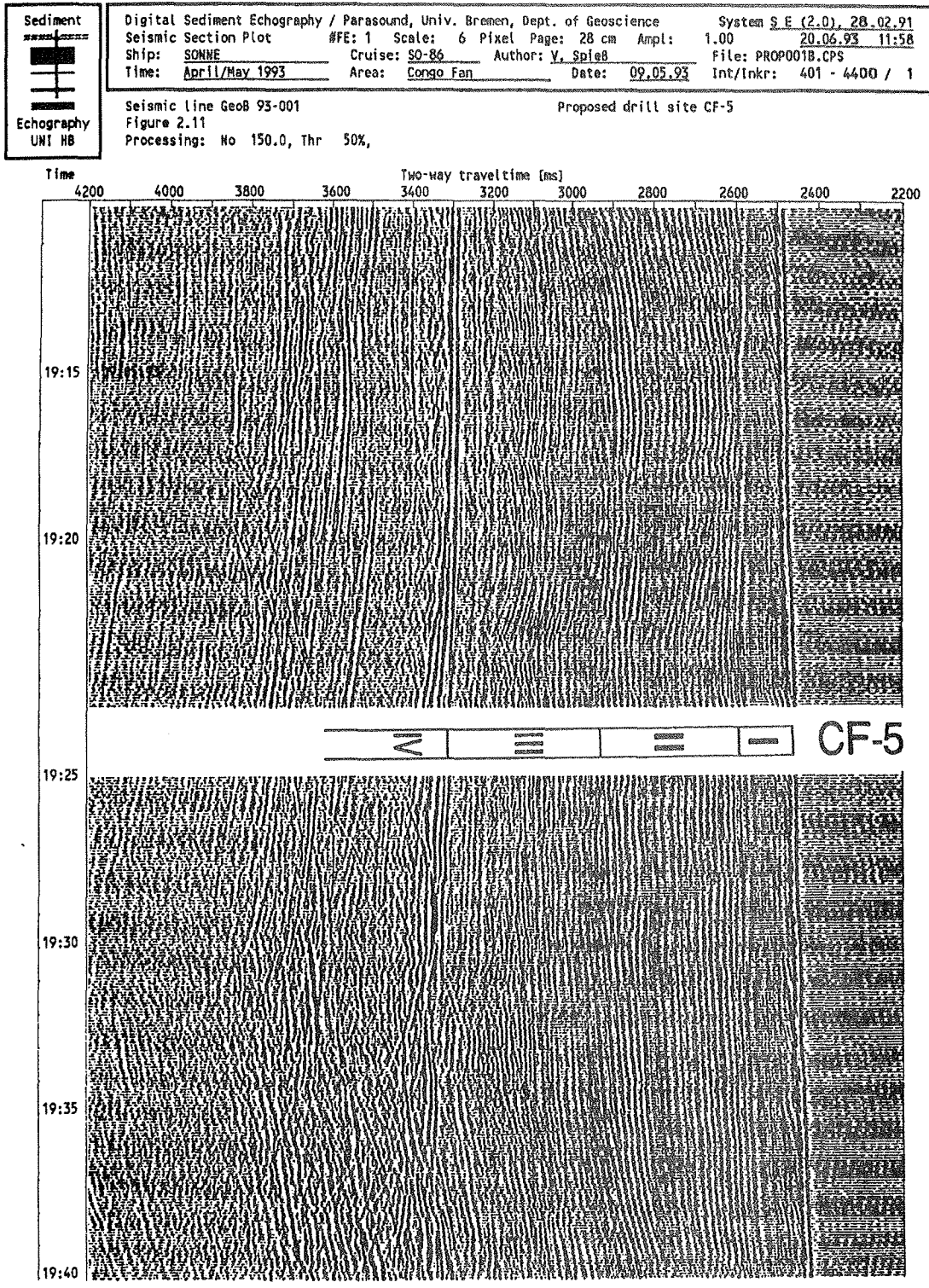


Figure 13

Seismic record at the proposed drilling location CF-6 (see Table 3 for details).

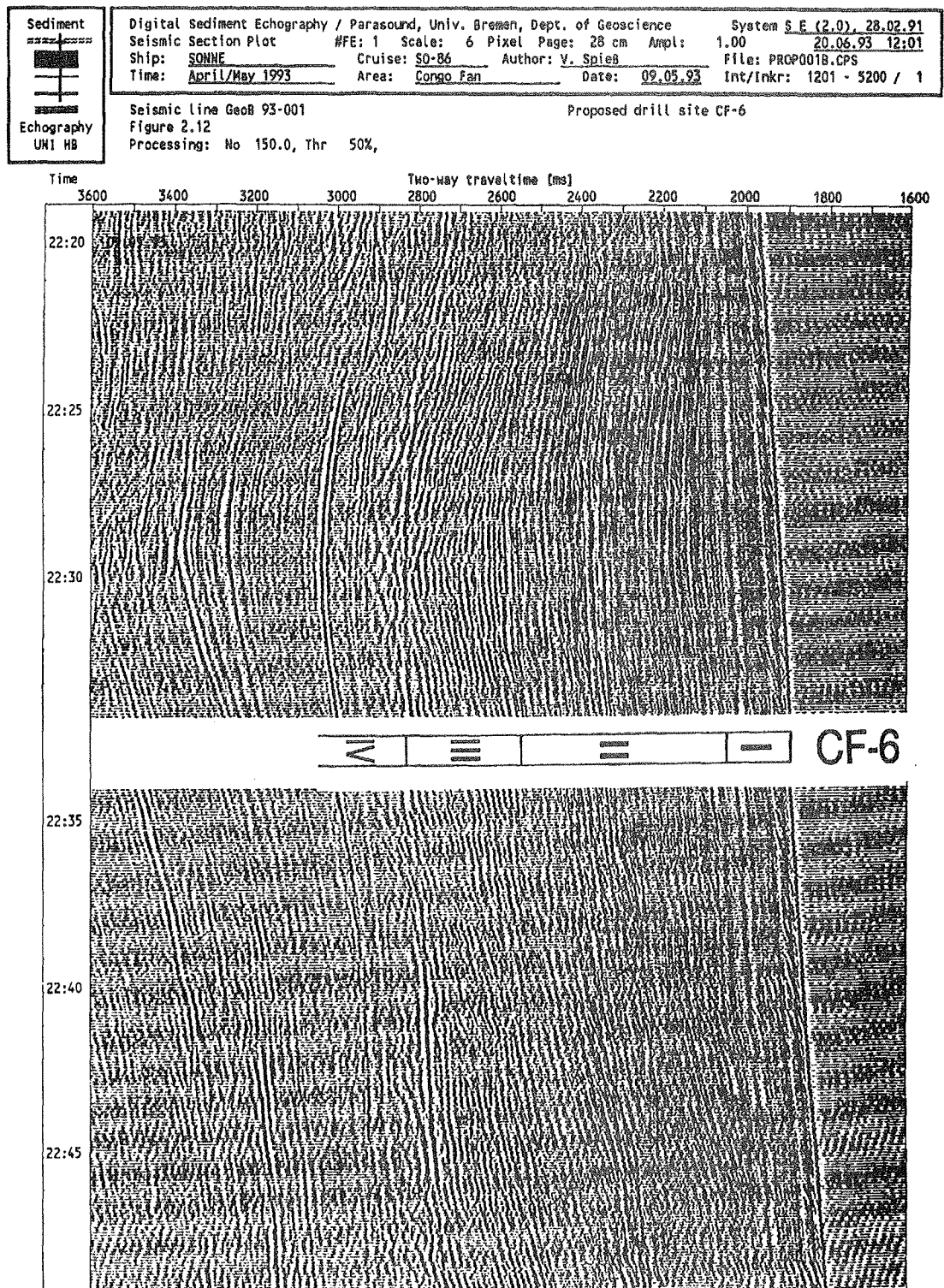
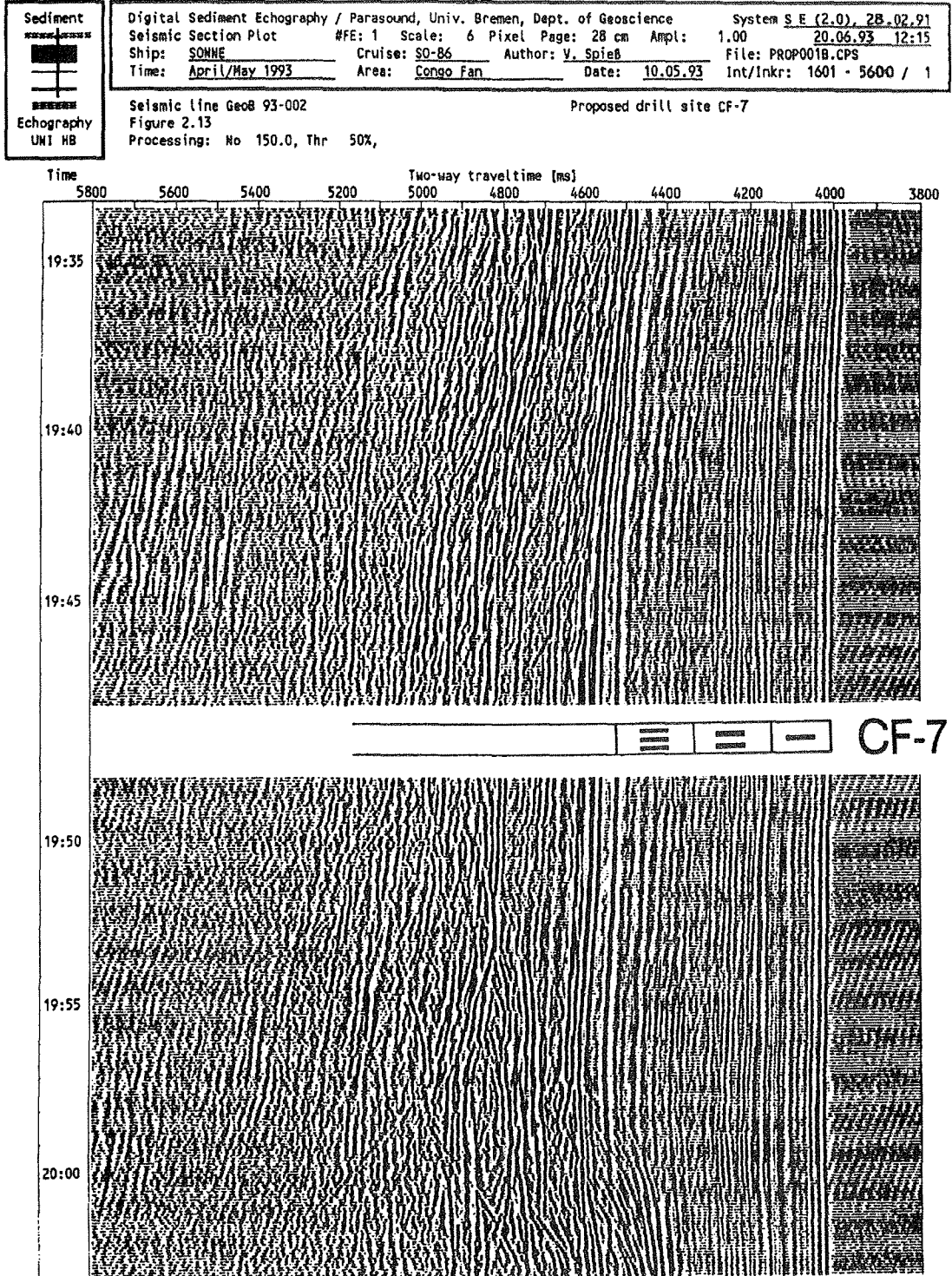


Figure 14

Seismic record at the proposed drilling location CF-7 (see Table 3 for details).



several stronger reflectors are observed which probably originate from thicker sedimentary units each deposited during a single event. As this unit is significantly thicker than at deeper sites, downslope transport may in fact have been a major depositional process.

Site CF-6 in 1400 m water depth shows a seismic pattern which is apparently affected by the proximity to the shelf break and a high terrigenous sediment input. Reflection amplitudes are generally high indicating a strong variability in acoustic impedance. Diffractions are already observed in Unit I. Units II and III are difficult to distinguish, but further data processing should provide better information about the continuity of reflectors and the internal microtopography. Sediments at Site CF-6 probably were quite directly influenced by the development of the Congo Canyon system and related changes in coastal current intensity, sea level and downslope sediment transport.

Site CF-7 (Fig. 14) is the most distant location with respect to the Congo Canyon. Although the water depth is around 3000 m, only minor indications are found for typical fan deposits. All seismostratigraphic units can be clearly identified. As compared to the shallower water sites, their thickness is reduced. A zone of diffuse echoes between Units II and III may be interpreted as an interbedded slump deposit. Unit III is much more regular in reflector geometry than at all other sites and perhaps would allow a more detailed analysis of early stages of the regional Cenozoic paleo-oceanographic development.

4.4 Angola Diapir Field at 12°S

4.4.1 Introduction

The second working area was in the Angola Diapir Field at 12°S. It is located between the upwelling center off the Congo River and the Angola - Namibia upwelling cell. The location represents a typical (hemi-) pelagic depositional regime which is still under the influence of the Benguela Current. The sedimentation rates are expected to be generally lower than in the Congo Fan area due to a reduced coastal upwelling.

The regional morphology is controlled by a rift basin which developed during the early opening of the South Atlantic. In Aptian - Albian times a shallow water basin was repeatedly flooded and evaporitic layers of altogether several hundred meter thickness accumulated (BAUMGARTNER & VAN ANDEL, 1971; LEYDEN et al., 1972; EMERY et al., 1975b; KENNETT, 1982; EMERY & UCHUPI, 1984). The subsequent phase of sea floor spreading disrupted this basin. A major portion between the equator and about 13°S remained at the African continental margin forming a plateau in water depths above 2500 to 3000 meters. Its seaward boundary, the Angola Escarpment, can be traced as a prominent morphological and structural feature.

Soon after deposition of the salt layers buoyant forces already initiated vertical movements which are also observed in the coastal basins (BRICE et al., 1982; EMERY et al., 1975b). They continued during the late Cretaceous and Cenozoic, when several kilometers of sediments were accumulated on the continental margin and the plateau. This salt tectonism has shaped the morphology of the area and dominates the regional sedimentation pattern. Numerous diapiric structures in the relict rift basin were imaged and analysed in some detail by the seismic surveys of BAUMGARTNER & VAN ANDEL (1971), LEYDEN et al. (1972) and BRICE et al. (1982). Intensive salt tectonism is associated with the diapirism. Because of the short average distance between diapirs, the identification of suitable potential drill sites with undisturbed sedimentary sequences was rather complicated.

4.4.2 Strategy of Site Survey

The preliminary site proposals in this region were based on seismic line #44 of EMERY et al. (1975b). As the new bathymetric map of CHERKIS et al. (1989) indicates relatively complex topographic structures around this profile, an area further to the south at about 12°S was surveyed. All drill sites proposed here are on line GeoB 93-015 for which 6 crossings are available (Fig. 15). Additional high resolution seismic profiles were recorded across DSDP Sites 364 and 365 to establish a seismostratigraphic correlation with the former drilling results.

4.4.3 Bathymetry

A bathymetric chart of the HYDROSWEEP tracks is shown in Figure 16. The water depth in the selected area amounts to less than 2000 meters. West of about 12°40'E on the outer plateau and less pronounced on the inner plateau to about 12°50'E, the morphology is irregular with slightly elongated NNW - SSE trending features of 50 to 100 m amplitude. Salt diapirism, which reaches close to the surface and thereby also affects the topography, has created this sequence of peaks and troughs. As the basins between the diapiric structures are only around 10 km wide, appropriate locations for first priority paleoceanographic drill sites could not be identified. East of 12°50'E the upper continental slope is smooth. The proposed drill sites are all located between 550 and 1560 m water depth in this area.

4.4.4 Seismostratigraphy

Vertical salt movements, the predominant tectonic process in the Angola Diapir Field have directly affected the regional morphology and sediment deposition. In the western part of the plateau diapiric structures nearly reach the surface. The sediment structures on top and on the flanks are deformed, indicating postdepositional salt

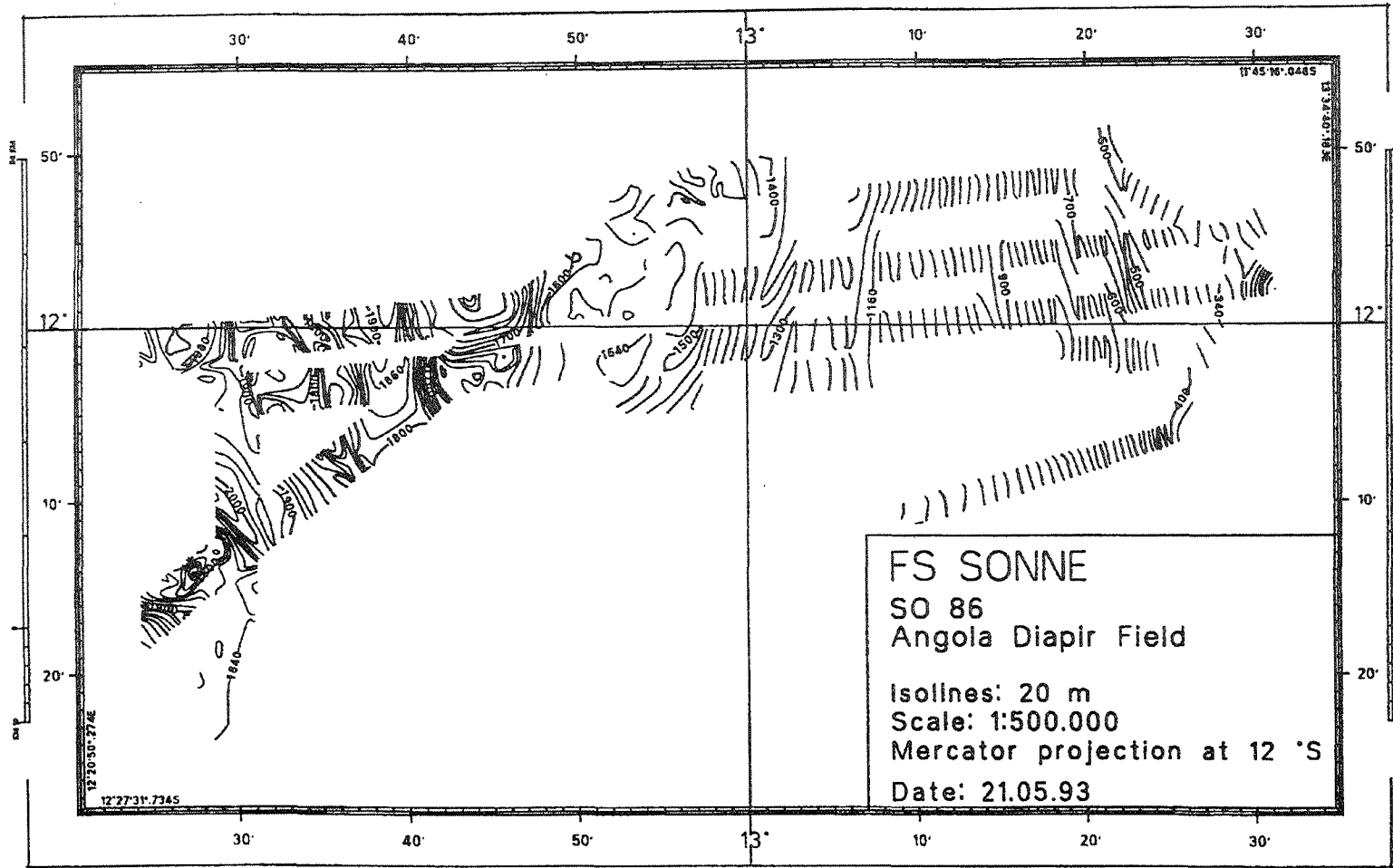


Figure 16 Bathymetry in the Angola Diapir Field area.

tectonics. Nevertheless, major reflectors can be correlated along the profiles even over vertical steps of 500 to 1000 ms. Apparently many of the small basins between the diapirs are almost unaffected by deformation and faulting, but their uplift may have caused local slumping of minor sediment packages.

The most obvious similarities between the seismic results at 12°S and the Congo Fan area are found in small basins on the western plateau. Figures 17 and 18 illustrate two examples from 12°26'E and 12°45'E, respectively. The first shows alternately continuous layering and irregular reflector surfaces, in some cases associated with small hyperbolae. The upper ~200 ms are undisturbed. Below several layers appear to reveal a basin fill from slumping events whereas other rough reflectors can be traced to the tops of the diapirs. In the second example a deep penetration into a thick sequence of regularly deposited sediments is observed. The sub-bottom depth to the base of the trough amounts to 1.5 - 2 seconds. Hyperbolic echoes indicating rough internal surfaces are of minor importance.

A subdivision into seismostratigraphic units is less straightforward than in the Congo Fan area, not the least, because the alternation of pelagic sedimentation and mass flow/fan deposition is missing here. A distinct marker for the seismostratigraphic interpretation should again be Horizon A of EMERY et al. (1975b) which was tentatively identified, e.g. at ~400 ms TWT in Figure 18. This is shallower than in the Congo Fan, where the depth of Horizon A varies between 520 and 920 ms TWT at the proposed drill sites. The following preliminary seismostratigraphic classification has been developed for this working area.

- Unit I A series of distinct reflectors, on some seismic lines cut by V-shaped troughs or channels producing wide angle diffractions. The internal surfaces are sometimes rough or undulating. Thickness 100 - 220 ms.
- Unit II Unit II can be subdivided into two subunits. Unit IIa is acoustically transparent. Unit IIb comprises a series of reflectors with a strong reflector at the base. In some intervals this base reflector is clearly identified as an unconformity. Its characteristics are very similar to Horizon A in the Congo Fan area, but an unequivocal interpretation is not yet possible at present. Thickness 100 to 220 ms.
- Unit III Acoustically almost transparent unit showing significant variations in thickness from 0 to 150 ms.
- Unit IV In some intervals this unit of mostly weaker reflectors clearly resides on an erosional contact. Thickness ~250 ms.
- Unit V Irregularly deposited sedimentary sequence with a large number of small hyperbolae.

Figure 17

Seismic record of Angola Diapir Field deposits (outer plateau, line GeoB 93-015, ~12°27'E).

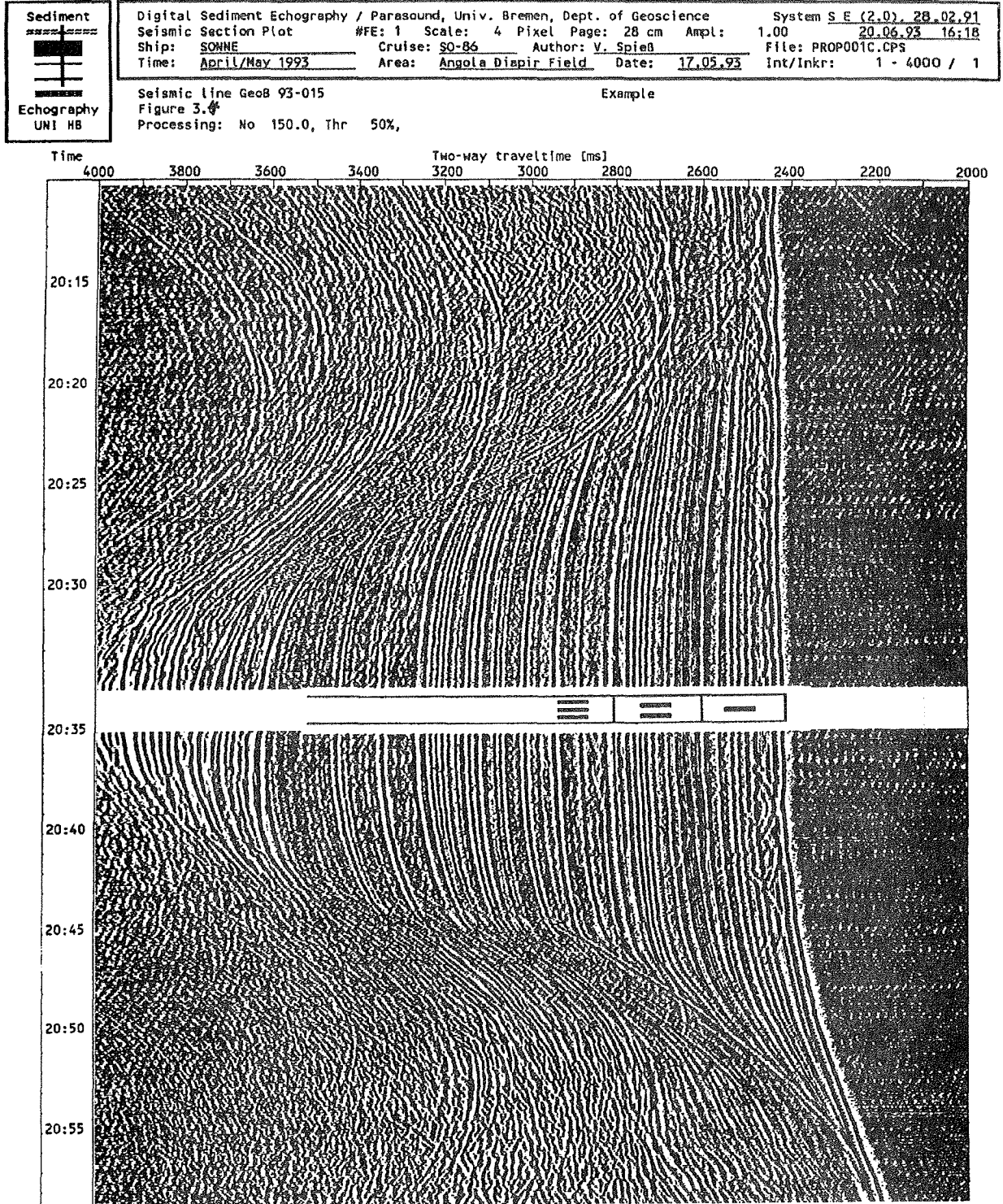
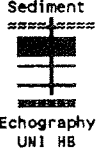
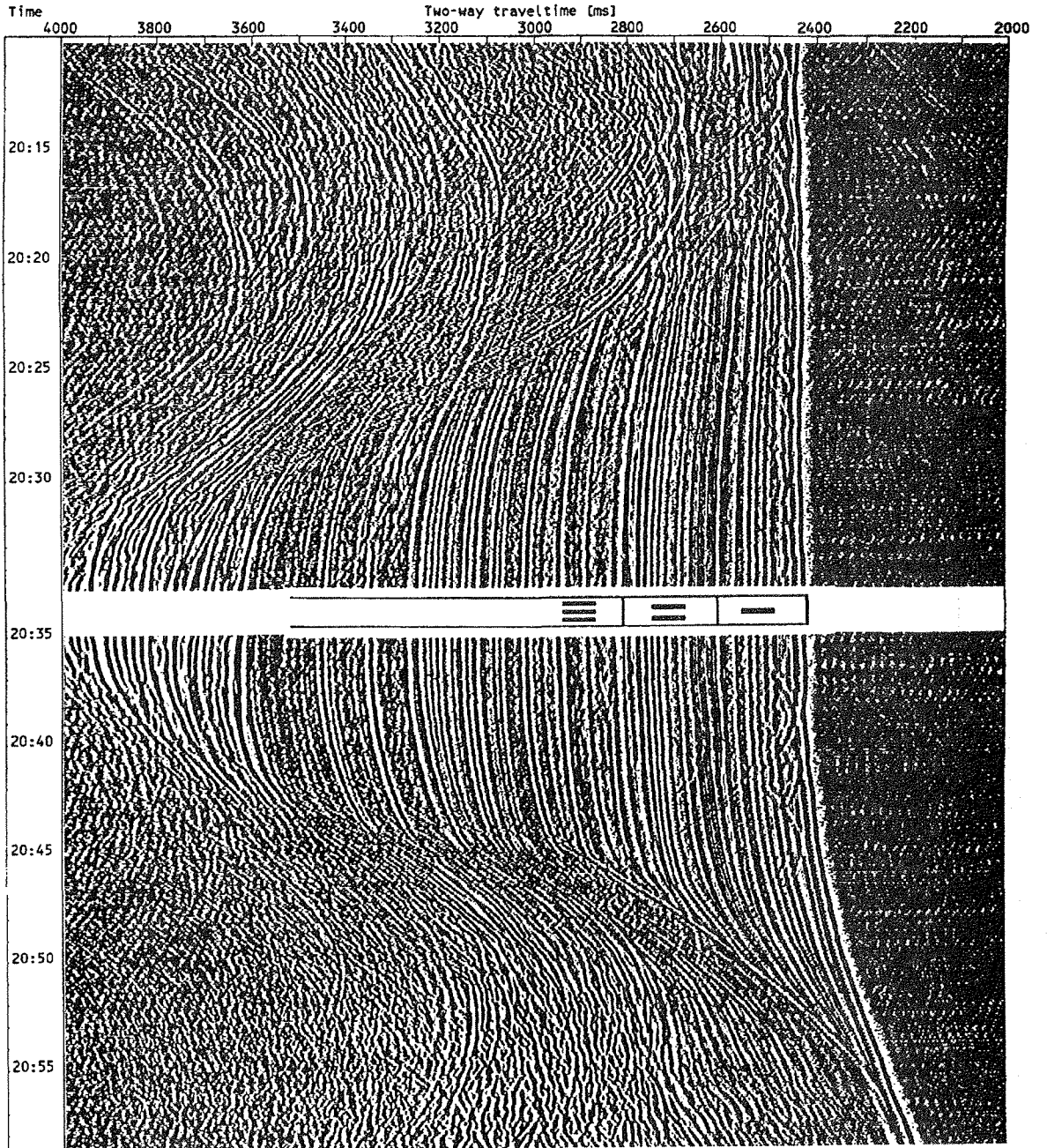


Figure 18

	Digital Sediment Echography / Parasound, Univ. Bremen, Dept. of Geoscience		System <u>SE (2.0), 28.02.91</u>
	Seismic Section Plot	#FE: 1 Scale: 4 Pixel Page: 28 cm Ampl: 1.00	20.06.93 16:18
	Ship: <u>SONNE</u>	Cruise: <u>SQ-86</u> Author: <u>V. Spieß</u>	File: <u>PROP001C.CPS</u>
	Time: <u>April/May 1993</u>	Area: <u>Angola Diapir Field</u> Date: <u>17.05.93</u>	Int/Inkr: 1 - 4000 / 1
Seismic line Geob 93-015		Example	
Figure 3.			
Processing: No 150.0, Thr 50%,			



Seismic record of Angola Diapir Field deposits (inner plateau, line Geob 93-015, ~12°45'E) with a preliminary seismostratigraphic classification.

A detailed correlation of these units to the seismostratigraphic sequence defined in the Congo Fan area is not yet possible at present. Horizon A, which was tentatively assigned to the base of seismostratigraphic Unit II here, is the only available marker. If its identification is correct, the resulting average sedimentation rates are by 10 to 30% lower than off the Congo River. Some support for this interpretation is provided by studies on Quaternary sediments resulting in rates of up to 4 cm/kyr as compared to 5 to 8 cm/kyr in the Congo Fan area (SCHEIDER, 1991). The sediment thickness above Horizon A at the proposed drill sites varies between 300 and 400 ms which should be well within the range of hydraulic piston coring.

4.4.5 PARASOUND Acoustostratigraphy

Analyses of the digital PARASOUND data revealed some most interesting details with respect to the impact of salt tectonism on the overlying sediments. Frequently a strong deformation with faulting and folding is observed. On top of the diapiric structures the uplifted sediment series are sometimes eroded and a cover of recent sediments could not always be identified. Many of the small basins on the outer and inner plateau allow a penetration of the high frequency signal of more than 100 m. There, the sediments show parallel layering without distortion or indications of slumping (Fig. 19) and therefore should be well suited to drill several shallow holes with penetrations on the order of 100 m.

Further upslope, between 1600 and 1200 m water depth, sediment waves or small channels/troughs are found (Fig. 20) which produce hyperbolic echoes in the seismic records. From water depths shallower than 1200 meters layered sediments can be traced up to the shelf edge. The signal penetration is mostly on the order of 80 to 100 meters. No evidence for downslope transport by mass movements is observed below 400 meter water depth.

4.4.6 Proposed Drill Sites

All drill sites proposed in the Angola Diapir Field are located on seismic line GeoB 93-015, because the sediments were found to be significantly influenced by slumping of shelf deposits and turbidity currents along the more southerly profile GeoB 93-017. Only smooth changes in near surface reflection patterns are observed on line GeoB 93-015 indicating the absence of mass flow deposition. For each of the six sites proposed, a crossing seismic profile was shot perpendicular to line GeoB 93-015. They cover a depth range from 550 to 1560 m over a distance of 28 nm. Also numerous other places were found both on the upper continental slope and in the plateau region in about 2000 m water depth, where the penetration of the PARASOUND signal is on the order of 100 m showing an undisturbed sedimentary regime. Table 4 summarizes all relevant data of the proposed drill sites ADF-1 to ADF-6.

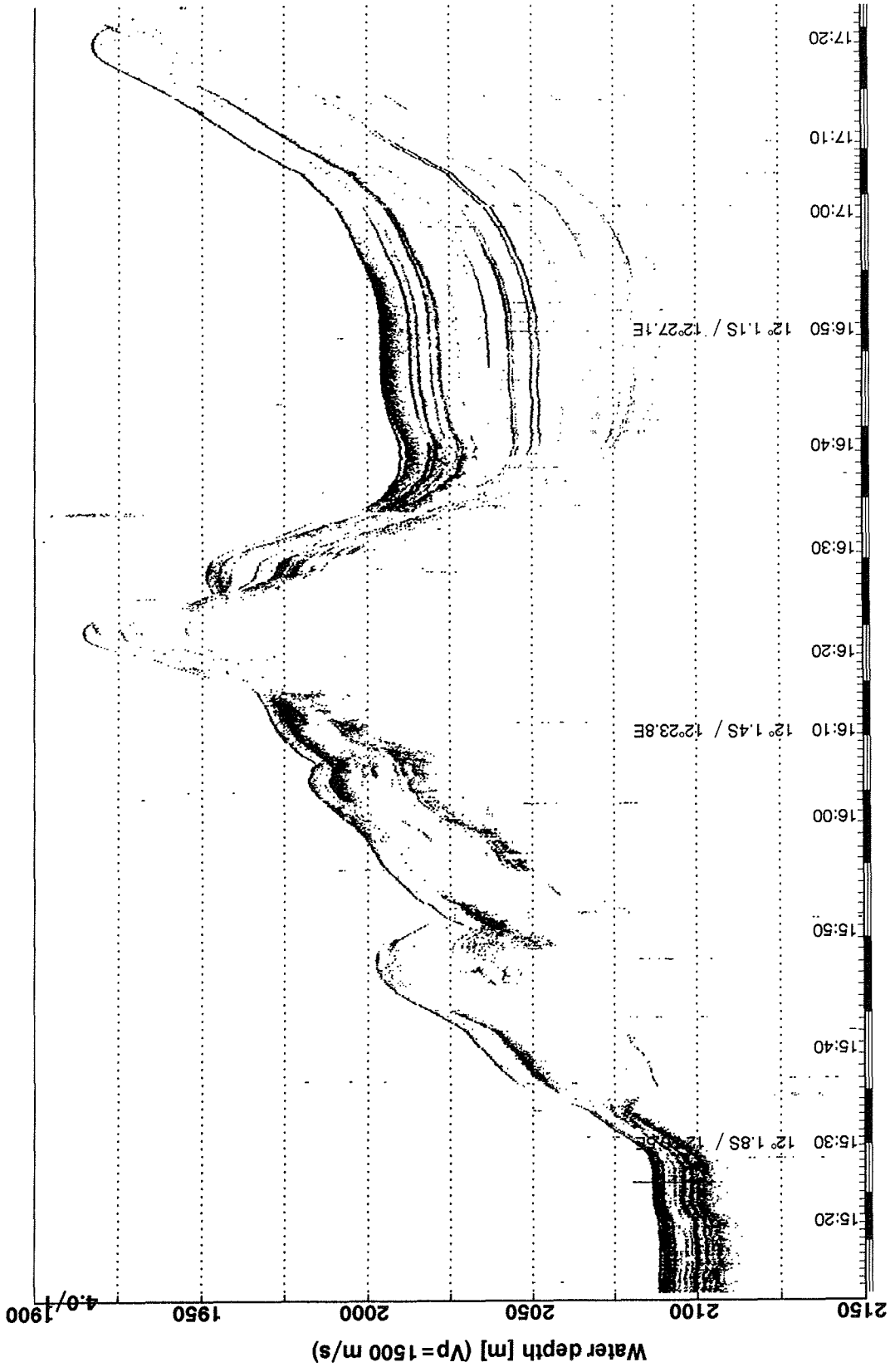


Figure 19 PARASOUND record on the outer plateau of the Angola Diapir Field (line GeoB 93-015, ~12°27'E). The right half of the section corresponds to the seismic record shown in Figure 17.

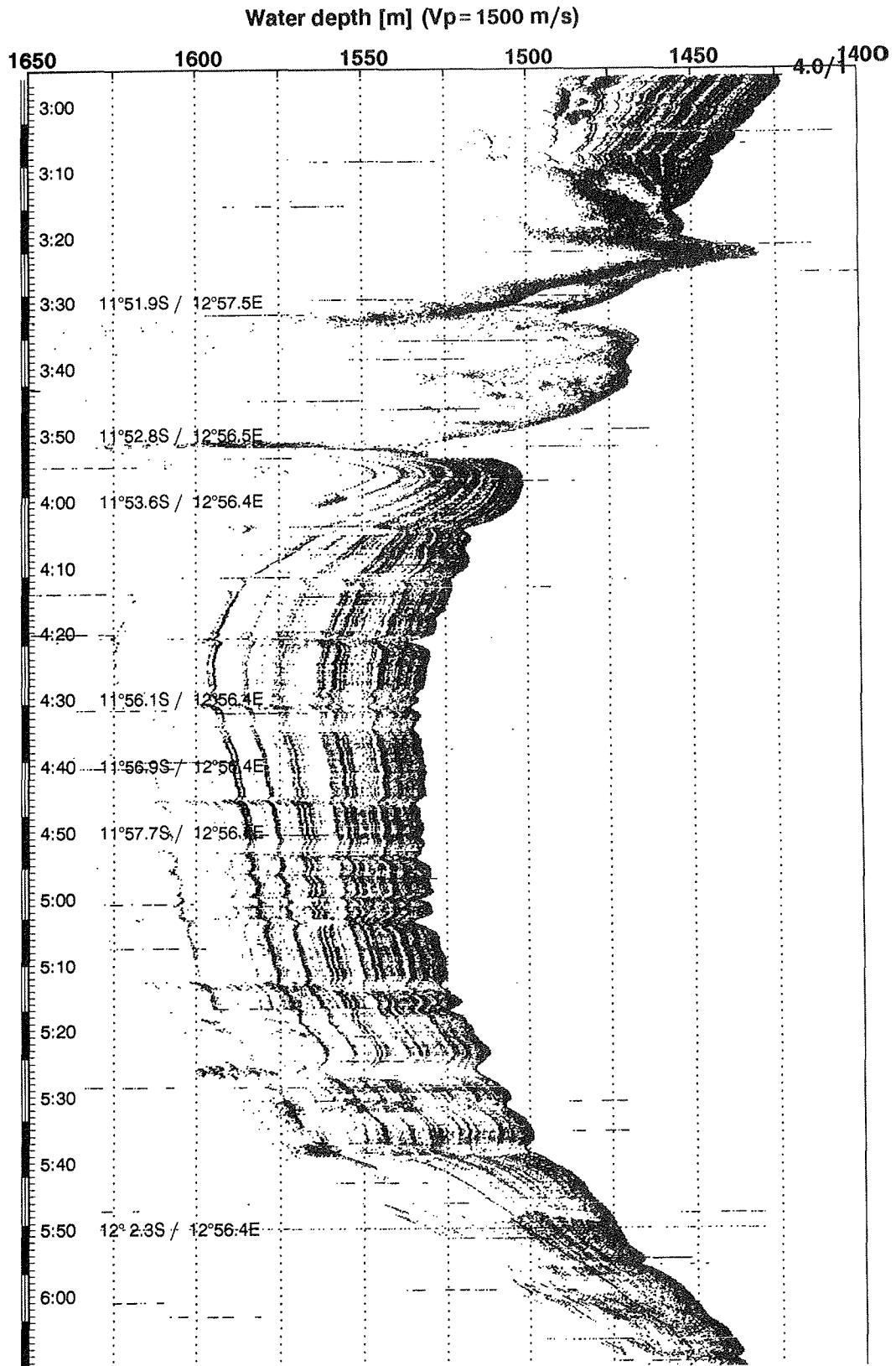


Figure 20 PARASOUND record of lower slope deposits in the Angola Diapir Field (line Geob 93-026, ~12°57'E near proposed drilling location ADF-5, see Fig. 25).

Table 4 Proposed drill sites in the Angola Diapir Field area. For each site the geographical coordinates and seismic line numbers as well as the date, time and water depth at crossings are listed.

Site	Geographic		Seismic Line	Date	Time	Water Depth (m)
	Latitude	Longitude				
ADF-1	11°55.4'S	13°21.5'E	GeoB 93-015	18.05.93	3:50	550
			GeoB 93-019	19.05.93	13:48	552
ADF-2	11°55.7'S	13°19.0'E	GeoB 93-015	18.05.93	3:15	719
			GeoB 93-021	19.05.93	17:56	715
ADF-3	11°56.9'S	13° 7.0'E	GeoB 93-015	18.05.93	0:50	1178
			GeoB 93-023	19.05.93	21:58	1175
ADF-4	11°57.7'S	13° 1.9'E	GeoB 93-015	17.05.93	23:50	1351
			GeoB 93-025	20.05.93	1:18	1346
ADF-5	11°58.0'S	12°56.4'E	GeoB 93-015	17.05.93	22:45	1530
			GeoB 93-027	20.05.93	4:54	1532
ADF-6	11°58.4'S	12°53.1'E	GeoB 93-015	17.05.93	22:05	1559
			GeoB 93-029	20.05.93	7:56	1559

Sites ADF-1 and ADF-2 in about 550 and 720 m water depth are the shallowest on the selected transect (Figs. 21 and 22). Unit I comprises a dense sequence of parallel internal reflectors of 180 to 220 ms thickness. A few thin transparent intervals interrupt this pattern. The about 150 to 200 ms thick Unit II is mostly transparent with several rather diffuse parallel layers. Below, more prominent reflectors are encountered beneath a relatively transparent zone. This Unit III is disturbed by hyperbolic echoes further downslope. The base of Unit II is tentatively interpreted as Horizon A, the Miocene to Oligocene/Eocene unconformity. Assuming an age of ~23 Ma for its termination, the average sedimentation rate would amount to ~4 cm/kyr, an about identical value as found in the Quaternary sediments. At present, it cannot be excluded, therefore, that the base of Unit I may coincide with Horizon A.

Sites ADF-3 and ADF-4 are located in water depths between 1350 and 1530 meters (Figs. 23 and 24). The general appearance of the seismostratigraphic units is similar to the shallower sites. A pronounced reflector marks the transition between Units I and II, while the base of Unit II is less easily identified. The average thicknesses amount to ~140 ms for Unit I and ~210 ms for Unit II.

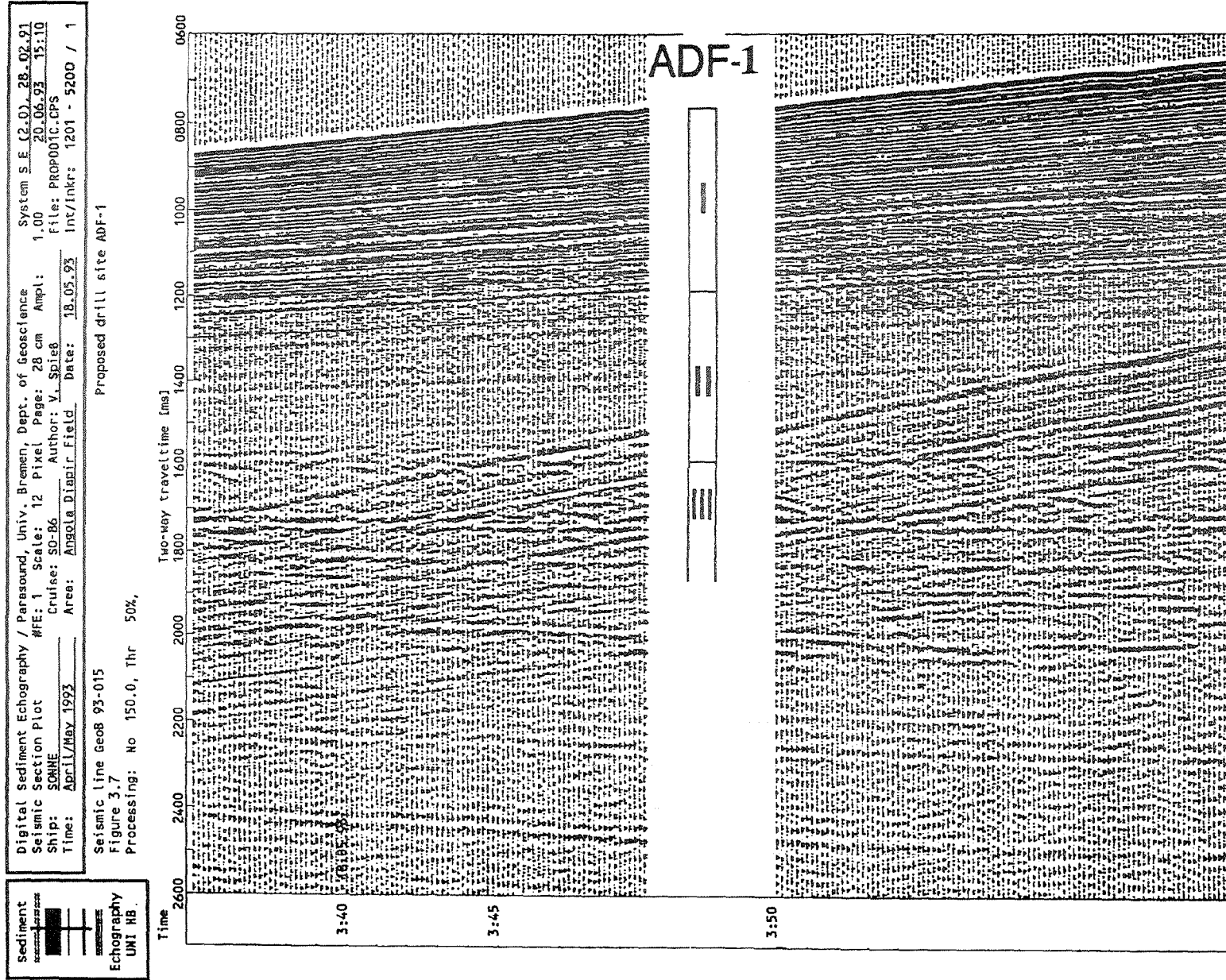


Figure 21 Seismic record at the proposed drilling location ADF-1 (see Table 4 for details).

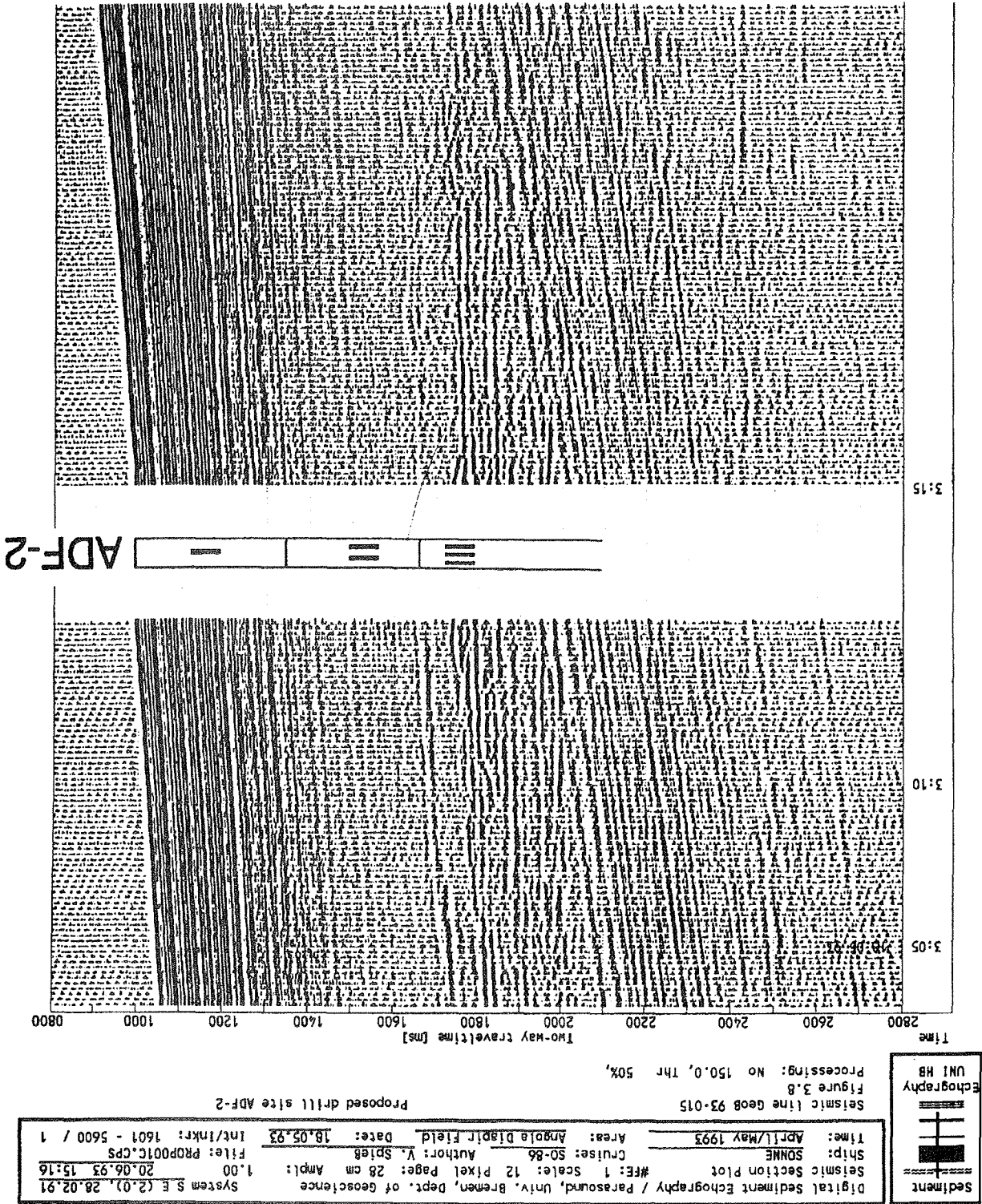


Figure 22 Seismic record at the proposed drilling location ADF-2 (see Table 4 for details).

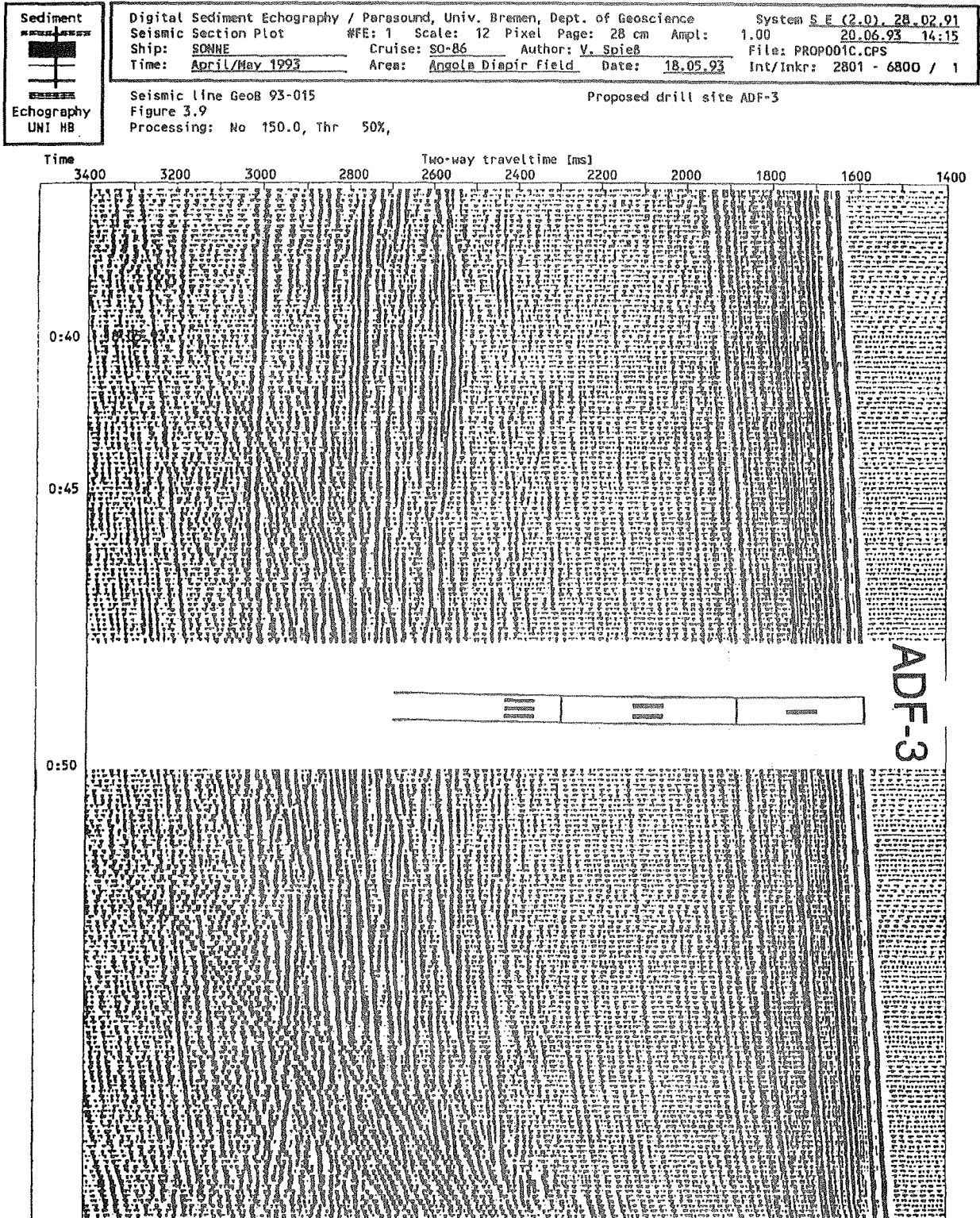


Figure 23

Seismic record at the proposed drilling location ADF-3 (see Table 4 for details).

Sediment  Echography UNI HB	Digital Sediment Echography / Parasound, Univ. Bremen, Dept. of Geoscience		System S E (2.0), 28.02.91	
	Seismic Section Plot #FE: 1 Scale: 6 Pixel Page: 28 cm Ampl: 1.00		20.06.93 12:34	
	Ship: SONNE	Cruise: SO-86	Author: V. Spieß	File: PROP001B.CPS
	Time: April/May 1993	Area: Congo Fan	Date: 17.05.93	Int/Inkr: 1201 - 5200 / 1
Seismic line GeoB 93-015		Proposed drill site ADF-4		
Figure 3.10				
Processing: No 150.0, Thr 50%,				

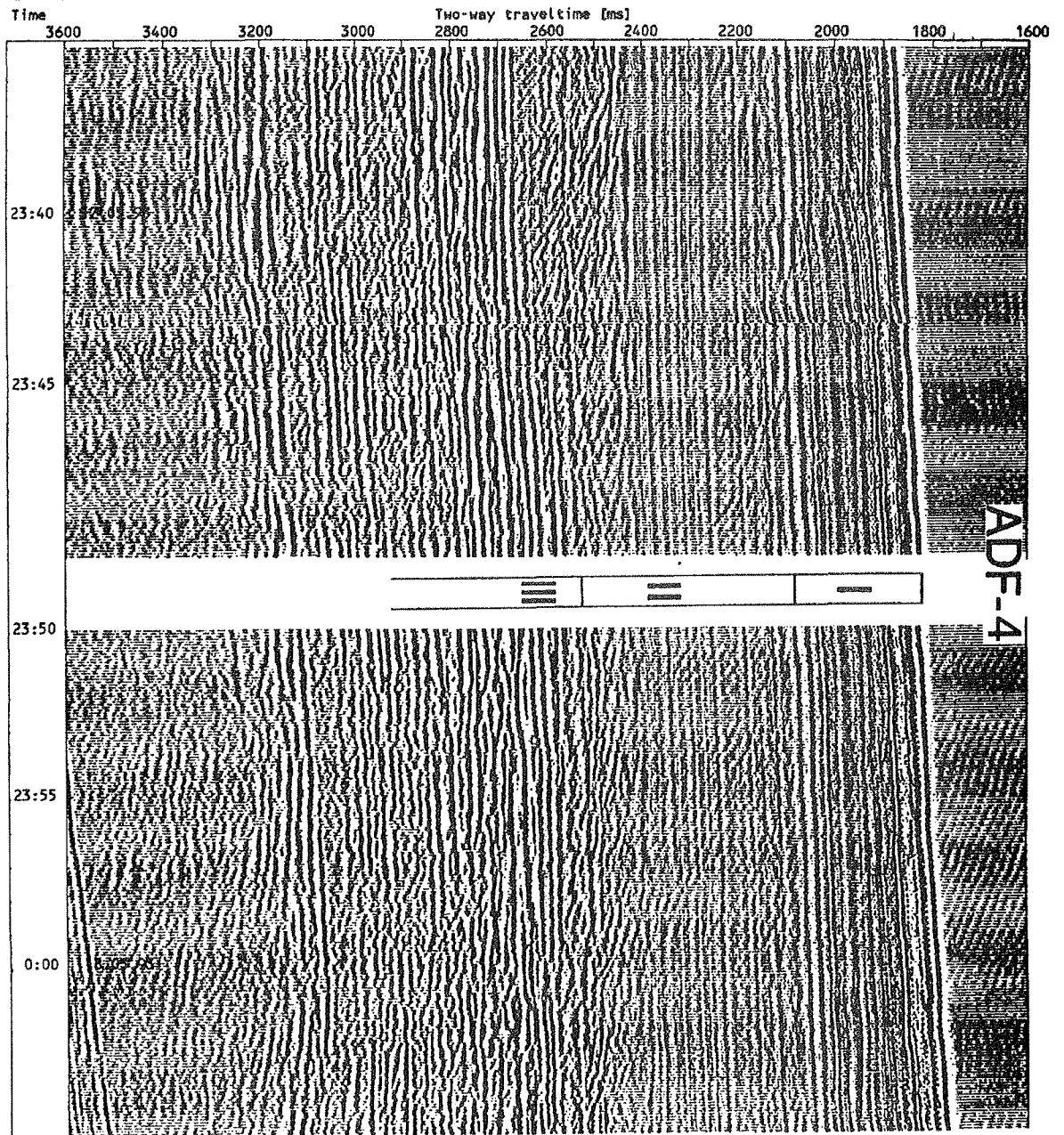


Figure 24

Seismic record at the proposed drilling location ADF-4 (see Table 4 for details).

Sediment  Echography UNI HB	Digital Sediment Echography / Parasound, Univ. Bremen, Dept. of Geoscience System <u>SE (2.0)</u> , <u>28.02.91</u>	Seismic Section Plot #FE: 1 Scale: 6 Pixel Page: 28 cm Ampl: 1.00 Date: <u>20.06.93</u> <u>15:32</u>
	Ship: <u>SONNE</u> Cruise: <u>SO-86</u> Author: <u>V. Spieß</u>	File: <u>PROP001C.CPS</u>
	Time: <u>APRIL/May 1993</u> Area: <u>Angola Diapir Field</u> Date: <u>17.05.93</u>	Int/Inkr: <u>1601 - 5600 / 1</u>
	Seismic line <u>GeoB 93-015</u> Figure 3.11 Processing: No 150.0, Thr 50%,	Proposed drill site <u>ADF-5</u>

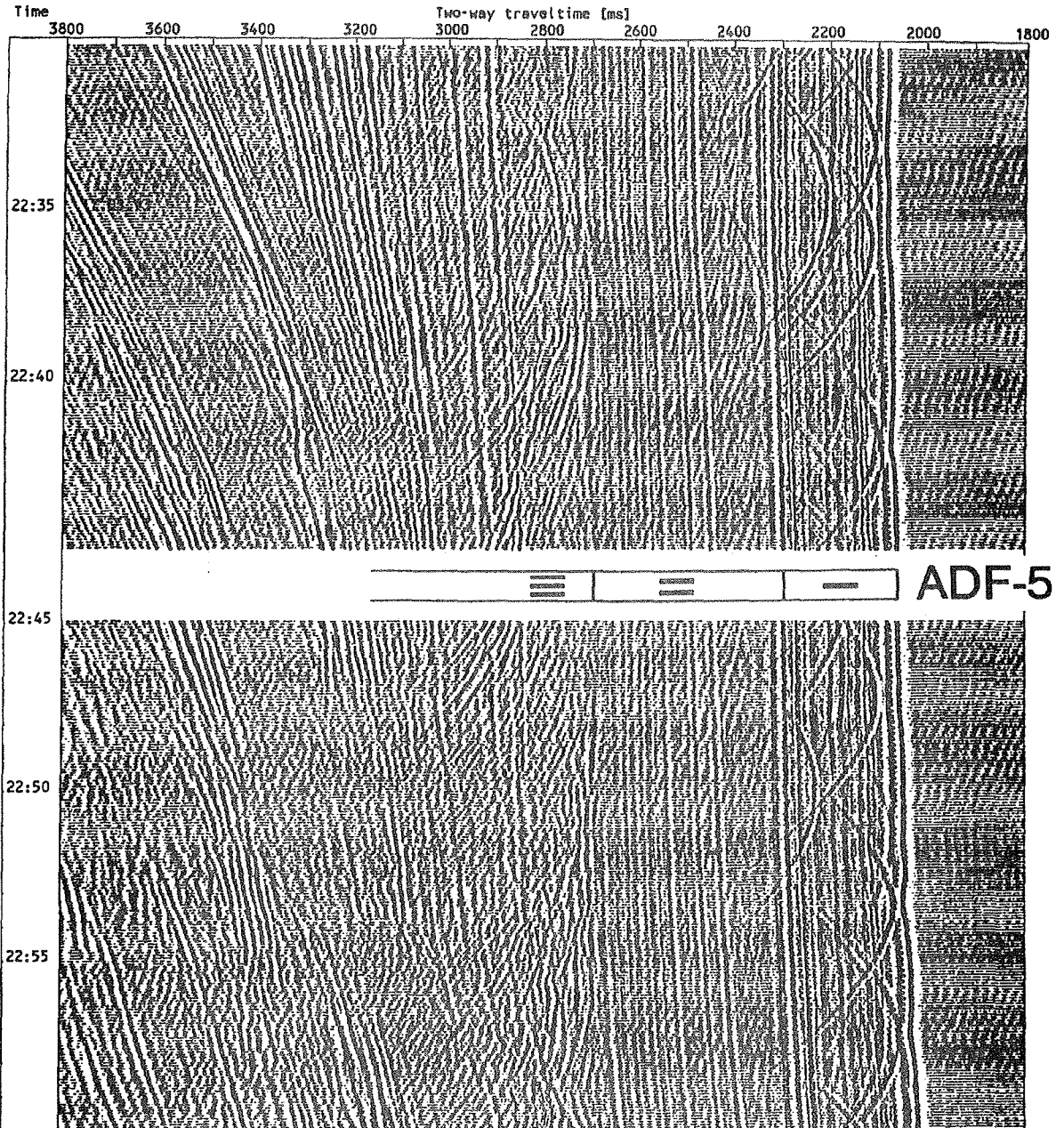
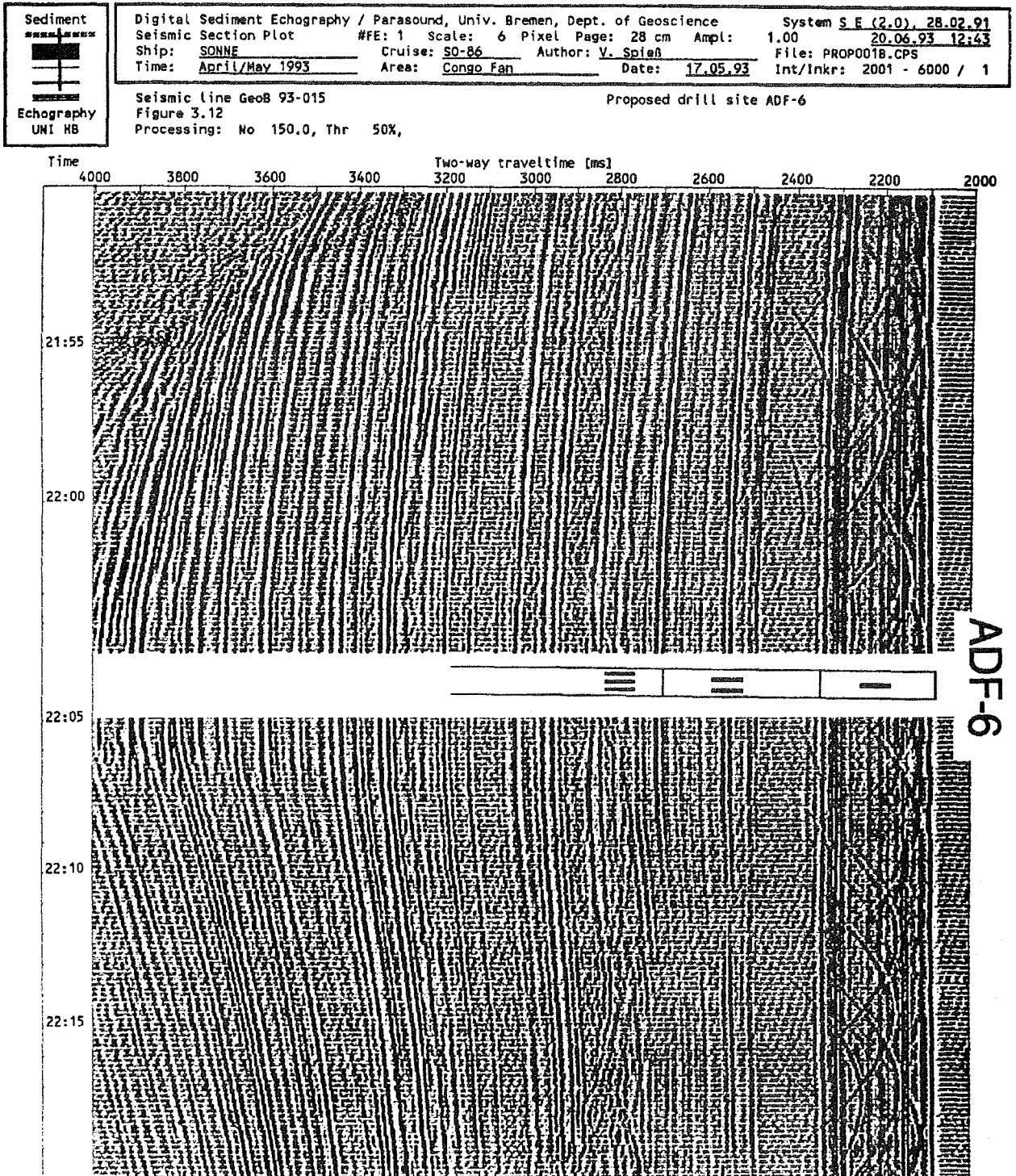


Figure 25 Seismic record at the proposed drilling location ADF-5 (see Table 4 for details).

Figure 26

Seismic record at the proposed drilling location ADF-6 (see Table 4 for details).



At Sites ADF-5 and ADF-6 in around 1500 to 1600 m water depth, sediment waves or small channels produce hyperbolic echoes in seismostratigraphic Unit I (Figs. 25 and 26). Furthermore, the character of Unit II has somewhat changed as a series of reflectors with increasing amplitudes appear in its central portion. There are indications for an erosional contact at the base of Unit II. The thicknesses of Units I and II amount to ~130 ms and 180 to 200 ms, respectively.

4.5 Namibia - Angola Upwelling at 17°S

4.5.1 Introduction

The northern part of the Angola - Namibia coastal upwelling cell (SCHELL, 1970; NELSON & HUTCHINS, 1983; STRAMMA & PETERSON, 1989) is located at ~17°S between the Angola Diapir Field and the Walvis Ridge. The continental margin is rather narrow as the relict of a rift basin is absent here and may eventually be traced at the South American side. Due to an intense current activity on the shelf and the steepness of the continental slope, downslope sediment transport by slides, debris flows and turbidity currents has shaped the area (EMBLEY & MORLEY, 1980). The morphology is further complicated by sedimentary tectonism and giant sediment slides. Although the pelagic sedimentation rates are high due to coastal upwelling off Namibia and Angola, only a few places could be identified with a clear pelagic sediment pattern.

4.5.2 Strategy of Site Survey

As multiple major and minor slides are documented in the survey region, highest priority was given to the identification of areas with an apparently undisturbed sedimentation. Because of the generally steep slopes, the most promising depth ranges were expected in the mid and lower stretches of the continental margin. The initial seismic line was oriented along an earlier PARASOUND profile (R/V METEOR Cruise M20/2) which had revealed undisturbed near surface sediments in a number of places. Only two suitable drill sites could be identified in water depths between 2200 and 3000 meters and were crossed by additional seismic lines (Fig. 27). All areas shallower than 2200 m and deeper than 3000 m were found to be affected by intensive slumping.

4.5.3 Bathymetry

The bathymetric records (Fig. 28) confirmed the complex nature of the depositional environment. Although the survey was not sufficient to analyse all structures in detail, it became clear from the combined HYDROSWEEP and PARASOUND echosounder data sets that only very few potential drill sites may be found in the region. The locations selected for additional seismic lines are apparently protected from mass movements by the local topography, perhaps featuring an underlying basement high.

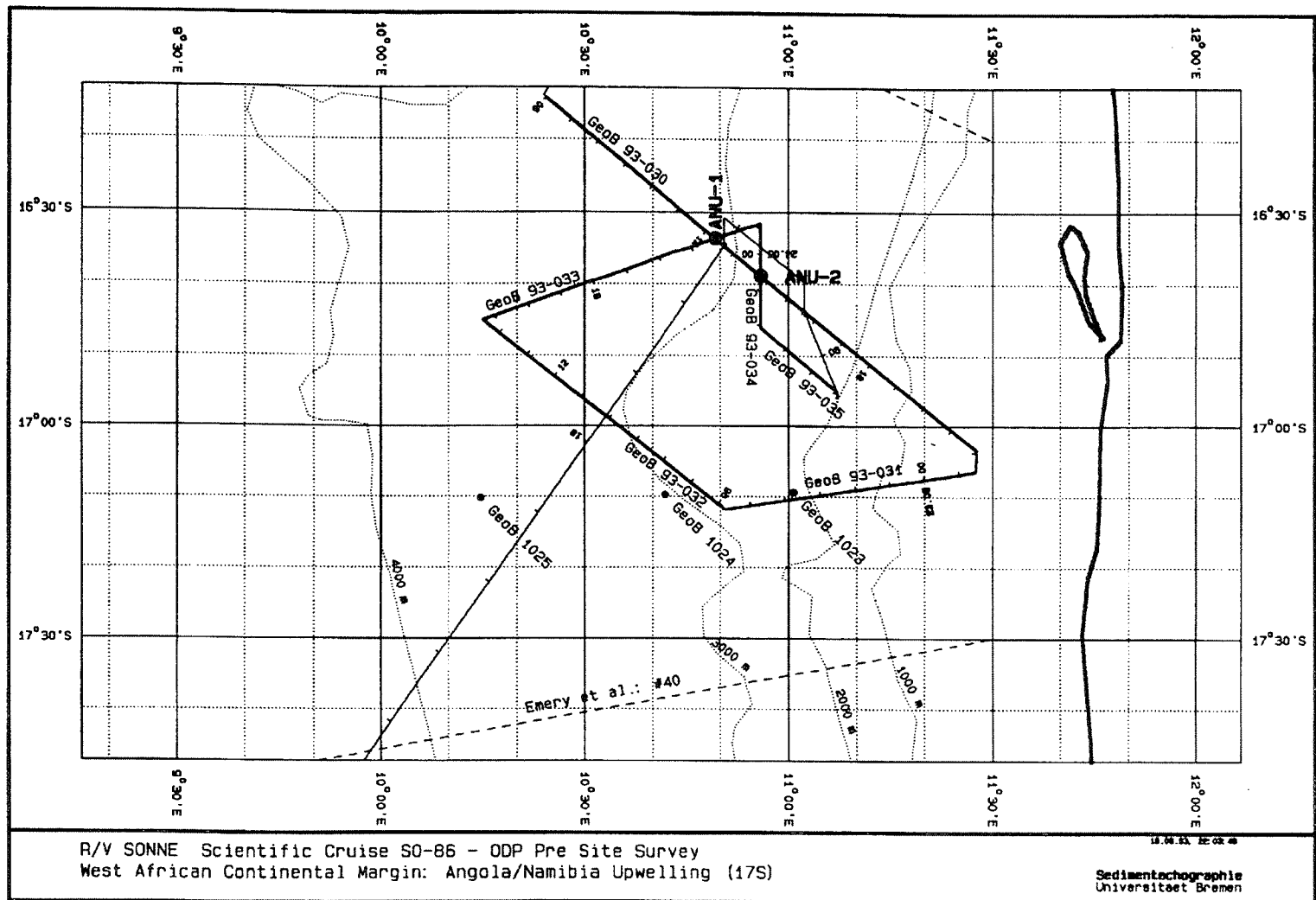


Figure 27 SO 86 track chart in the Namibia - Angola Upwelling area. Thick lines denote seismic and echographic profiles, thin lines echographic profiles only. Seismic profile #40 of EMERY et al. (1975b) is indicated by a broken straight line. Dots mark potential ODP drill sites.

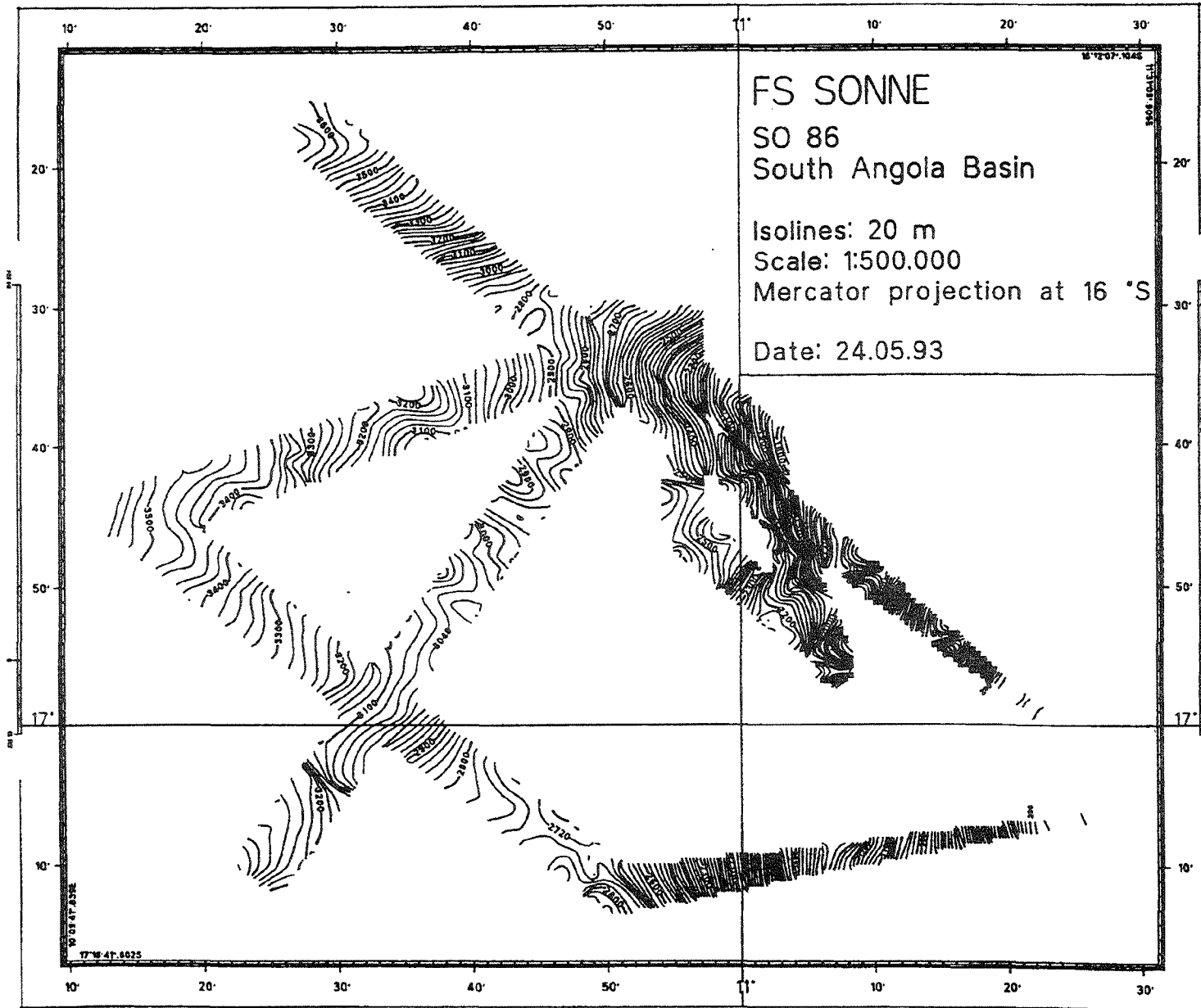


Figure 28 Bathymetry in the Namibia - Angola Upwelling area.

4.5.4 PARASOUND Acoustostratigraphy

The selection of drill sites in the Angola - Namibia Upwelling region was primarily based on digital PARASOUND data. Only they allowed a clear distinction between chaotic and regular sediment structures on a meter scale. Seismic data often showed a continuous layering, while the PARASOUND system was imaging a microtopography with rough, scattering surfaces. The signal penetration on the order of 50 to 75 meters was generally lower than in the survey areas further north, possibly resulting from lower clay and higher silt/sand concentrations. This may indicate an intensified deposition of planktic foraminifera or, more likely, higher proportions of shelf materials transported downslope. The selected drill sites (Figs. 29 and 30) show undisturbed sediment structures which should represent a continuous and primarily hemipelagic sedimentation documenting the regional productivity and upwelling history.

4.5.5 Seismostratigraphy and Proposed Drill Sites

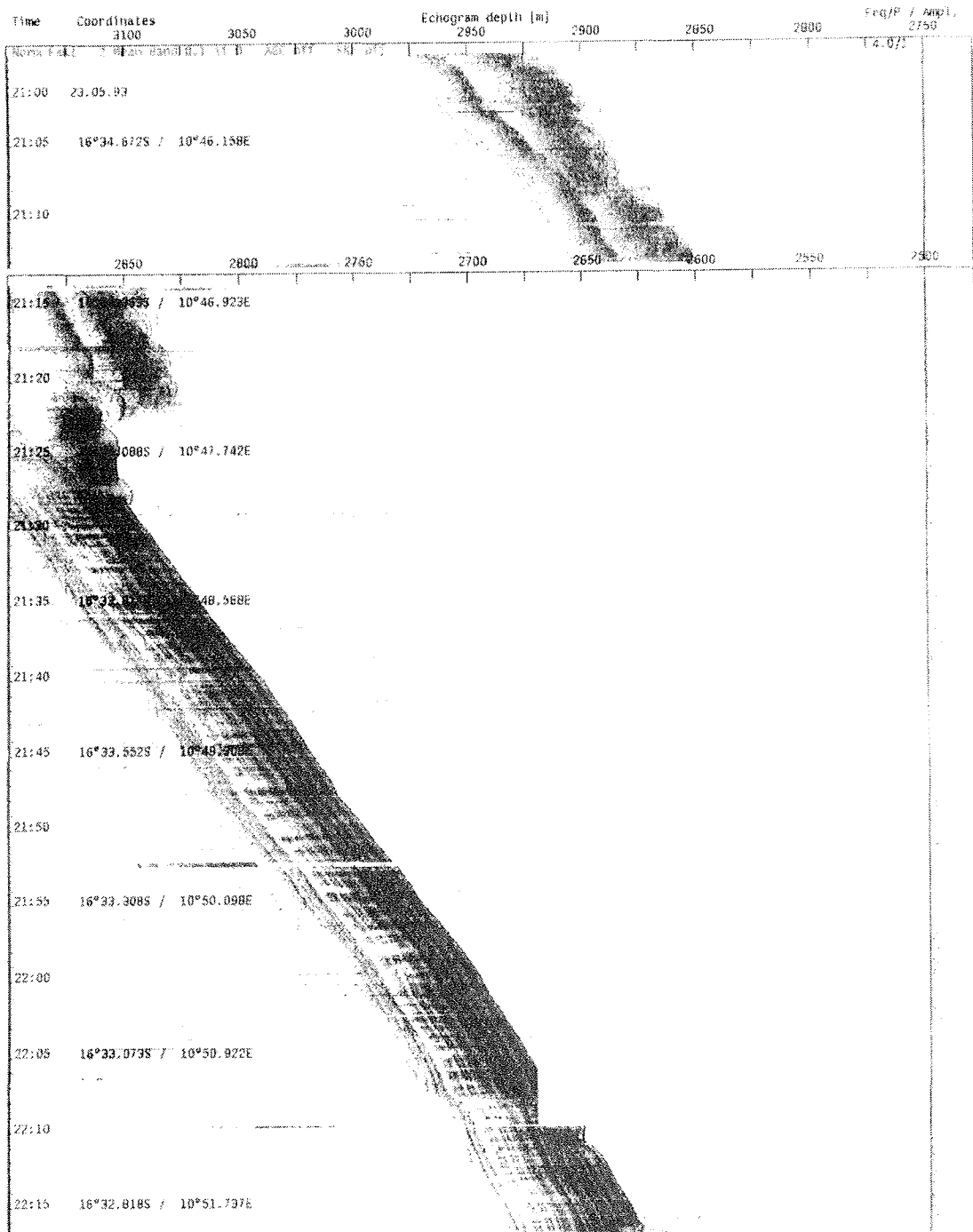
Figures 31 and 32 show sections of seismic line GeoB 93-030 across the two proposed drill sites (Table 5). The reflection pattern is predominantly regular comprising several stronger continuous reflectors. Occasionally small hyperbolic echoes indicate undulating surfaces or a rough microtopography which cannot be distinguished due to the limited resolution of the seismic data. It should be taken into account, however, that the frequency band of the source as well as the recording system extends to several hundred Hz providing a comparatively detailed image of the sedimentary structures. If only the frequency band below 100 Hz had been considered - as for usual multichannel seismic surveys - the reflection pattern would appear much more regular.

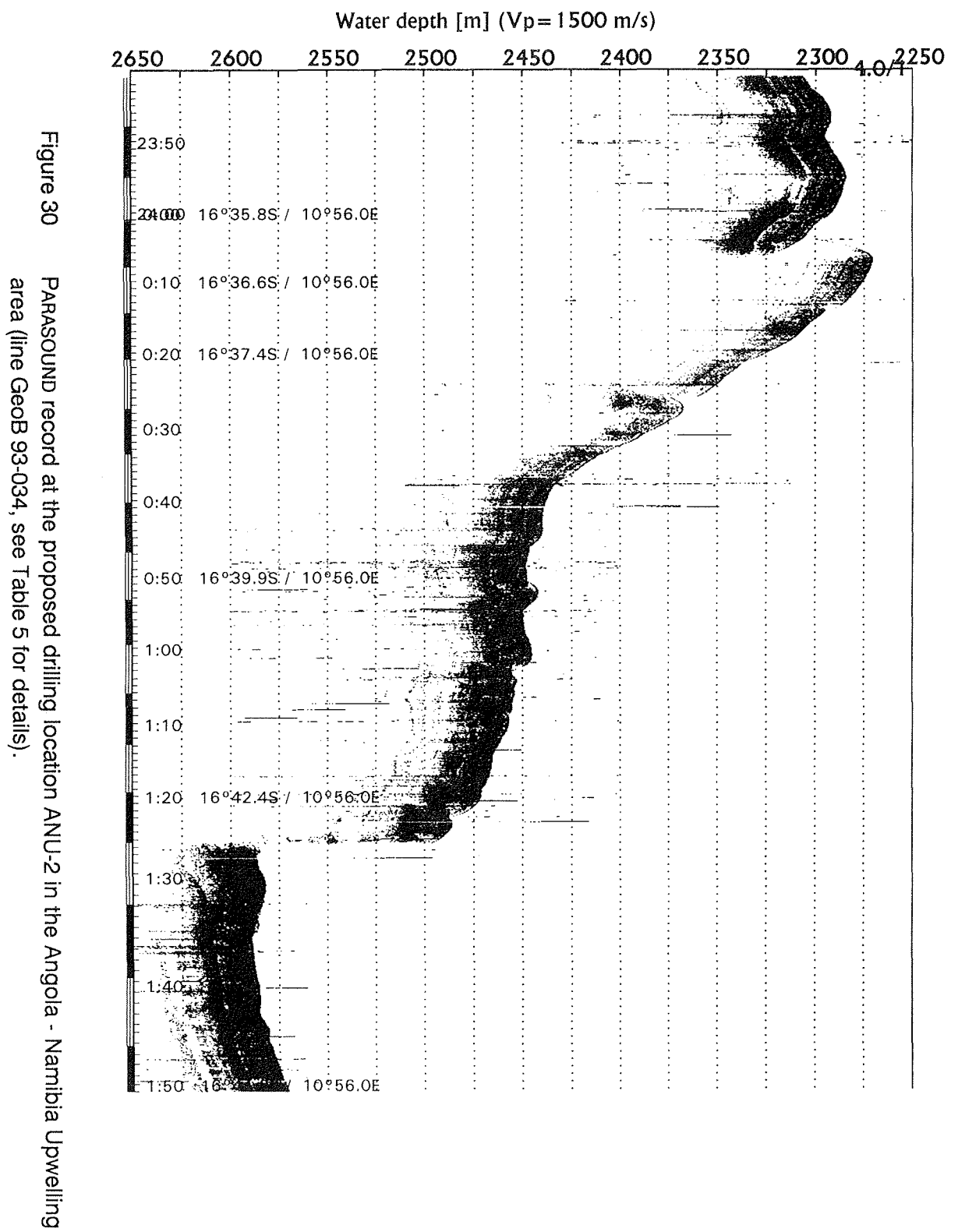
Table 5 Proposed drill sites in the Angola - Namibia Upwelling area. For each site the geographical coordinates and seismic line numbers as well as the date, time and water depth at crossings are listed.

Site	Geographic		Seismic Line	Date	Time	Water Depth (m)
	Latitude	Longitude				
ANU-1	16°33.6'S	10°49.3'E	GeoB 93-030	22.05.93	12:20	2775
			GeoB 93-033	23.05.93	21:45	2770
ANU-2	16°38.8'S	10°56.0'E	GeoB 93-030	22.05.93	14:00	2423
			GeoB 93-034	24.05.93	0:35	2425

Figure 29

PARASOUND record at the proposed drilling location ANU-1 in the Angola - Namibia Upwelling area (line GeOB 93-033, see Table 5 for details).





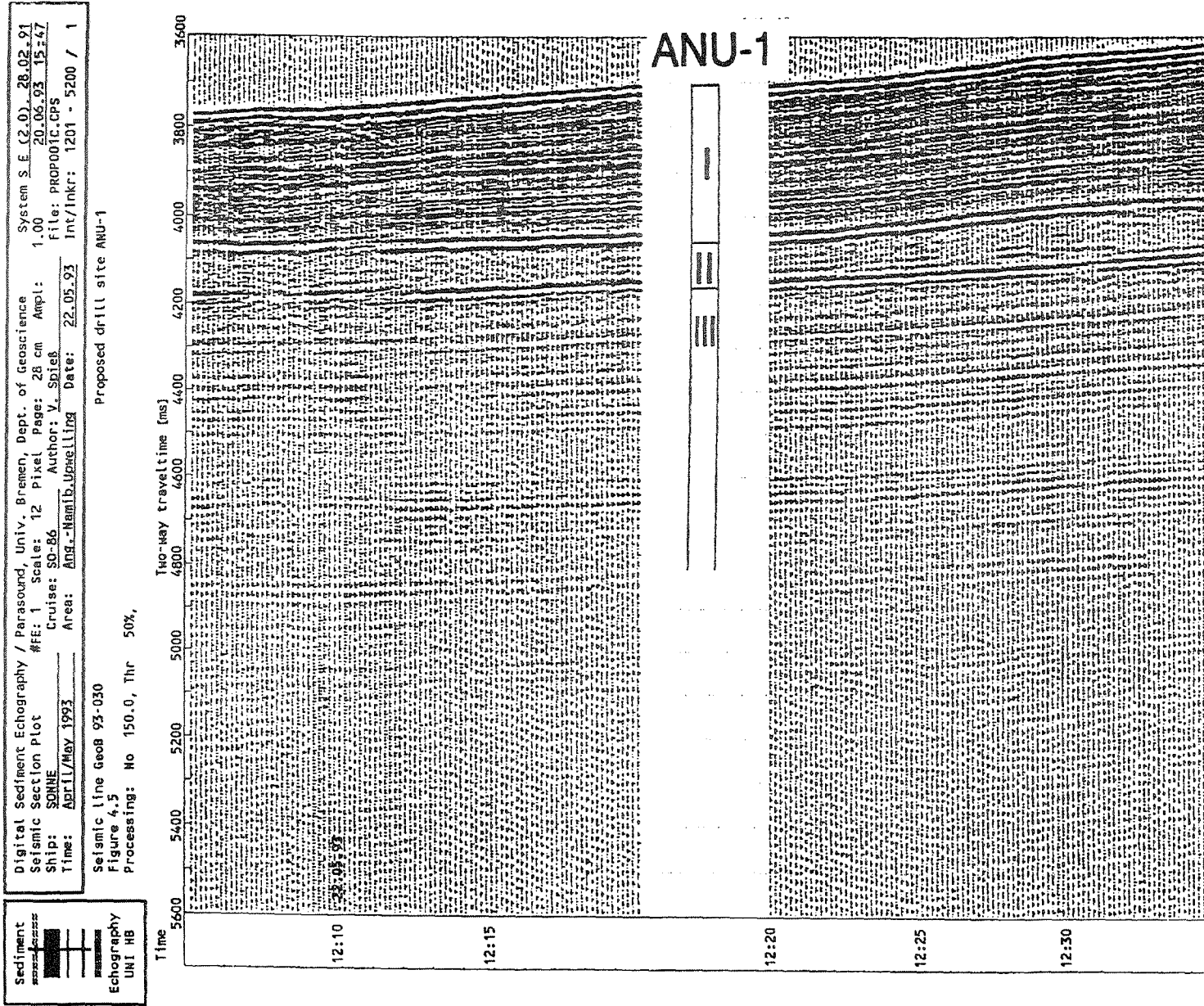
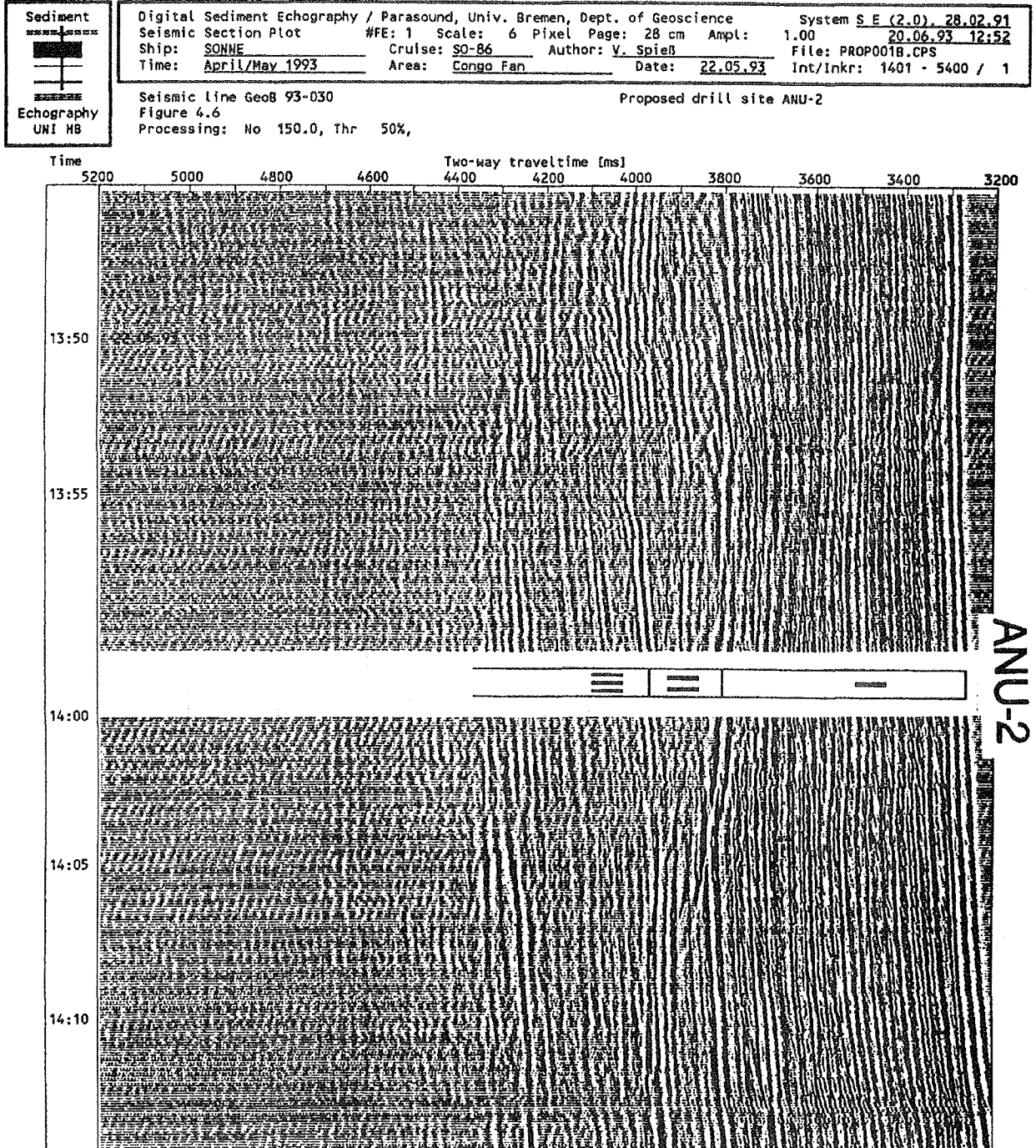


Figure 31 Seismic record at the proposed drilling location ANU-1 (see Table 5 for details).

Figure 32

Seismic record at the proposed drilling location ANU-2 (see Table 5 for details).



The local and small scale disturbances in the sedimentary sequences produced by the depositional environment might possibly complicate an interpretation of the drilling results. On the other hand, the selected sites are among the very few places in the area with a reasonably clear, parallel reflector pattern which should allow the reconstruction of the regional sedimentation history.

At this stage, the available evidence to identify seismostratigraphic units in the seismic records is even more tenuous than at the other survey areas. Tentatively assigning the distinct high amplitude reflectors marking the base of Unit II at 230 and 350 ms, respectively, to Horizon A would result in relatively low average sedimentation rates of 2.5 - 4 cm/kyr since earliest Miocene. The base of Unit I is associated with a general change in reflection pattern to lower amplitudes. The upper series of sediment may thus represent upwelling conditions, while the mainly transparent packages below are affected and to a large extent deposited by turbidity currents. Similar characteristics were also observed at DSDP Site 530 in the southernmost Angola Basin.

4.6. Additional Seismic Surveys

Two additional areas were investigated with seismic lines at the end of Cruise SO 86 which should be of substantial interest for the future planned drilling operations.

On the northern flank of the Walvis Ridge a detailed survey was performed in the vicinity of DSDP Sites 530 and 532 and connected by a line over the ridge flanks (Fig. 33). The data will be used to calibrate the actual seismostratigraphies with previous drilling results using lithologic, sedimentologic and physical core logs as well as logging data. Compared to available multichannel seismic data, the resolution could now be increased by a factor of 5 to 10.

A second survey (Fig. 34) was carried out across proposed drill sites NCB-1 and NCB-3 in the Northern Cape Basin (EMERY et al., 1975a), where multichannel data have been provided by the University of Texas (AUSTIN & UCHUPI, 1982). The crossing of Site NCB-1 shows undisturbed sedimentary sequences almost without lateral changes. Immediately after passing over Site NCB-3 further seismic measurements had to be abandoned due to problems with the seismic source. Although the crossing line could not be completed, the results obtained also indicate an undisturbed sedimentation in the vicinity of this site.

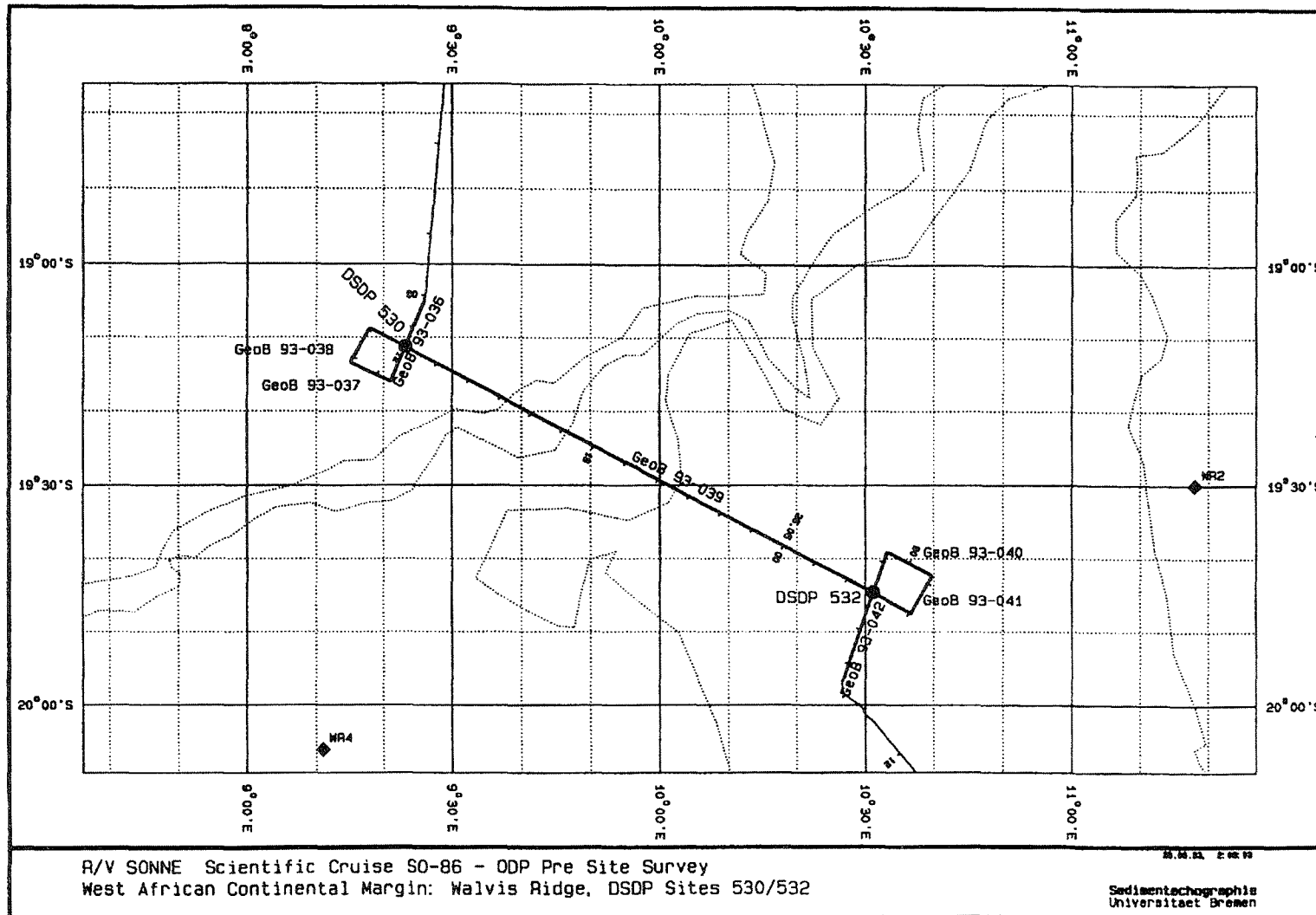


Figure 33 SO 86 track chart at the Walvis Ridge in the vicinity of DSDP Sites 530 and 532. Thick lines denote seismic and echographic profiles, thin lines echographic profiles only.

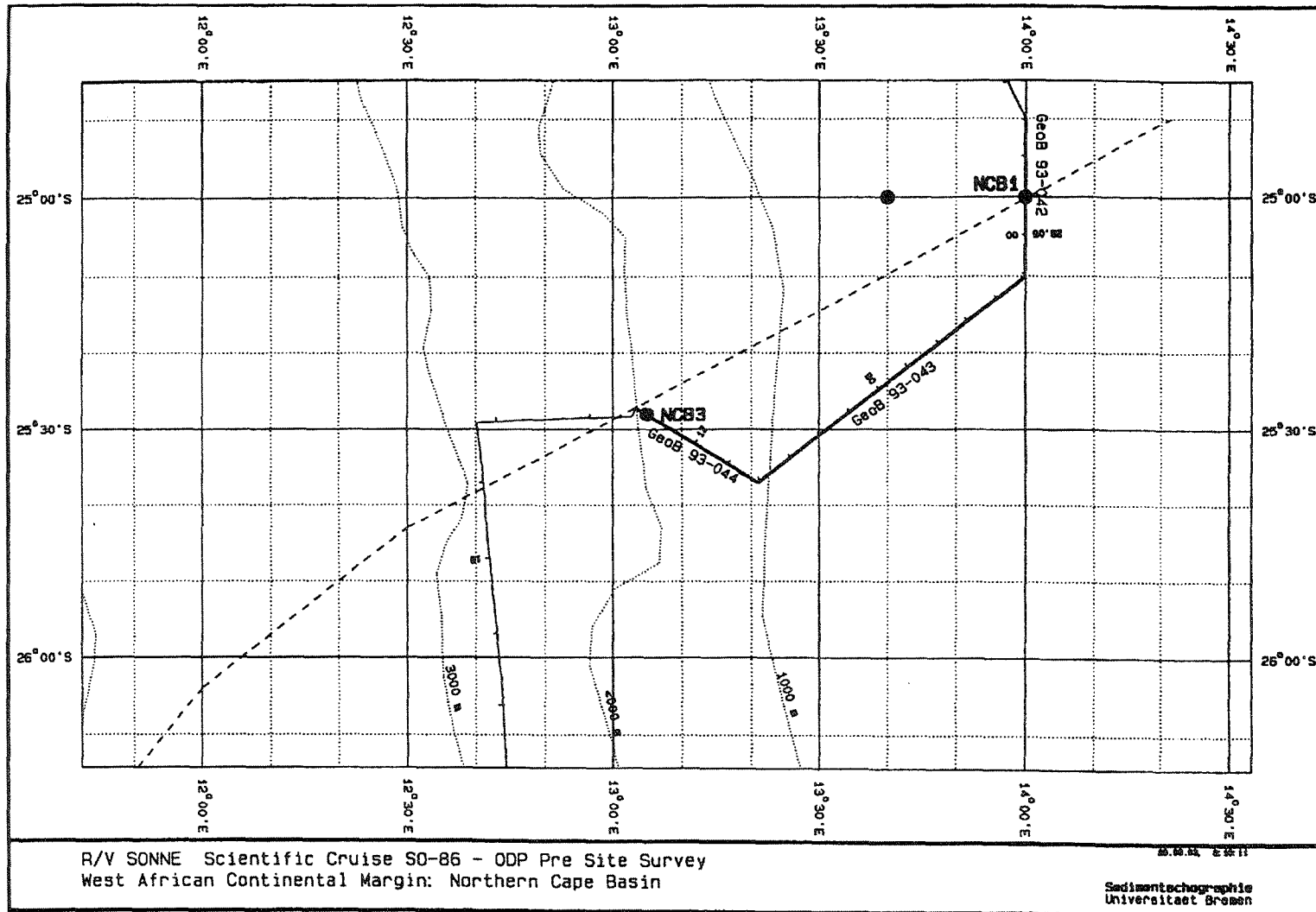


Figure 34 SO 86 track chart in the northern Cape Basin in the vicinity of proposed drill sites NBC-1 and NBC-3. Thick lines denote seismic and echographic profiles, thin lines echographic profiles only. An echographic profile obtained during R/V METEOR Cruise M23/1 is indicated by a broken line.

5 Sediment Sampling

R. Schneider, L. Dittert, P. Helmke, U. Rosiak

A multicorer and a gravity corer were used to recover surface and late Quaternary sediments at 10 stations on the southwest African continental margin off Congo, Angola and Namibia from water depths between 400 and 3000 m. A series of in each case 3 stations was positioned along transects across the northern flank of the Congo Fan (Fig. 2) and in the Angola Diapir Field (Fig. 15). One station is located just north, another 2 are located just south of the Angola Benguela Front. The last station of this cruise was sampled in the Cape Basin near the upwelling center off Walvis Bay. All relevant details of the sediment sampling operation are summarized in the station list (Table 6).

5.1 Multicorer

The multicorer is designed to recover undisturbed surface sediment sections together with the overlying bottom water. The device used during Cruise SO 86 was equipped with 4 small (6 cm diameter) and 10 large (8 cm diameter), 60 cm long plastic tubes. At most stations all tubes successfully retrieved the uppermost 22 to 45 cm of sediment covered with bottom water. In general, the following sampling scheme was applied:

- 3 large tubes for the investigations of planktic and benthic foraminiferal assemblages were cut into 1 cm slices;
- 1 large tube for organic carbon geochemistry was also cut into 1 cm slices and frozen;
- 0 - 2 cm of surface sediment from 2 large tubes was sampled for the investigation of radiolarian assemblages;
- 0 - 3 cm of surface sediment from 1 small and 2 large tubes was sampled to supplement the Atlantic surface water reference data set based on planktic foraminiferal transfer functions (Pflaumann, Kiel);
- 2 small tubes were stored for investigations of magnetic bacteria;
- 1 small and 2 large tubes were frozen as archive cores;
- 2 bottom water samples (250 and 100 ml) for analyses of stable oxygen and carbon isotopes were stored in glass bottles.

Table 6 List of Sampling Stations, SONNE Cruise 86

GeoB No.	Date 1993	Coring Device	Bottom Contact (UTC)	Latitude	Longitude	Water Depth (m)	Core Recovery (cm)	Remarks
NORTHERN CONGO FAN								
2301-1	12.05.	MC	05:25	5°04,0'S	11°06,7'E	1377	38	homogeneous mud, olive-green, 4 small / 7 large tubes
2301-2	12.05.	SL12	06:27	5°04,0'S	11°06,7'E	1379	-	surface sediment in weight
2301-3	12.05.	SL18	10:47	5°04,0'S	11°06,7'E	1378	1532	
2302-1	12.05.	MC	14:00	5°06,4'S	10°05,5'E	1830	37	homogeneous mud, olive-green, H ₂ S, bioturbated, 4 small / 9 large tubes
2302-2	12.05.	SL18	14:24	5°06,4'S	10°50,9'E	1830	1418	277 to 301cm disturbed during sampling, CC: homogeneous mud, olive-green, H ₂ S
2303-1	12.05.	MC	19:53	5°11,5'S	10°22,0'E	2491	45	homogeneous mud, olive-green, 3 small / 10 large tubes
2303-2	12.05	SL18	21:35	5°11,4'S	10°22,0'E	2494	1736	CC: homogeneous mud, olive-green, H ₂ S, 0 - 15 cm missing
ANGOLA DIAPIR FIELD 12°S								
2304-1	18.05.	MC	23:13	12°01,3'S	12°27,0'E	1998	35	homogeneous mud, dark olive-green, hard, H ₂ S, ~ 5 cm oxidated layer, 4 small / 9 large tubes
2304-2	19.05.	SL12	00:43	12°01,2'S	12°27,1'E	2003	554	CC: homogeneous mud, olive-green, hard, H ₂ S
2305-1	19.05.	MC	06:16	11°56,1'S	13°15,1'E	897	26	homogeneous mud, olive-green, 4 small / 10 large tubes
2305-2	19.05.	SL12	07:02	11°56,1'S	13°15,1'E	897	495	CC: homogeneous mud, olive-green
2306-1	19.05.	MC	09:01	11°55,3'S	13°23,0'E	476	28	homogeneous mud, olive-green, foraminifers, 4 small / 10 large tubes
2306-2	19.05.	SL12	09:51	11°55,3'S	13°23,0'E	479	358	CC: homogeneous mud, olive-green, hard, H ₂ S

Table 6 continued

GeoB No.	Date 1993	Coring Device	Bottom Contact (UTC)	Latitude	Longitude	Water Depth (m)	Core Recovery (cm)	Remarks
ANGOLA BENGUELA FRONT								
2307-1	21.05.	MC	15:40	14°13,8'S	11°31,1'E	2888	33	homogeneous mud, grey-green, brown oxidated layer, 4 small / 10 large tubes
2307-2	21.05.	SL12	17:30	14°13,9'S	11°31,1'E	2892	724	CC: homogeneous mud, grey-green hard, foraminifers rare
2308-1	24.05.	MC	07:19	16°43,6'S	11°02,3'E	2121	24	homogeneous mud, olive-green, foraminifers, fluffy-layer, 4 small / 10 large tubes
2308-2	24.05.	SL12	08:44	16°43,7 S	11°02,3'E	2114	1133	CC: homogeneous mud, olive-green, H ₂ S, foraminifers
2309-1	24.05.	MC	12:29	16°34,7'S	10°50,6'E	2672	29	homogeneous mud, olive-green, foraminifers, green fluffy-layer, 4 small / 10 large tubes
2309-2	24.05.	SL18	14:14	16°34,7'S	10°50,5'E	2675	878	CC: homogeneous mud, olive-green, H ₂ S
CAPE BASIN								
2310-1	27.05.	MC	03:22	22°15,9'S	12°32,4'E	1019	22	carbonate-rich mud, olive-green, foraminifers abundant, 4 small / 10 large tubes
2310-2	27.05.	SL18	04:17	22°16,0'S	12°32,3'E	1024	686	CC: homogeneous mud, olive-green, H ₂ S, foraminifers
Coring Device:		MC		Multicorer (10 tubes)				
		SL 12		Gravity Corer (Schwerelot), 12 m				
		SL 18		Gravity Corer (Schwerelot), 18 m				

5.2 Gravity Corer

With the gravity corer between 4 and 18 m long late Quaternary sediment sequences have been retrieved at 10 stations (Table 6). Immediately after recovery, the cores were sawed into sections of about 1 m length and stored in the laboratory to equilibrate to ambient temperature. Subsequent to the shipboard whole-core geophysical measurements (Chapter 5.4), the core sections were cut lengthwise into an archive and a working half. The sediments were described from the archive half (Figs. 35 to 44) which was then frozen and stored at -15 °C. The working half was stored in the cooling room at 4 °C after the electrical conductivity had been measured at 2 cm depth intervals.

With the exception of core GeoB 2307-2, the cores will be subsampled in Bremen for measurements and analyses of physical properties, stable isotopes, faunal assemblages and organic geochemistry. Core GeoB 2307-2 recovered near the present northern boundary of the Angola Benguela Front (ABF) at 14°14'S was extensively sampled on board. Two parallel series of syringe samples (10 ccm) were taken from the working half at intervals of 5 cm. This procedure will allow to start the planned shore based work on the ABF variability immediately after the cruise. The core was also sampled for a detailed paleomagnetic study.

5.3 Sediment Pattern

According to the visual inspection and core descriptions the sediments recovered with the multicorer and the gravity corer are probably all of late Quaternary age. They were buried under anoxic conditions as indicated by a strong H₂S odor emitted by all cores during opening. The sediments can be subdivided into five groups related to the specific oceanic environments which prevailed in the different working areas.

Congo Fan

In the northern part of the Congo Fan, where the longest cores of this cruise were obtained (Table 6), the sediments consist of homogeneous, dark olive-green, hemipelagic muds throughout the cores. The dark color hints to high organic carbon concentrations, while the carbonate content is presumably low. Only small numbers of foraminifers could be detected visually. The muds are very soft down to 10 - 12 meters and are characterized by large burrows which sometimes are open or filled with very soft sediments containing large amounts of water. Open burrows have been observed down to about 6 m core depth.

These muds are typical for the deposits in the upper part of the Congo Fan and have also been described from the area south of the Congo Canyon (JANSEN et al., 1984; SCHNEIDER, 1991). They reflect the high concentration of fine terrigenous

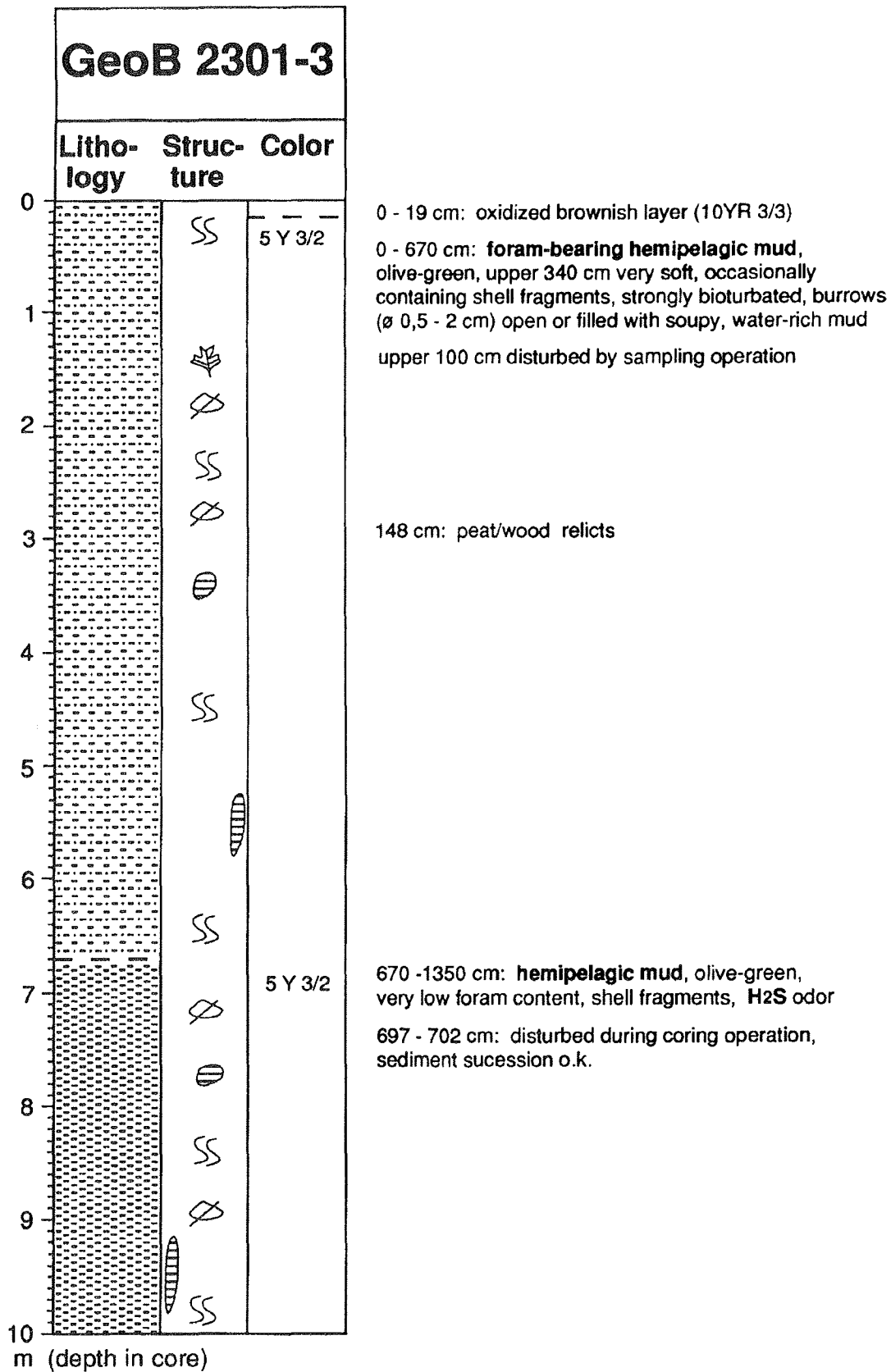
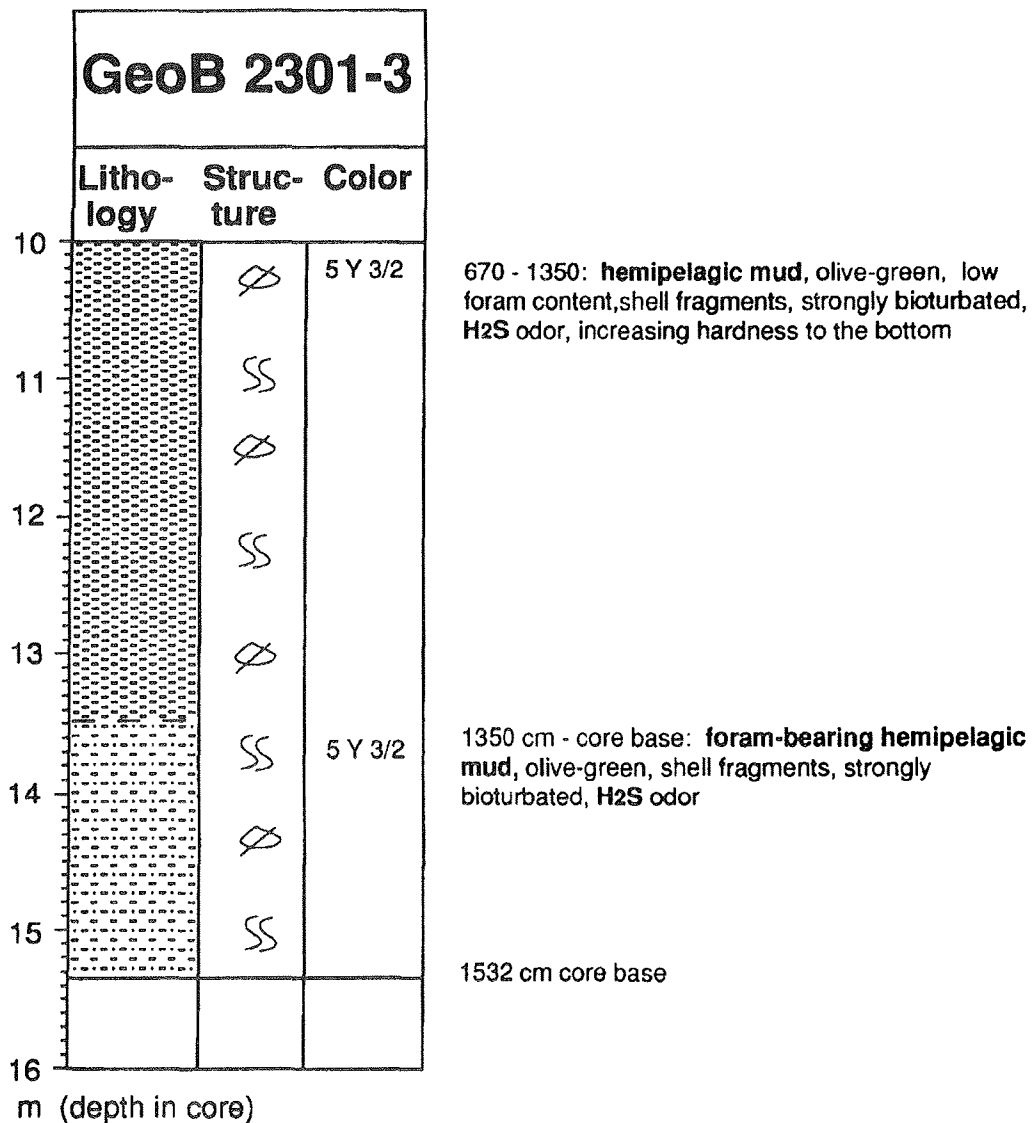
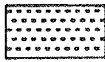
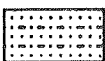


Figure 35 Gravity core GeoB 2301-3 (northern Congo Fan area): Core description.



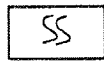
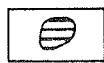
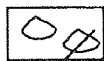
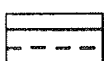
Summary of symbols used in the graphic core descriptions

Lithology

-  hemipelagic mud, very low foraminifera content *
-  foram-bearing hemipelagic mud
-  foram-rich hemipelagic mud
-  silt/sand layer
-  foram-rich calcareous ooze

* foram content estimated by eye

Structure

-  bioturbation
-  burrows** open or filled with water-rich sediment
-  mollusk shells, intact or broken
-  plant debris
-  lithologic boundary, sharp or bioturbated

**origin of burrows sometimes not clear: gas cracks or bioturbation ?

Figure 35 continued.

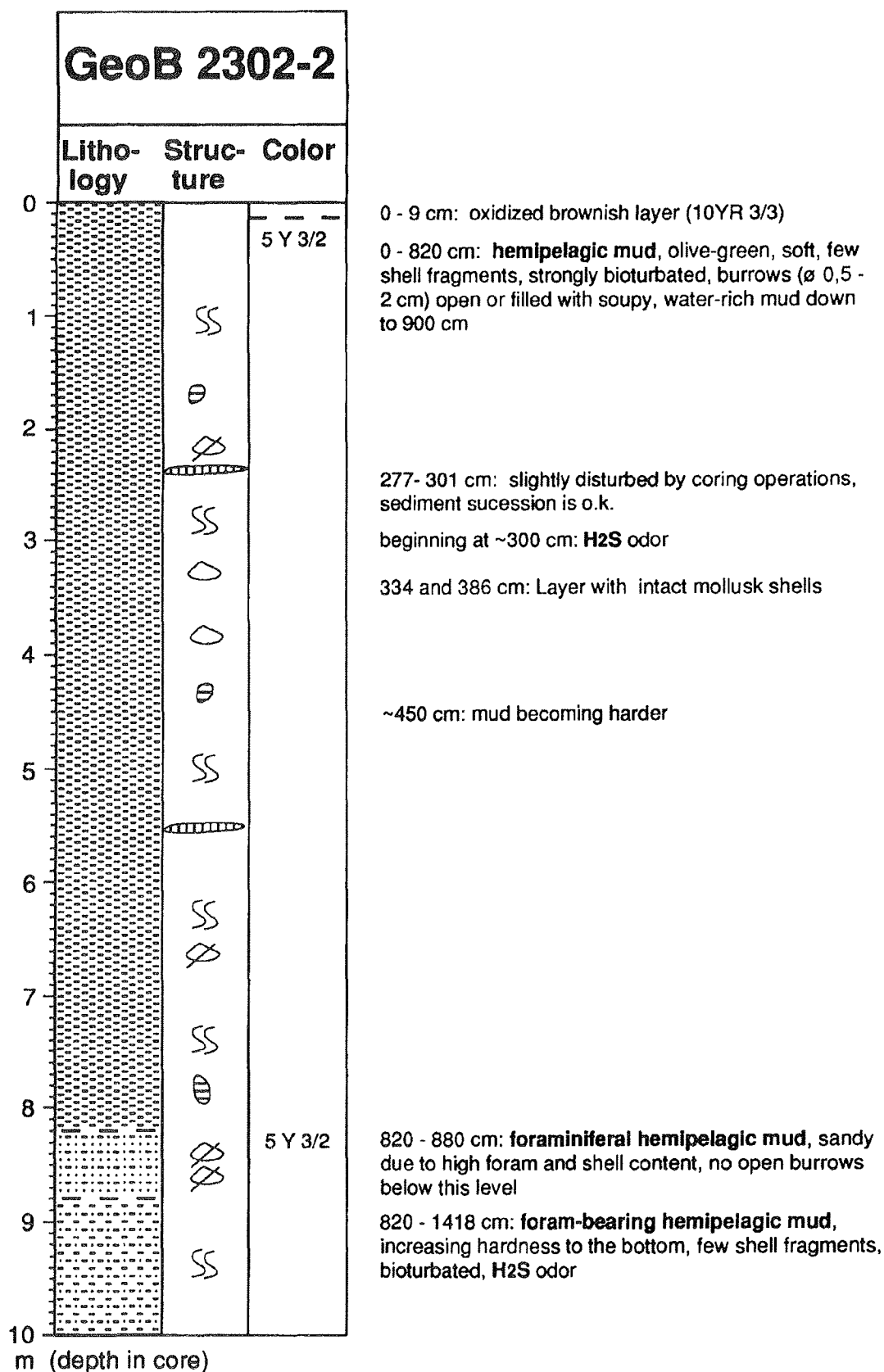


Figure 36 Gravity core GeoB 2302-2 (northern Congo Fan area): Core description.

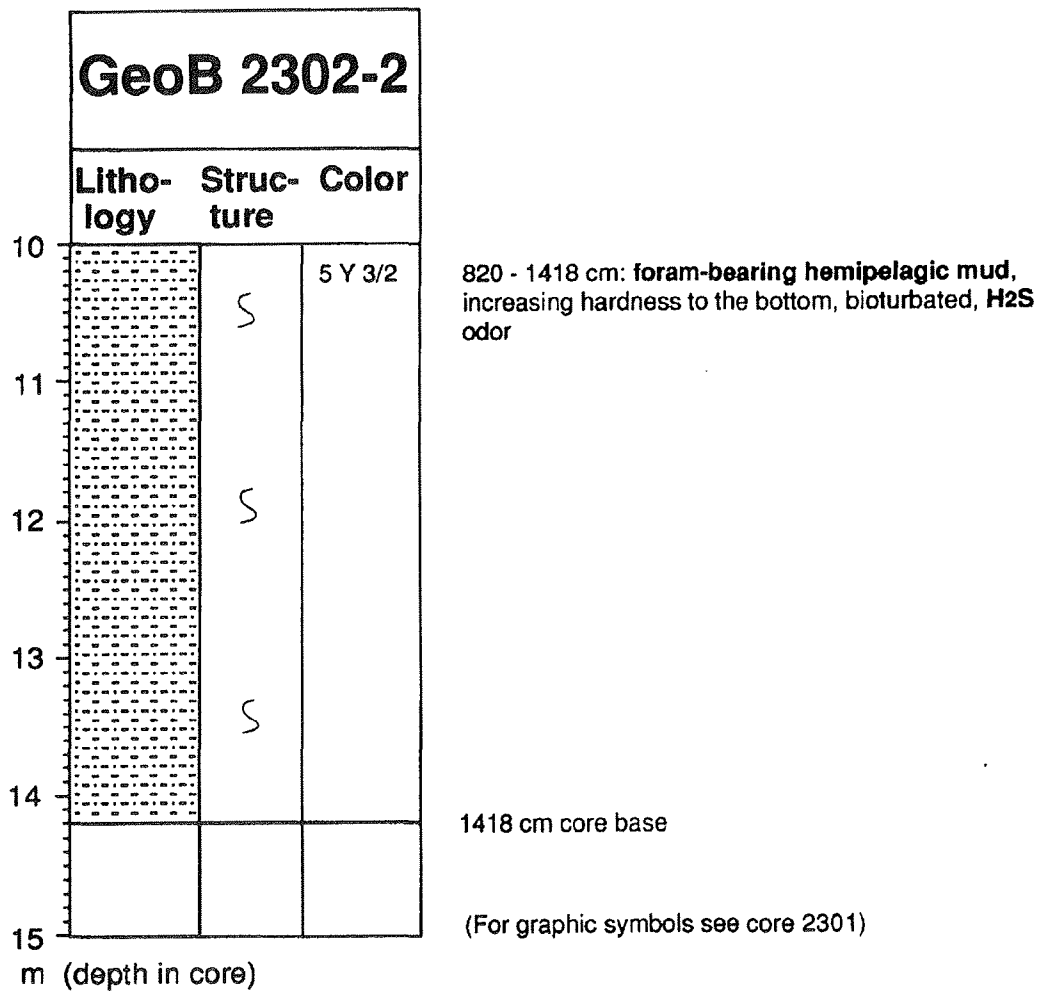


Figure 36 continued.

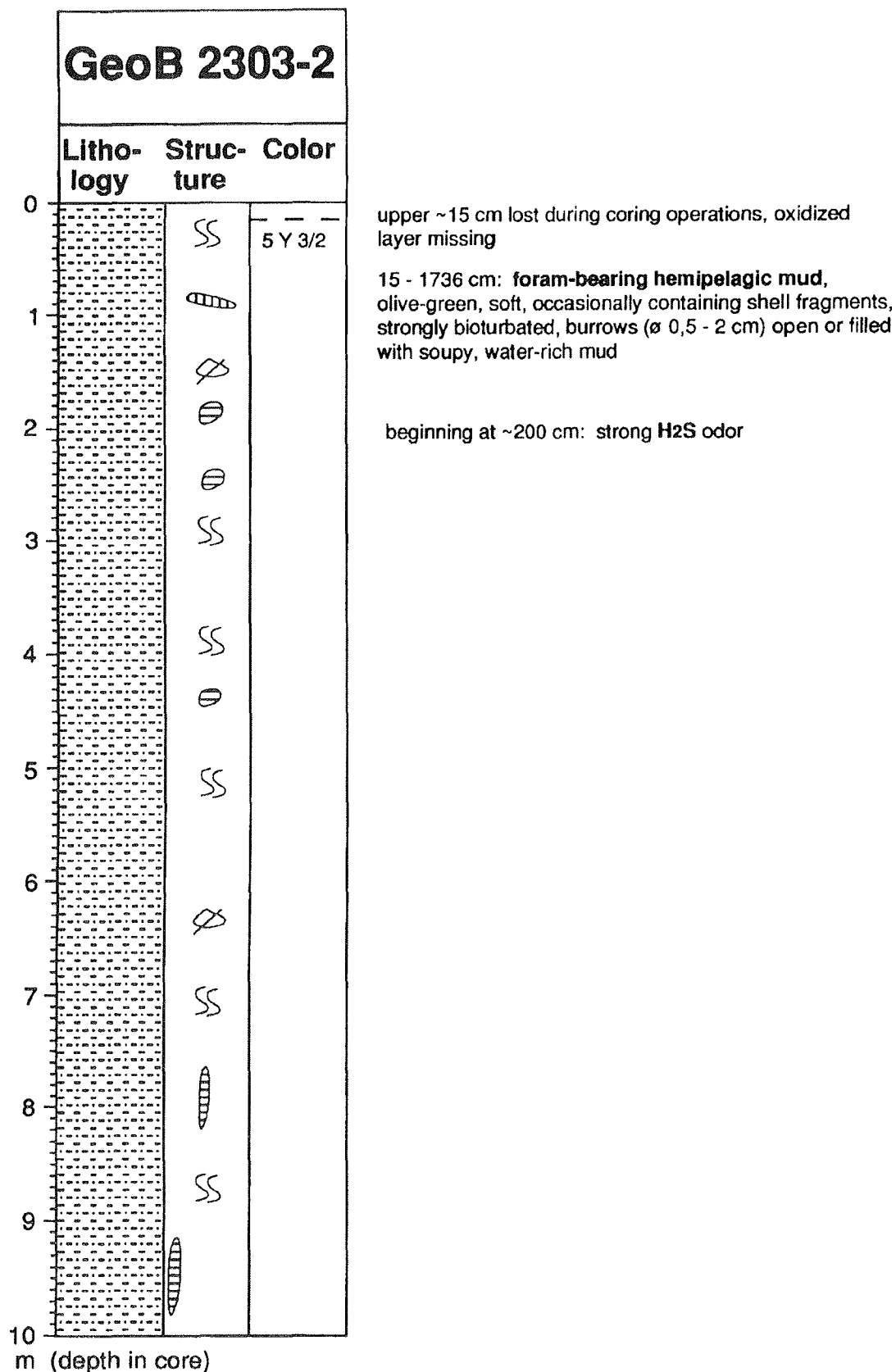


Figure 37 Gravity core GeoB 2303-2 (northern Congo Fan area): Core description.

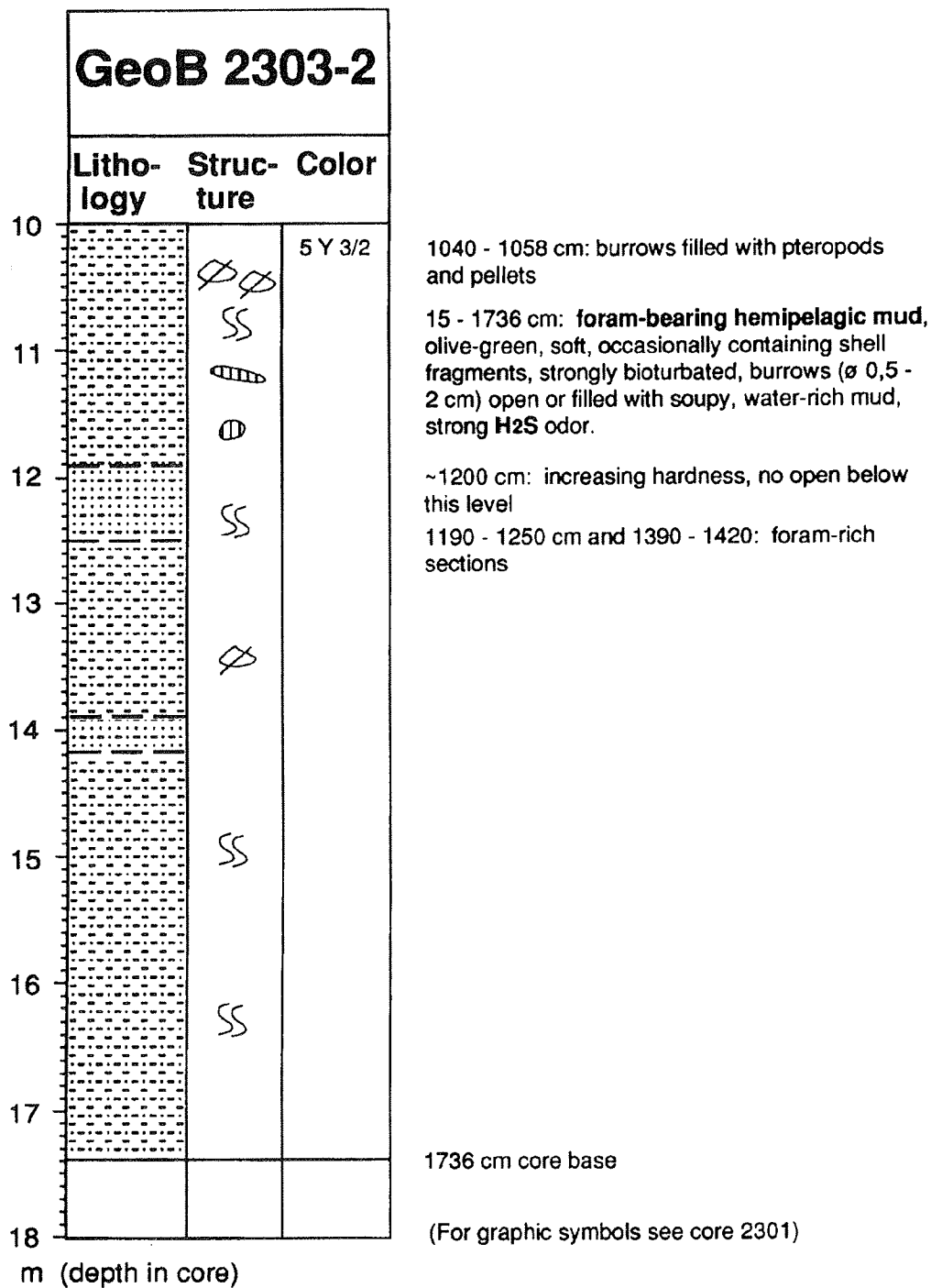


Figure 37 continued.

material originating from fluvial input of the Congo River. High organic carbon contents are derived from the combination of terrigenous plant detritus and an intense marine productivity. The latter results from a river-induced upwelling and nutrient supply, as well as a local coastal upwelling.

Angola Diapir Field

The three cores taken along a profile at 12°S also consist of hemipelagic muds, but the sediments are not as soft those found off Congo. The numbers of foraminifers seem to be in the same range as in the Congo Fan deposits. From the dark olive-green color and the H₂S smell it can be assumed that the sediments also contain high amounts of organic carbon, although the existence of coastal upwelling during the last 200,000 years off central Angola is highly improbable. The origin of the organic carbon is rather related to high fertility in the surface waters induced by the doming of nutrient-rich subsurface waters with the eastern Angola Basin Gyre (SCHNEIDER, 1991).

Angola Benguela Front

Core GeoB 2307-2 was taken at 14°14'S to study late Quaternary northward shifts of the Benguela Coastal Current (BBC) cold-water boundary. In the modern ocean this boundary, the Angola Benguela Front, fluctuates seasonally between 14 and 16°S. The sediments recovered at this location were dark-gray to greenish-gray hemipelagic muds. A 5 cm thick brownish horizon at the top of the multicorer indicates well oxygenated bottom water and surface sediment conditions. The older sediment column in the gravity core exhibits prominent cycles, starting at the core top with a light greenish-gray sediment sequence which changes to a dark gray and back to a light section again, repeating this pattern to about 5 m depth in the core. As the lighter sections are characterized by higher numbers of foraminifers than the dark intervals, it can be assumed that these light - dark cycles represent the change from sediments relatively rich in carbonate and poor in organic carbon during interglacials to the opposite sediment composition within glacial periods. This pattern can be explained by the back and forth of the front driven by alternating warm and cold climatic periods. During warm stages the ABF was presumably located more to the south restricting the influence of cold and nutrient-rich waters associated with the BBC at the sampling location. As a consequence, high productivity and organic carbon flux was reduced in the interglacials and carbonate dissolution was not as high as during glacials. Below 5 m core depth this light - dark sequence is disturbed by the occurrence of intercalated layers of muds which can be differentiated by their color change from black to light gray or greenish-blue. Also little sand lenses were observed in this deepest sediment section. It is not bioturbated and lacks the high amounts of foraminifers recognized in the upper part of the core. Thus we assume that the core GeoB 2307-2 contains a turbiditic sequence originating from mudflows below 5 m core depth.

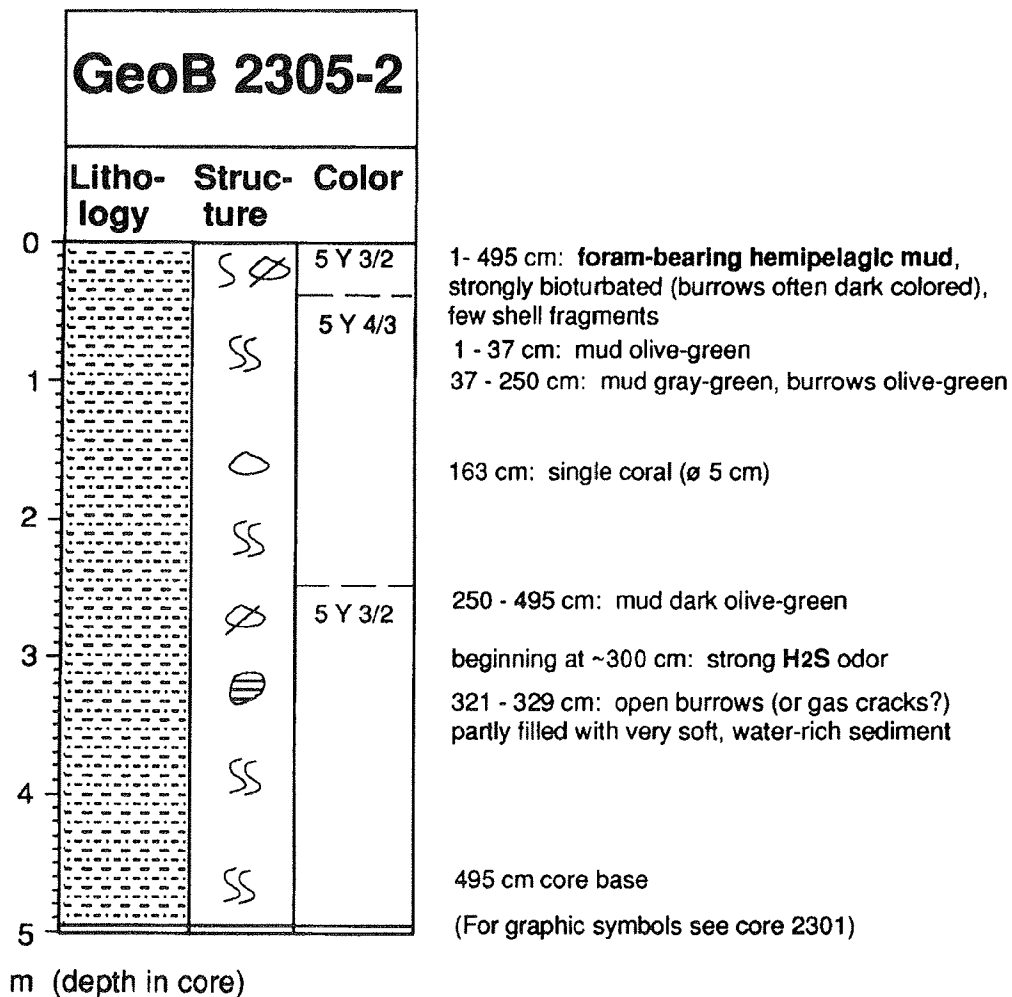


Figure 39 Gravity core GeoB 2305-2 (Angola Diapir Field area): Core description.

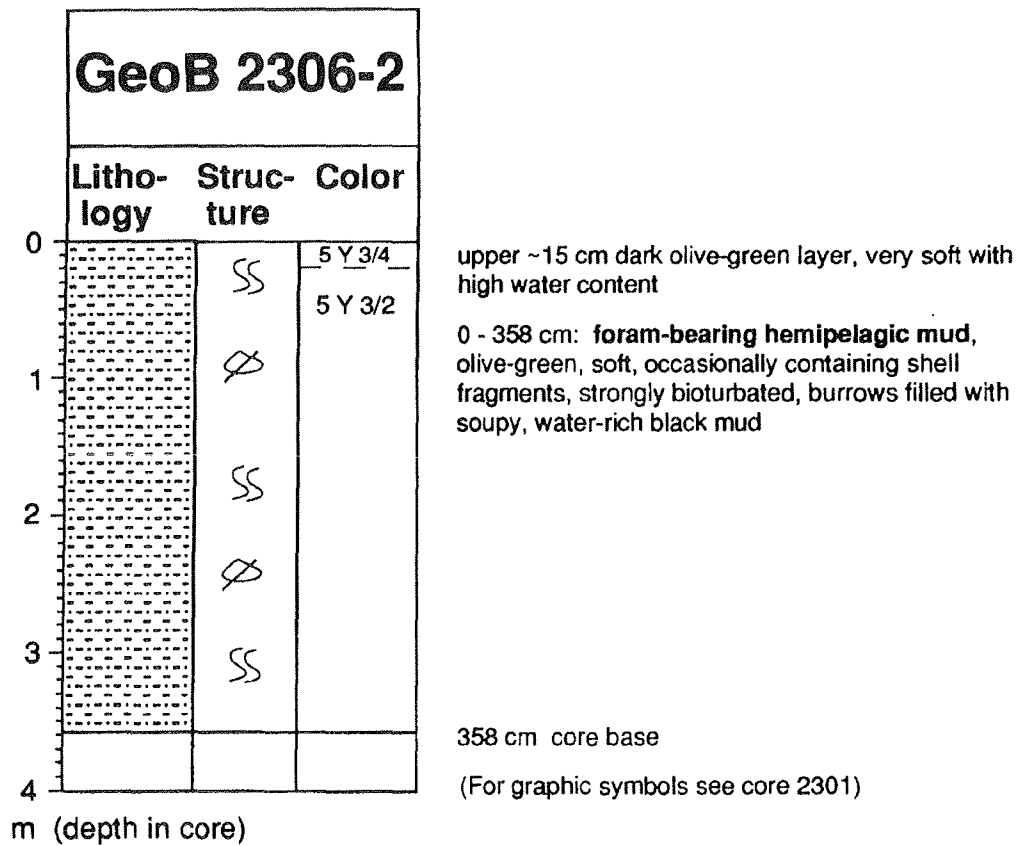


Figure 40 Gravity core GeoB 2306-2 (Angola Diapir Field area): Core description.

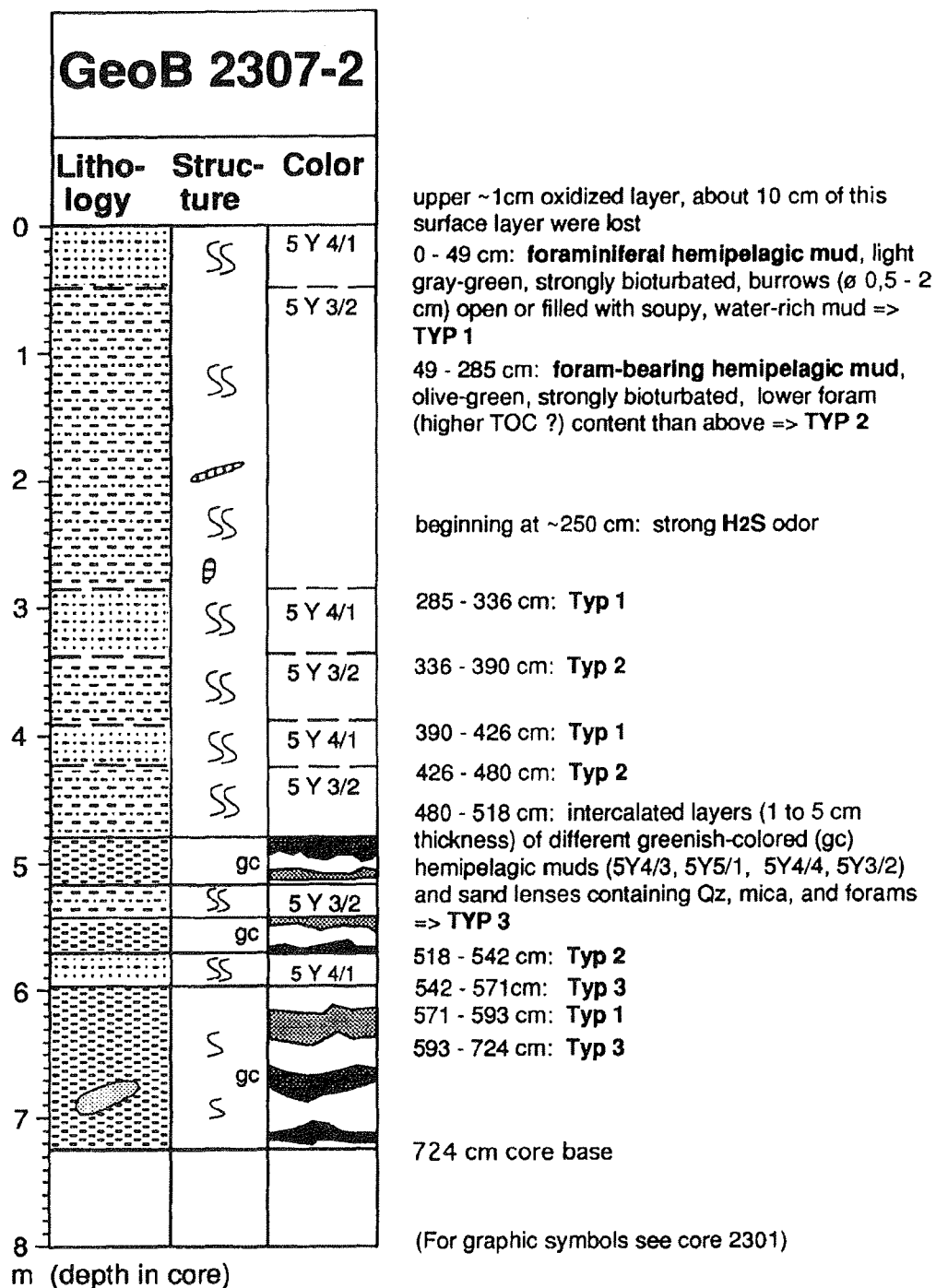


Figure 41 Gravity core GeoB 2307-2 (Angola Benguela Front area): Core description.

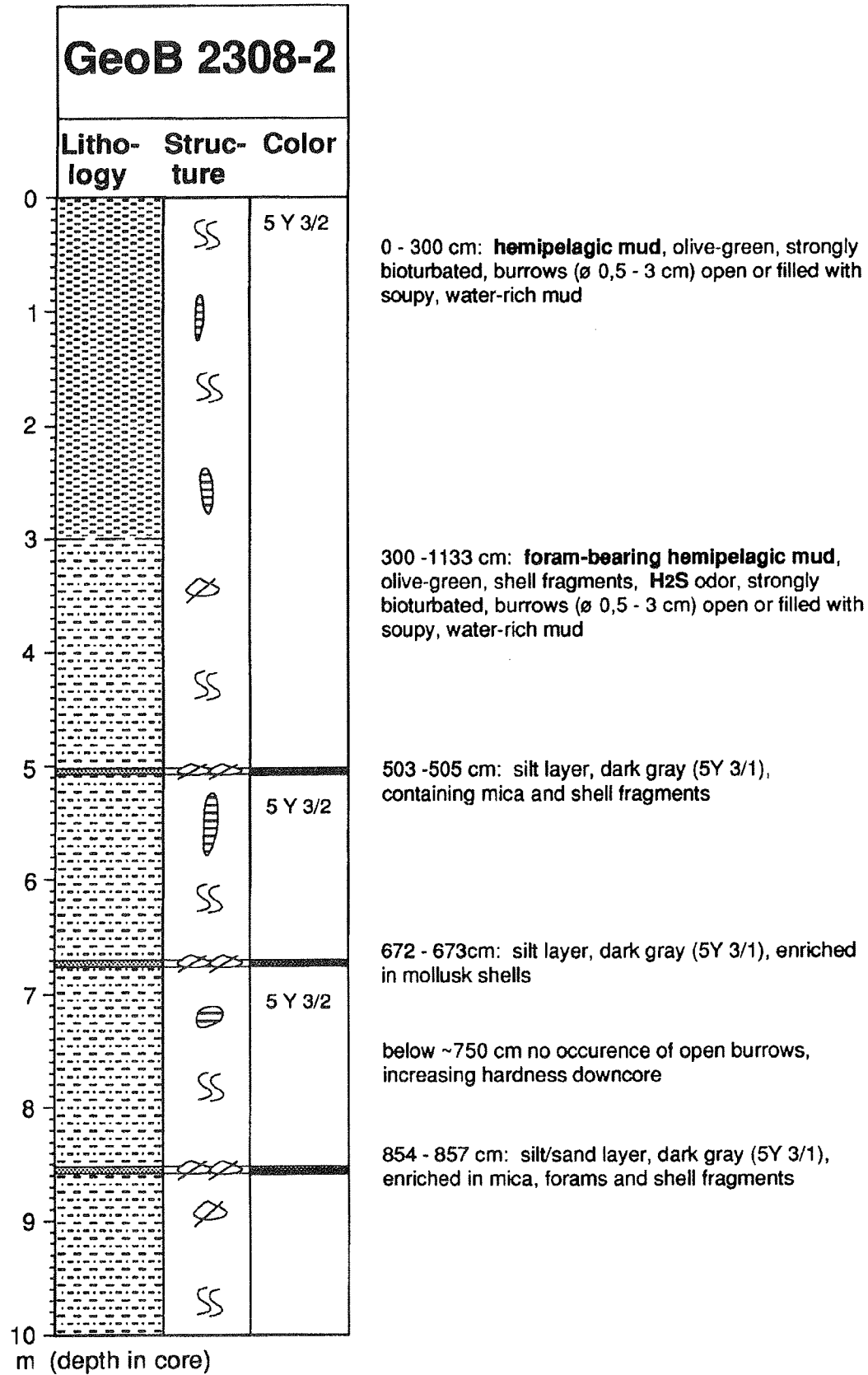


Figure 42 Gravity core GeoB 2308-2 (Angola Benguela Front area): Core description.

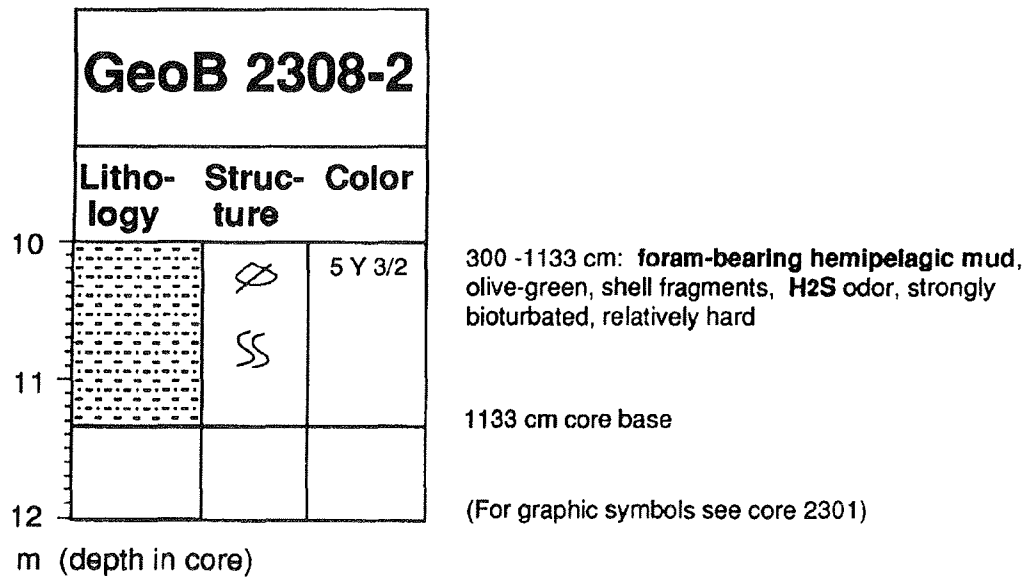


Figure 42 continued.

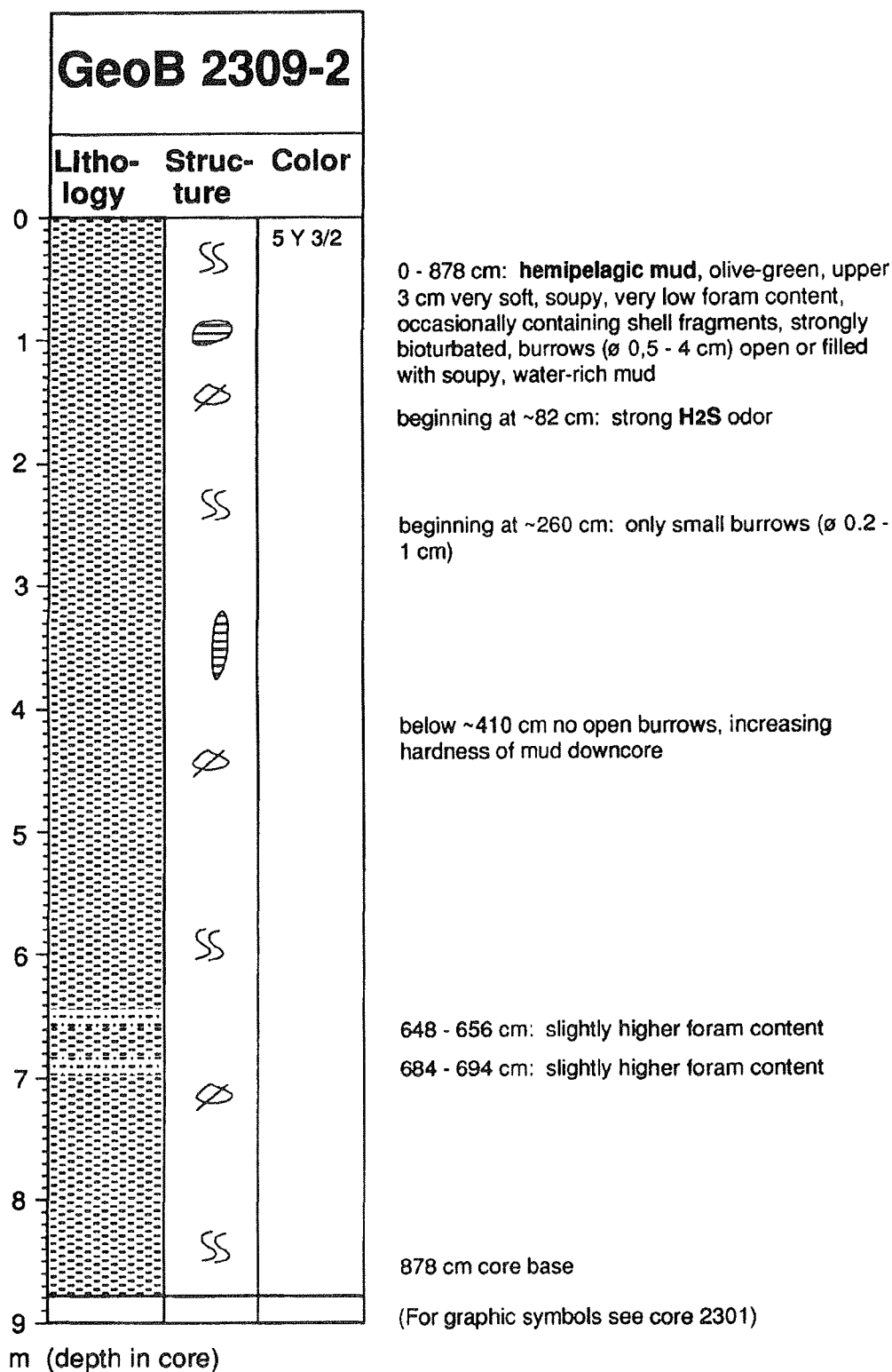


Figure 43 Gravity core GeoB 2309-2 (Angola Benguela Front area): Core description.

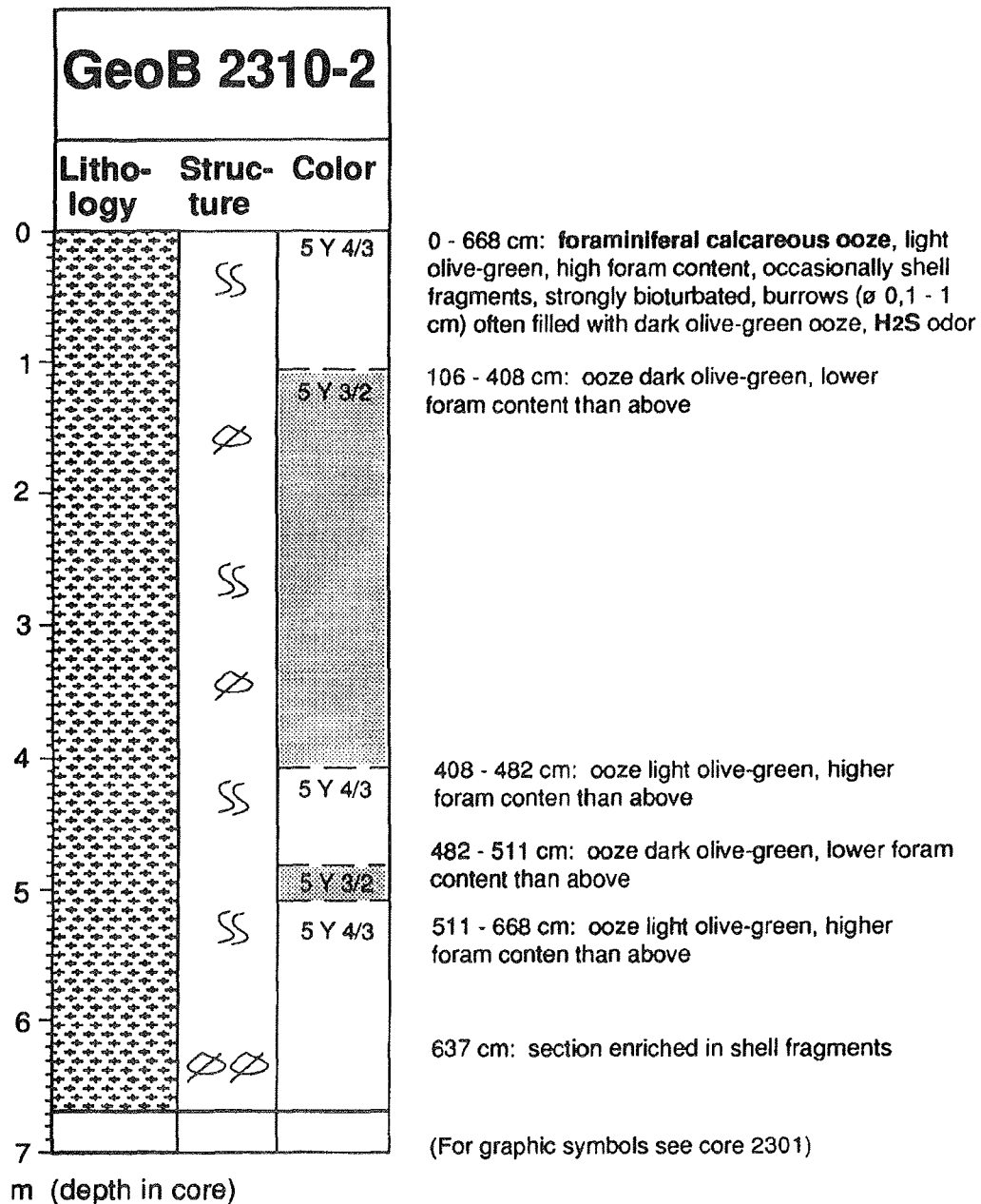


Figure 44 Gravity core GeoB 2310-2 (northeastern Cape Basin): Core description.

Homogeneous, olive-green, hemipelagic muds were found off southern Angola at 16.7°S. These deposits are in general comparable with those found north of the Congo River mouth. They contain a little higher amounts of sand, however, which originate from an eolian input coming from the Namibian desert and/or from a fluvial input by the Cunene River which enters the Angola Basin at about 17°S. The source for the high organic carbon contents (dark color, anoxic conditions throughout the core) should have been the Southwest African coastal upwelling cell during the whole Late Quaternary which at present is confined between 15 and 17°S.

Cape Basin

The last core of this cruise was taken in the northeastern Cape Basin. The upper slope sediments at this station, which under modern surface water conditions lies at the western boundary of the upwelling cell located above the shelf, consist of carbonate-rich muds with high amounts of foraminifers. Their olive-green color and the H₂S odor point to high organic carbon concentrations. The terrigenous input appears to be lower than in the Angola Basin presumably because the winds and eolian transport are predominantly directed alongshore towards the north and also no larger river system reaches the northern Cape Basin coast. The high carbonate content may be explained by a weaker carbonate dissolution in the Cape Basin as compared to the semi-closed Angola Basin and also a lower dilution by terrigenous components.

5.4 Physical Properties Studies

M. Breitzke, K. Däumler, H. Keil, B. Pioch, F. Pototzki, T. Schwenk

5.4.1 Introduction

Ten gravity cores with a total length of 95 m were retrieved during the Cruise SO 86 and investigated with respect to their physical properties, comprising measurements of P-wave velocity, wet bulk density and magnetic susceptibility. P-wave velocities and magnetic susceptibilities were determined from the unsplit cores, wet bulk densities from the split core halves.

5.4.2 Physical Background and Experimental Techniques

P-wave velocity

P-wave velocities were measured with an automated full wave form logging system (BREITZKE & SPIEB, 1993). Figure 45 shows a diagram of the system configuration. It mainly consists of three units,

- i) a signal generation and recording unit, including two equivalent ultrasonic transducers, a broad-banded high-voltage pulse generator, an analogue amplifier and a programmable, digital 8-bit storage oscilloscope;
- ii) an automated transducer movement and distance/diameter measurement unit, including a stepping motor, two digital measuring tools and a multiplexer;
- iii) a PC based data storage and system control unit, including a PC with different interface cards, floppy, 100 MByte hard disc and a printer.

The unsplit (or split) cores are analysed by transmission seismograms travelling radially through the sediment cores. Signal emission and reception is performed by a pair of equivalent, diametrically arranged wheel probes of 374 kHz dominant frequency (C.N.S. ELECTRONICS LTD.) which are mounted in a carriage. A spring-loaded jig presses them onto the core liner. A sufficient coupling is achieved by plastic tires surrounding the wheel probes. After analogue amplification the received transmission seismograms are digitized, recorded and stored by means of an oscilloscope (NICOLET 320) and transferred to the PC's hard disc. Recording parameters, e. g., sample rate, recording length and delay as well as data transfer to the PC's hard disc are controlled via a HPIB interface.

The wheel probe carriage is automatically moved along the core liner by a stepping motor. It stops at arbitrary, equidistant spacings to record a quasi-continuous section of transmission seismograms along the core segment. Stepping rate, acceleration and deceleration are controlled by a special PC interface (PCL 738B). Axial travel distance and core diameter are determined by digital measuring tools (MITUTOYO Digimatic Scale Unit 572) with an accuracy of 0.01 mm. The data are transferred to the recording and control program via two channels of a multiplexer (MITUTOYO MUX 10) and a serial interface.

The logging process, data transfer and data storage are controlled by an IBM compatible PC (HEWLETT PACKARD VECTRA QS/16S, 80386SX processor). The physical, geometrical and recording parameters of each core segment can be set individually in a menu driven FORTRAN control program. After assigning these parameters to a seismogram header, the transmission data are stored on the PC's hard disc using the DOS Real*4 format and - similar to the industry standard SEG-Y-header - an 800 Byte header per trace.

P-wave velocities are evaluated from the first arrivals of the transmission seismograms and the core diameter by an on-line routine. It is based on a cross-correlation of the transmission seismogram with the 'zero-offset' signal, i. e. the signal which is recorded before the logging process by bringing both wheel probes into close contact. Only a short wavelet of this 'zero-offset' signal with one or two periods duration is used for the cross- correlation so that the instant of the first arrival can

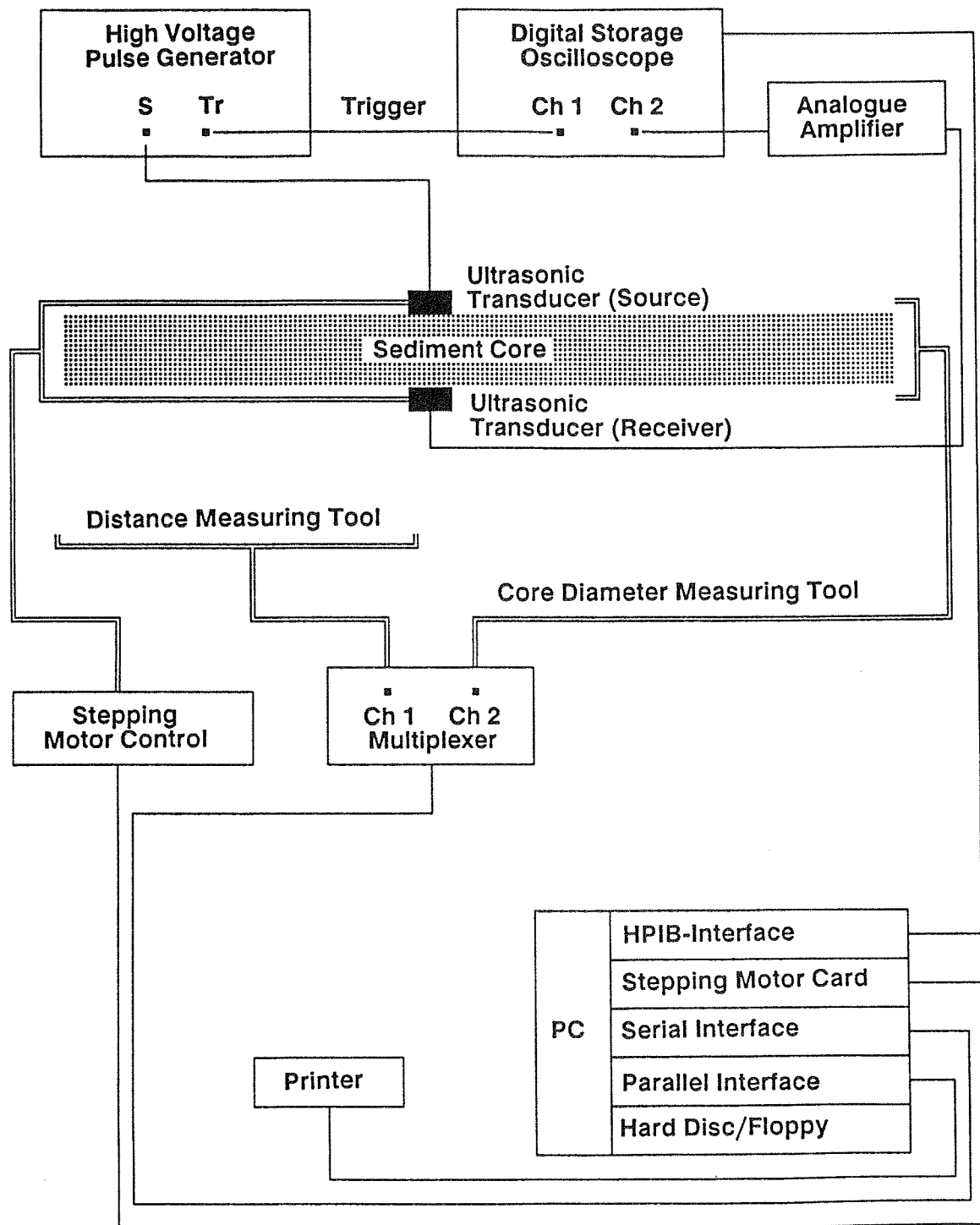


Figure 45 Block diagram of the P-wave logging system.

accurately be assigned to the first significant peak of the cross-correlogram resulting from the first maximum coherence between both signals. Numerically, this maximum is determined as the first positive excursion whose amplitude exceeds a given percentage amplitude threshold. In practice threshold values of 10 to 15% of the cross-correlogram's maximum proved to be suitable for a stable first arrival detection. Since the cross-correlogram only depends on the phase difference between the transmission seismogram and the 'zero-offset' wavelet, it is independent of the internal pulse delay within the wheel probes and only a correction for the travel times through the liner walls must be taken into account. Explicitly, if t is the picked first arrival time, t_L the pulse travel time across both liner walls, d the outside diameter of the core liner and d_L the double liner wall thickness, the P-wave velocity can be calculated from

$$v_P = (d - d_L) / (t - t_L)$$

P-wave velocity measurements on board are usually carried out only after the core segments have reached ambient temperature. Due to varying weather conditions temperature differences of up to 10 °C may occur from one core (segment) to another resulting in P-wave velocity variations of up to 30 m/s. To enable a precise comparison between the P-wave velocity profiles of different cores (or core segments), the sediment temperature is determined once per core segment with an accuracy of 0.1 °C and a correction of all laboratory P-wave velocities values to a constant temperature of 20 °C is applied using the approximation of SCHULTHEISS & McPHAIL (1989)

$$v_{20} = v_T + 3 \cdot (20 - T)$$

where v_{20} is the P-wave velocity at 20 °C (in m/s), v_T the P-wave velocity at T °C (in m/s), and T the temperature (in °C) of the core segment when logged.

Wet-bulk density

Wet bulk densities were derived from electrical resistivity measurements on the split halves of the sediment cores. Figure 46 shows a block diagram of the system. A probe comprising a miniature WENNER configuration is manually inserted into the sediment perpendicular to the core axis so that the integrating effect of the electrical field mainly acts in an about constant core depth. Four platinum wires (\varnothing 0.6 mm) which are cast into the solid plastic body of the probe with a spacing of 4 mm serve as electrodes. An NTC (SIEMENS, K29) is additionally integrated into the probe. It allows a fast determination of the sediment temperature with an accuracy of 0.1 °C while the resistivity is measured. Including this temperature sensor, the total dimensions of the probe are 22.3 x 4 x 135 mm. To improve the coupling to the sediment, the lower part of the probe is shaped to a triangular cross-section. A waveform generator and a current drive supply a constant, low-frequency alternating square wave current of 330 Hz and 400 μ A. The potential difference depending on the sediment's resistivity is determined across the inner pair of electrodes by means of a voltmeter after passing a differential amplifier and a phase sensitive detector.

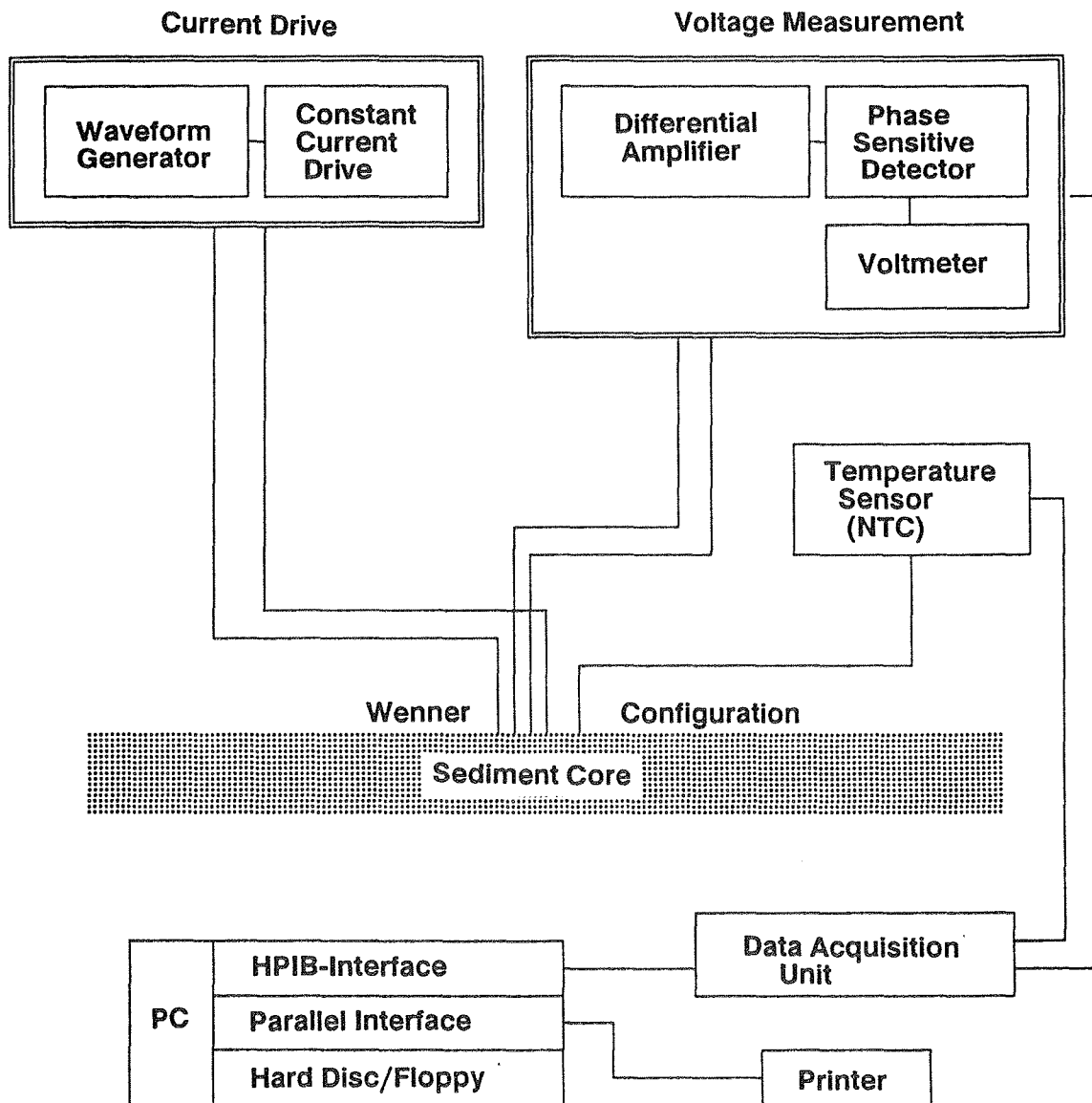


Figure 46 Block diagram of the electrical resistivity logging system.

The resistivity logging process is controlled and recorded by a menu driven FORTRAN program running on an IBM compatible, portable PC (ESCOM BLACKMATE NOTEBOOK, 386SX processor). Potential and temperature values are transferred to the PC's hard disc (40 MByte) via a data acquisition/control unit (HP 3421A) and a HPIB interface. An on-line routine converts the measured resistivity data to porosity and density. This conversion is based on ARCHIE's empirical equation

$$R_s/R_w = k \cdot \phi^{-m}$$

which relates the ratio of the sediment resistivity R_s and the interstitial water resistivity R_w to porosity ϕ . According to BOYCE (1968), appropriate values for the proportionality constant k and the power m are $k = 1.30$ and $m = 1.45$. The interstitial water resistivity R_w is derived from a calibration curve which describes the temperature - conductivity relation of sea water by the following fourth power law (SIEDLER & PETERS, 1986)

$$1/R_w = C_0 + C_1 \cdot T + C_2 \cdot T^2 + C_3 \cdot T^3 + C_4 \cdot T^4$$

The coefficients C_0 to C_4 depend on the geometry of the probe and are determined by a least-square approximation to the measured calibration values.

Assuming a two component model for the sediment with homogeneous sediment matrix and interstitial water densities ρ_m and ρ_w , the wet bulk density ρ_{wet} is computed using the porosity as weighting factor (BOYCE, 1976)

$$\rho_{wet} = (\phi \cdot \rho_w) + (1 - \phi) \cdot \rho_m$$

Values of $\rho_m = 1030 \text{ kg/m}^3$ and $\rho_w = 2670 \text{ kg/m}^3$ were used here for the interstitial water and the grain density.

Magnetic susceptibility

Magnetic susceptibilities were determined from the unsplit cores using a BARTINGTON magnetic susceptibility meter type MS2.C combined with a whole-core sensor.

5.4.3 Shipboard Results

P-wave velocities and wet bulk densities were determined at a spacing of 2 cm, magnetic susceptibilities at 1 cm intervals.

The transmission seismograms for the P-wave velocity determination were sampled at a rate of 20 MHz. The recording length was 200 μs , starting after a delay of 50 μs . A 'zero-offset' signal was measured before each gravity core. Cross-correlograms for the

first arrival detection were calculated with the first period (25 to 30 μ s) of this 'zero-offset' signal. The first peak of the cross-correlogram exceeding a threshold of 20% of the cross-correlogram's maximum was picked as the first arrival.

Electrical resistivities for the wet bulk density determination were measured at each depth point after waiting for 10 s to achieve stable potential differences.

The magnetic susceptibility measurements should provide a preliminary insight into the magnetic characteristics of the cores and were therefore done only with the low sensitivity option ($1.0 \cdot 10^{-6}$ SI).

Figures 47 to 56 show the three physical property logs for each gravity core. To facilitate a core to core comparison they are all plotted to the same depth scale. The P-wave velocity measurements occasionally suffered from coupling problems between the sediment and the liner wall, probably due to gas (H_2S) so that no transmission signal could be received for several depth intervals.

Congo Fan (GeoB 2301-03, 2302-02, 2303-02)

The P-wave velocity logs reveal only smooth variations of about 20 m/s per core. The mean values slightly increase with increasing water depth from 1493 m/s for the shallowest core GeoB 2301-03 to 1496 m/s for GeoB 2302-02 and to 1502 m/s for the deepest core GeoB 2303-02.

In contrast, the wet bulk density logs show a distinct increase from very low values (about 1100 kg/m^3) at the sea floor to values varying around 1400 kg/m^3 at greater depth. This density contrast is especially pronounced in gravity cores GeoB 2301-03 and 2302-02. A level of around 1400 kg/m^3 is reached at about 3.5 m depth in core GeoB 2301-03 coinciding with a density increase of the clayey mud visually identified in the core description. In gravity core GeoB 2302-02 the 1400 kg/m^3 level is already reached at about 2.0 m depth. In core GeoB 2303-02 the density values start at about 1200 kg/m^3 , slightly decrease to about 1100 kg/m^3 at 1.7 m depth and then increase to about 1400 kg/m^3 at around 5.2 m depth. The corresponding porosity values range from about 90 to 95% at the sea floor to about 75 to 80% at greater depths.

The magnetic susceptibility logs display a distinct decrease at about 4.2 m depth in core GeoB 2301-03 and at about 2.9 m depth in core GeoB 2302-02 which does not coincide with the pronounced variations in wet bulk density logs. For the deepest core, GeoB 2303-02, this decrease can still be identified at about 1.4 depth but it is much less obvious as the mean susceptibility only amounts to about $40 \cdot 10^{-6}$ SI compared to about $70 \cdot 10^{-6}$ and $60 \cdot 10^{-6}$ SI in cores GeoB 2301-03 and 2302-02, respectively.

GeoB 2301-03

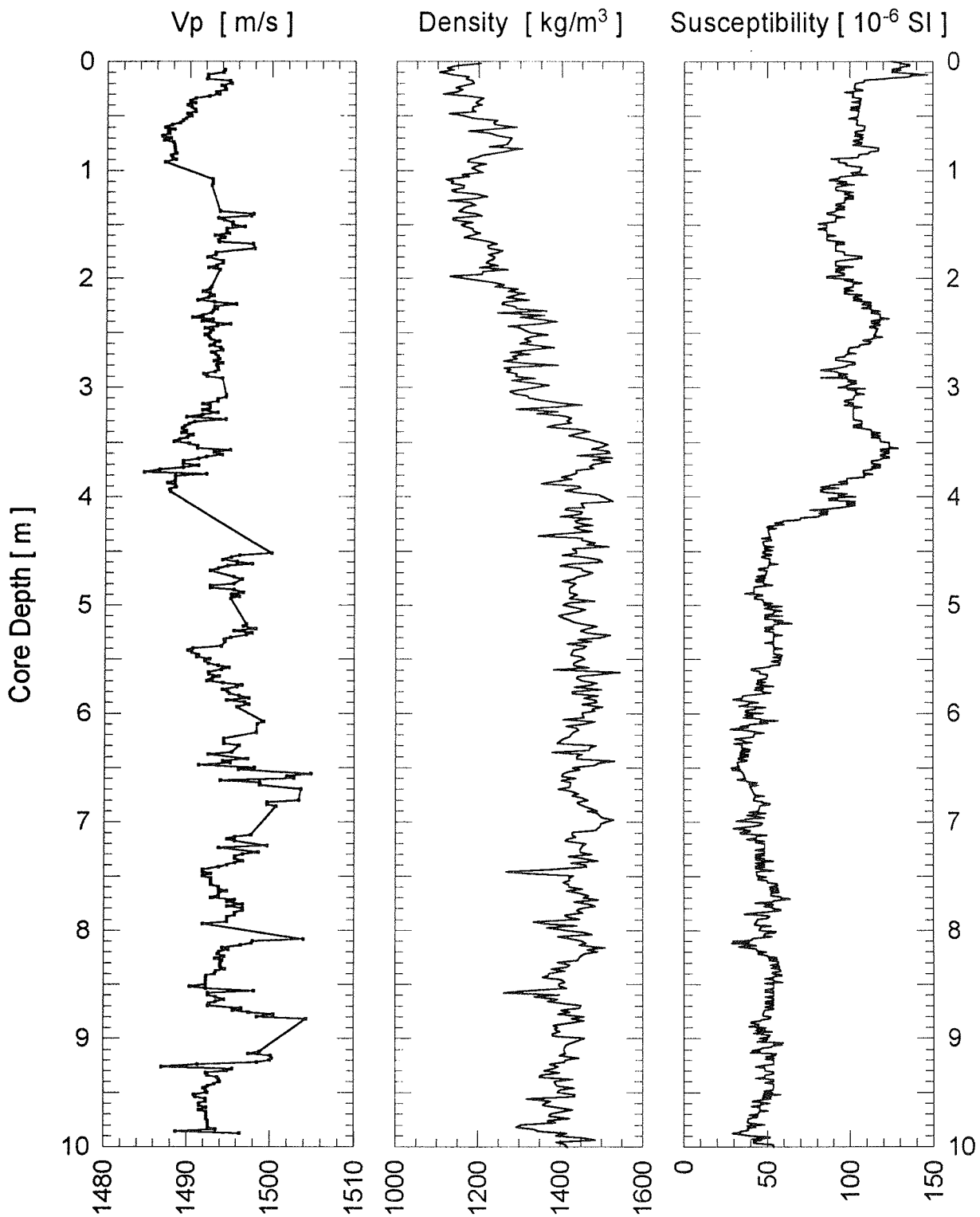
Date: 12.05.93 Pos: 05°04,0' S 11°06,7' E
Water Depth: 1378 m Core Length: 1532 cm

Figure 47 Gravity core GeoB 2301-3 (northern Cogo Fan area): Physical property logs.

GeoB 2301-03

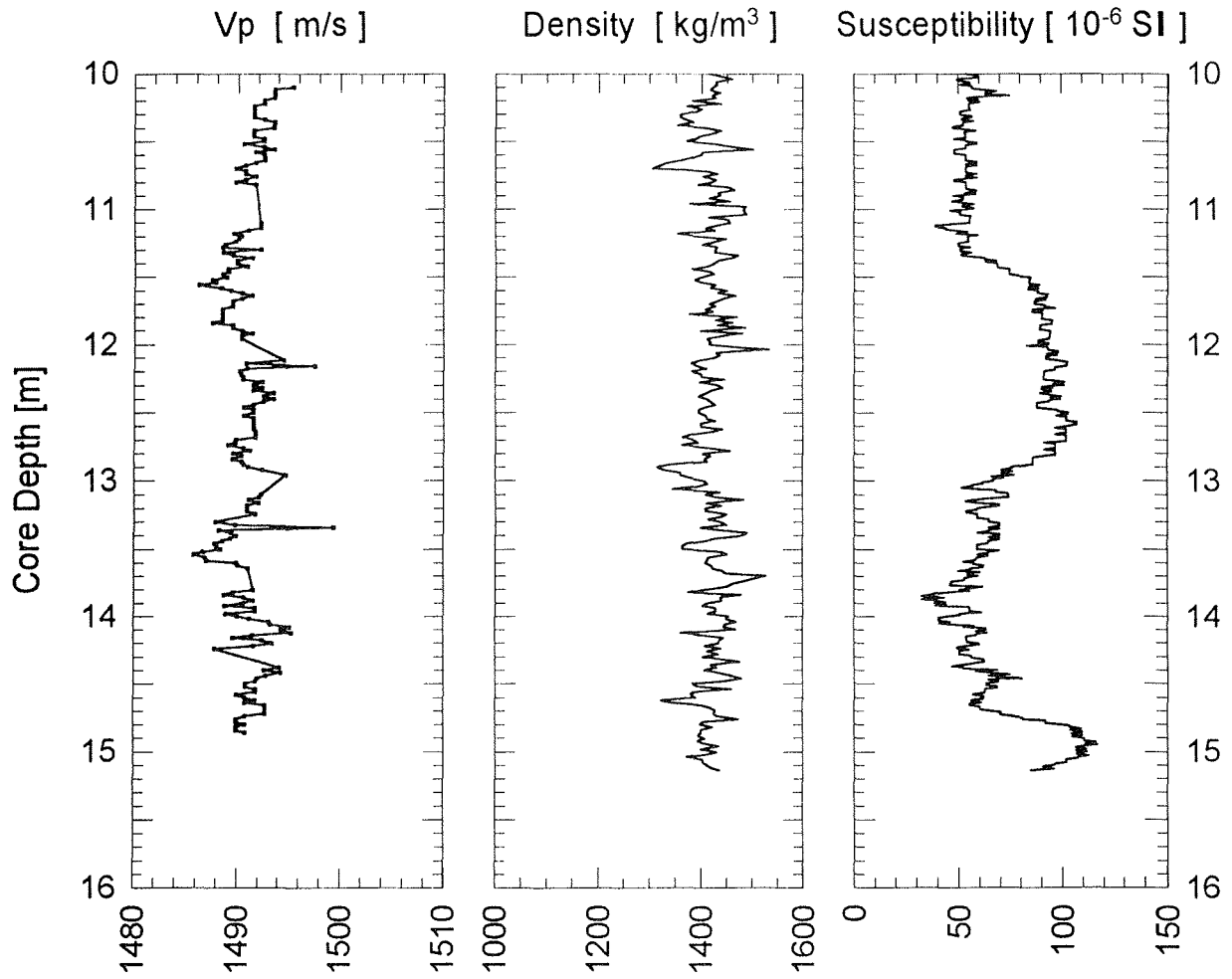
Date: 12.05.93 Pos: 05°04,0' S 11°06,7' E
Water Depth: 1378 m Core Length: 1532 cm

Figure 47 continued.

GeoB 2302-02

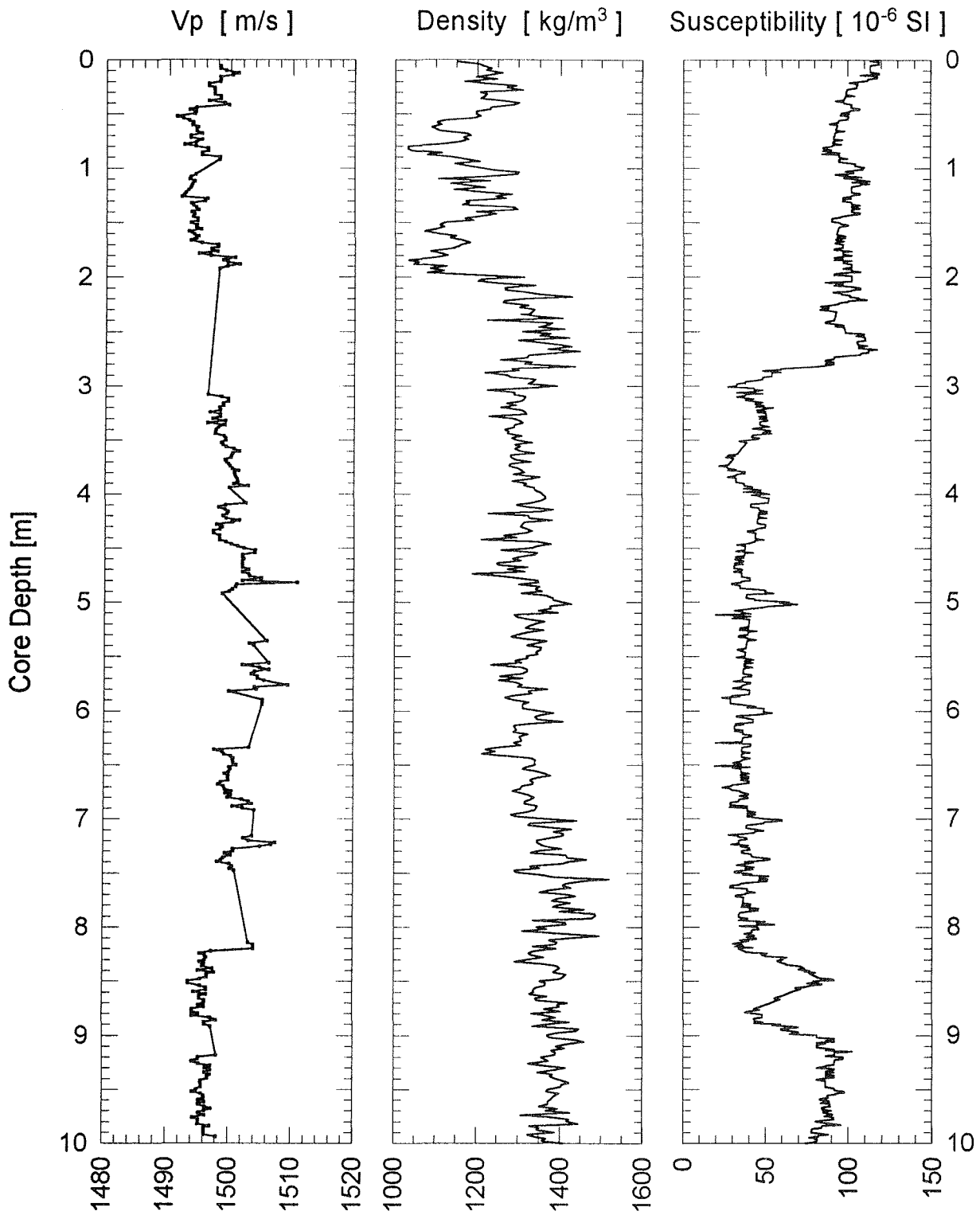
Date: 12.05.93 Pos: 05°06,4' S 10°50,9' E
Water Depth: 1830 m Core Length: 1418 cm

Figure 48 Gravity core GeoB 2302-2 (northern Cogo Fan area): Physical property logs.

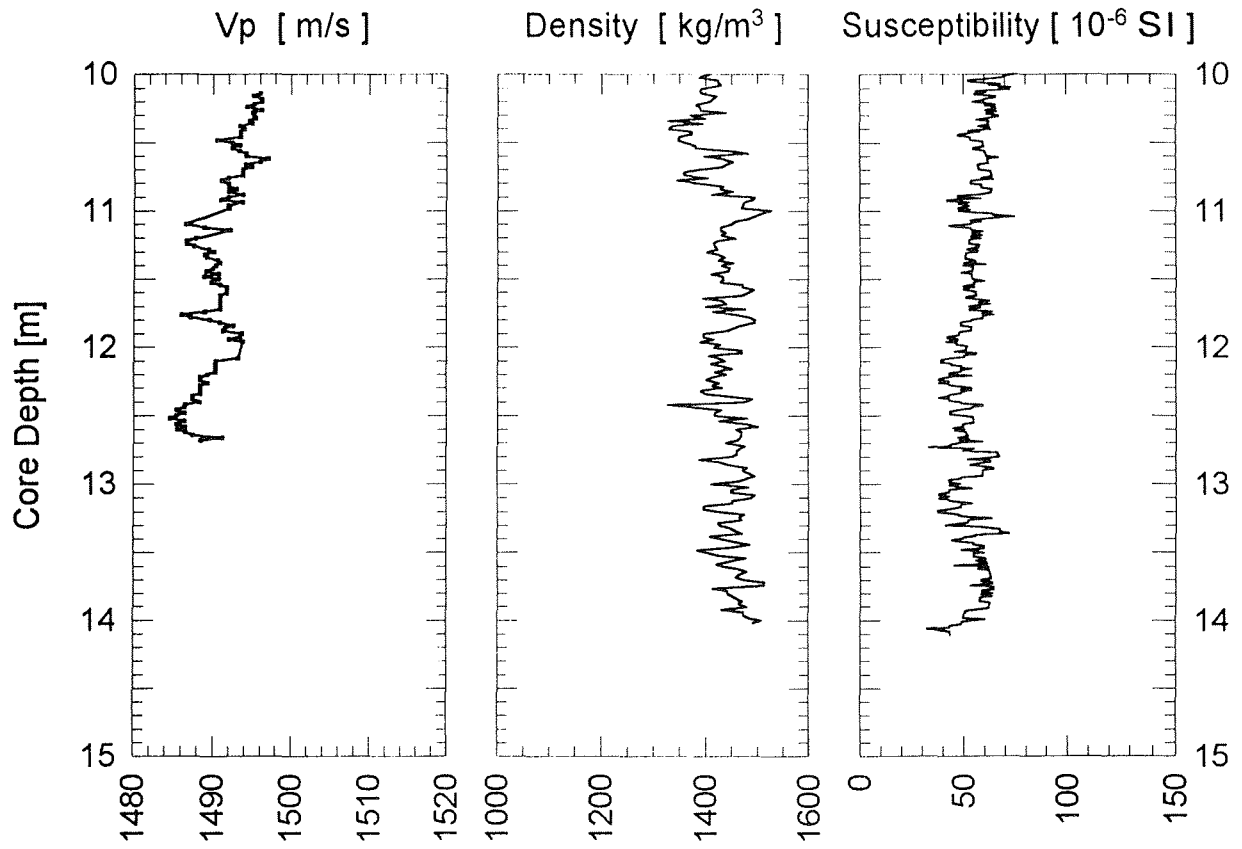
GeoB 2302-02Date: 12.05.93 Pos: 05°06,4' S 10°50,9' E
Water Depth: 1830 m Core Length: 1418 cm

Figure 48 continued.

GeoB 2303-02

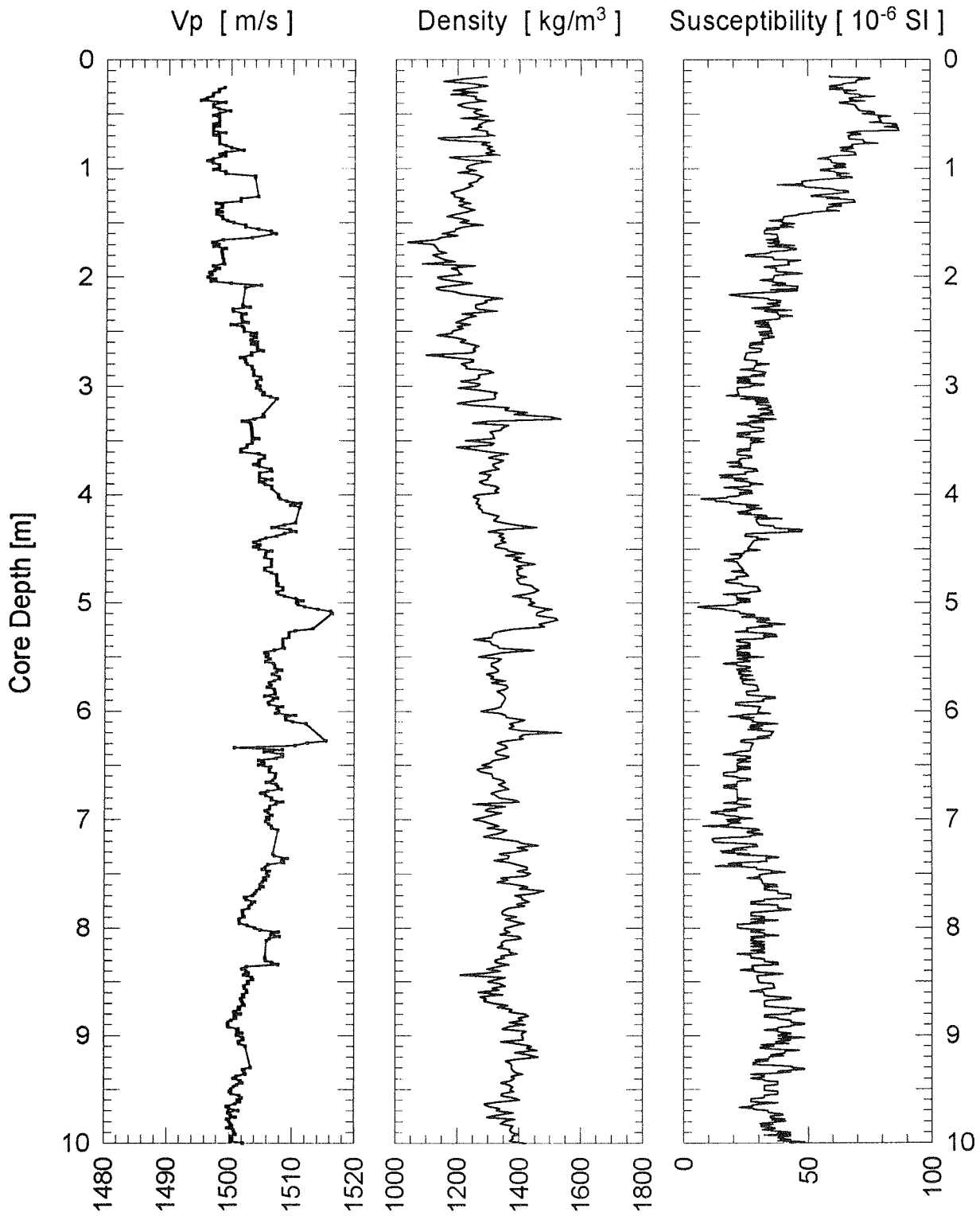
Date: 12.05.93 Pos: 05°11,4' S 10°22,0' E
Water Depth: 2494 m Core Length: 1736 cm

Figure 49 Gravity core GeoB 2303-2 (northern Cogo Fan area): Physical property logs.

GeoB 2303-02

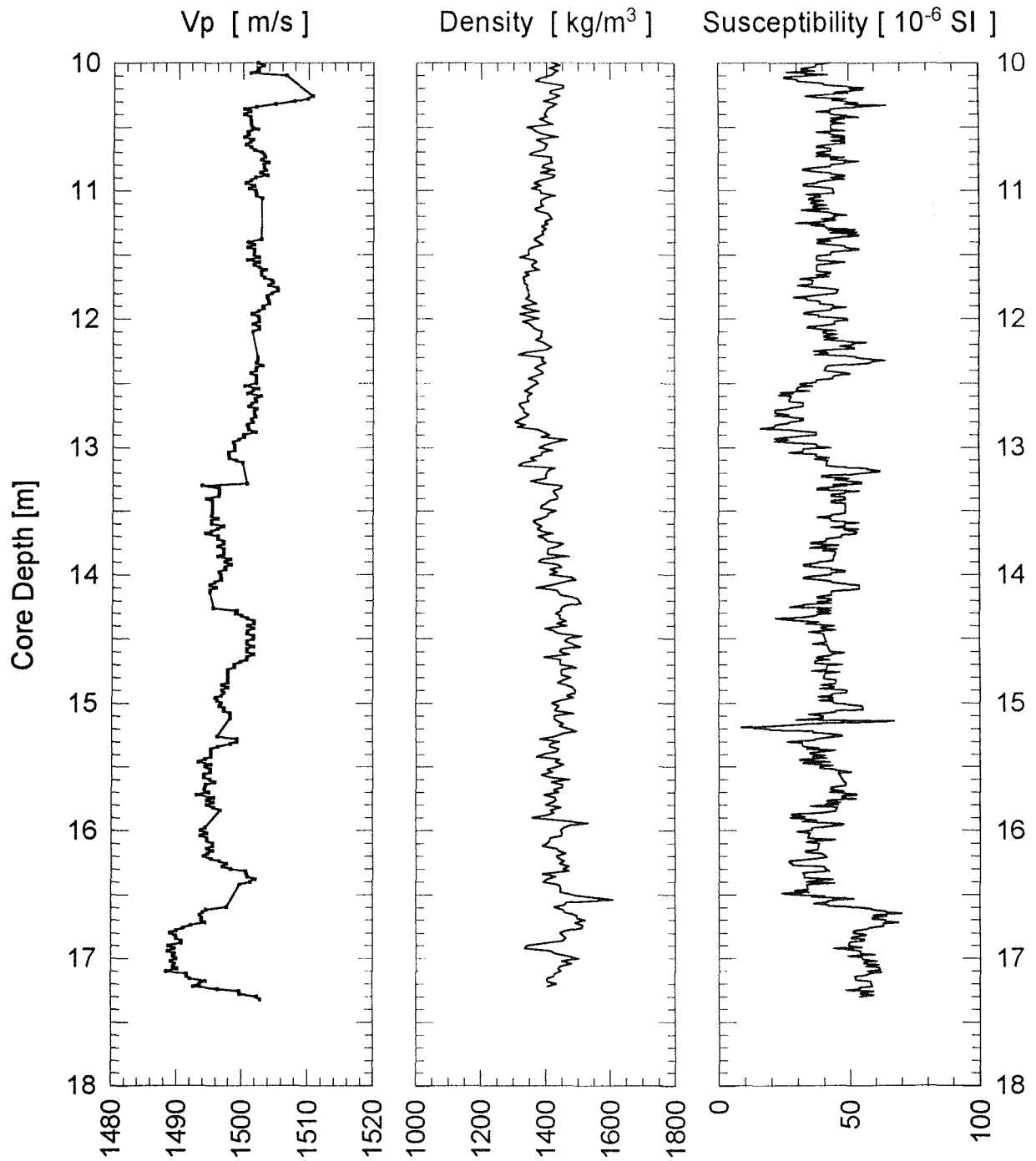
Date: 12.05.93 Pos: 05°11,4' S 10°22,0' E
Water Depth: 2494 m Core Length: 1736 cm

Figure 49 continued.

Angola Diapir Field (GeoB 2304-02, 2305-02, 2306-02)

Apart from a thin sandy layer at about 0.62 m depth, the P-wave velocity log of core GeoB 2304-02 does not show any prominent variations. A slight increase from about 1490 to 1505 m/s is observed downcore. Over the same range P-wave velocities of gravity core GeoB 2306-02 decrease from the top to around 2 m core depth.

All cores in the Angola Diapir Field area essentially reveal a trend of linearly increasing densities downcore. In contrast to the Congo Fan, values of about 1400 kg/m³ are typical at the sea floor, they increase to 1600 or 1700 kg/m³ at the base of the cores. The corresponding porosity data vary between 70 and 80% in the upper parts of the cores and decrease to about 60 to 65% in deeper layers. The thin sandy horizon at about 0.62 m depth in gravity core GeoB 2304-02 yields a very high density of around 2100 kg/m³.

The magnetic susceptibility logs of cores GeoB 2304-02 and 2305-02 show pronounced maxima of 130 to 140 · 10⁻⁶ SI in the upper part of the cores. Below about 1.2 and 1.5 m depth an almost constant level around 50 · 10⁻⁶ SI is reached which prevails in the whole sediment sequence of gravity core GeoB 2306-02.

Angola Benguela Front (GeoB 2307-02, 2308-02, 2309-02)

In gravity core GeoB 2307-02 P-wave velocities slightly increase from about 1490 m/s at the top of the core to 1500 m/s at 3.0 m depth. Beneath cyclic variations from about 1490 to 1510 m/s between 4.0 and 5.0 m depth for which there is no obvious explanation in the core description P-wave-velocities increase again from about 1490 to 1510 m/s at the base of the core.

Apart from two thin silty/sandy layers in gravity core GeoB 2308-02 with values of up to 1550 m/s, the P-wave velocity logs of the two other cores display only relatively smooth variations between 1490 and 1510 m/s.

In the upper part of the core 2307-02 wet bulk densities slightly decrease from about 1400 to 1300 kg/m³ at 2.7 m core depth. Following a rapid rise to some 1600 kg/m³, they further increase downcore to about 1750 kg/m³. A peak at 6.9 m depth, which also appears in the P-wave velocity log, probably results from a small sandy lens mentioned in the core description. Porosity values vary between 70 and 85% down to 2.7 m depth and then decrease to values between 50 and 60% to the base of the core.

In the two other cores of this area, wet bulk densities oscillate at relatively high frequency around mean values of 1440 kg/m³ in the shallower (GeoB 2308-02) and 1270 kg/m³ (GeoB 2309-02) in the deeper waters. Mean porosities for these two cores amount to 75% (GeoB 2308-02) and to 85% (GeoB 2309-02), respectively.

GeoB 2304-02

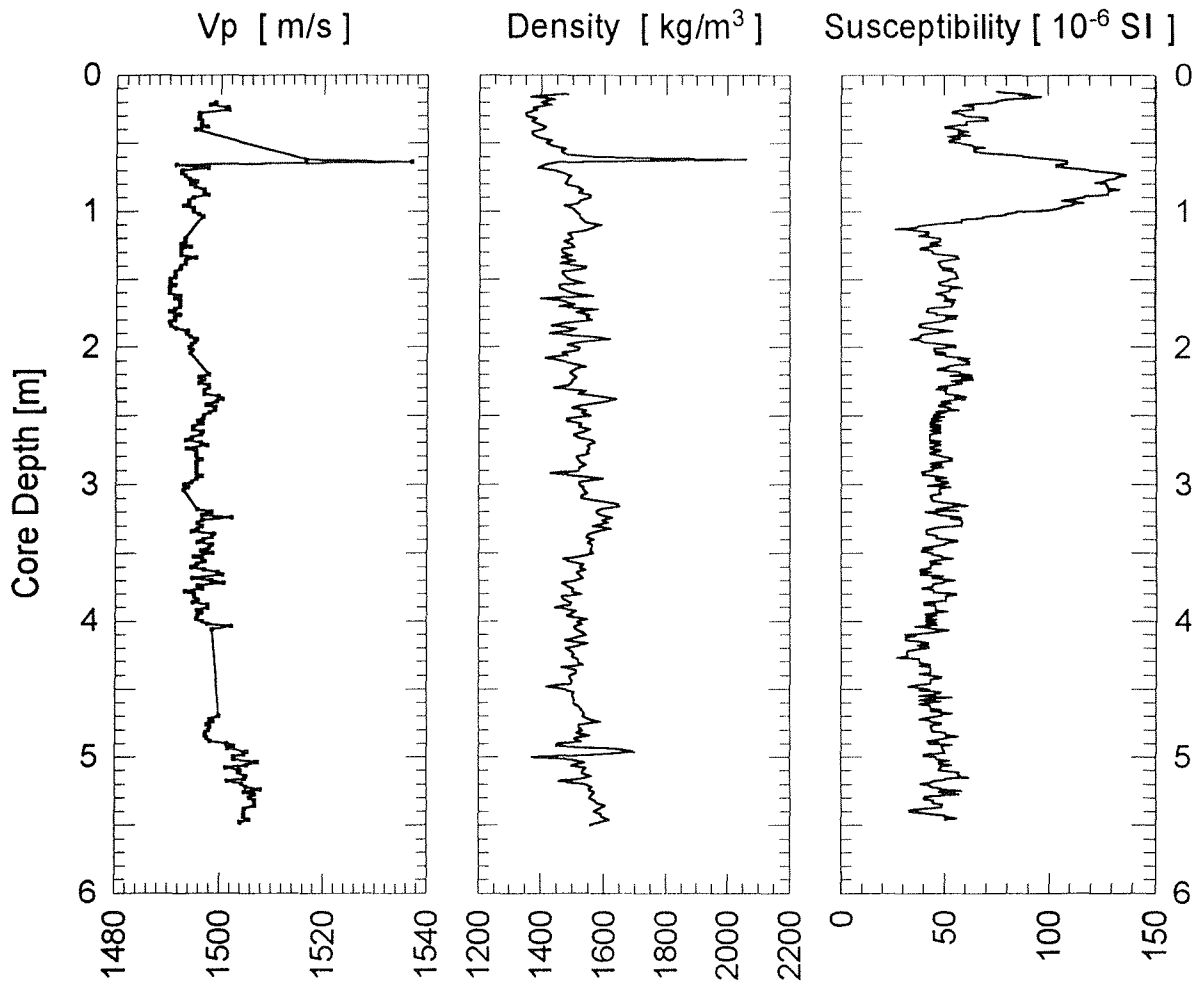
Date: 19.05.93 Pos: 12°01,2' S 12°27,1' E
Water Depth: 2003 m Core Length: 554 cm

Figure 50 Gravity core GeoB 2304-2 (Angola Diapir Field area): Physical property logs.

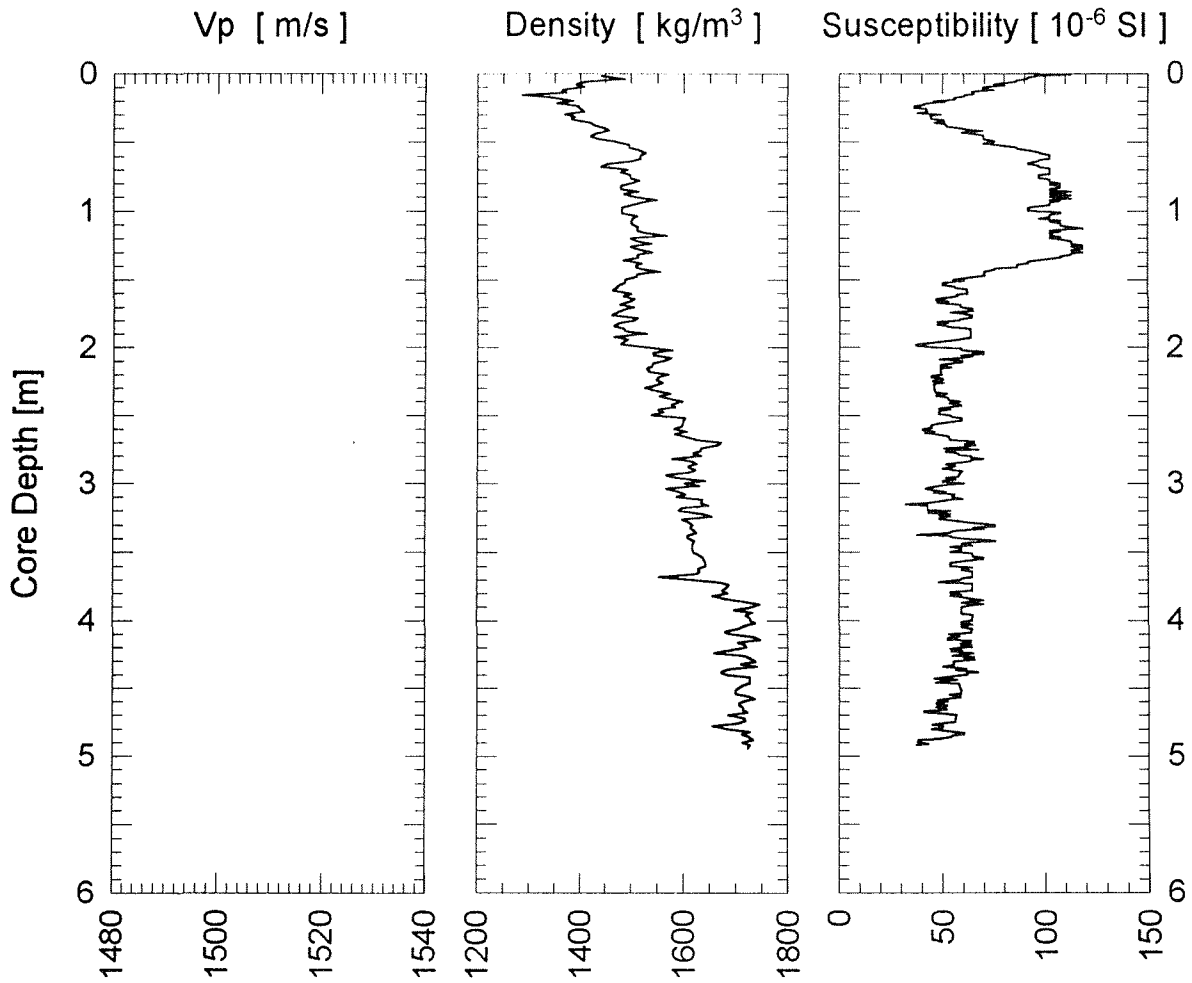
GeoB 2305-02Date: 19.05.93 Pos: 11°56,1' S 13°15,1' E
Water Depth: 897 m Core Length: 495 cm

Figure 51 Gravity core GeoB 2305-2 (Angola Diapir Field area): Physical property logs.

GeoB 2306-02

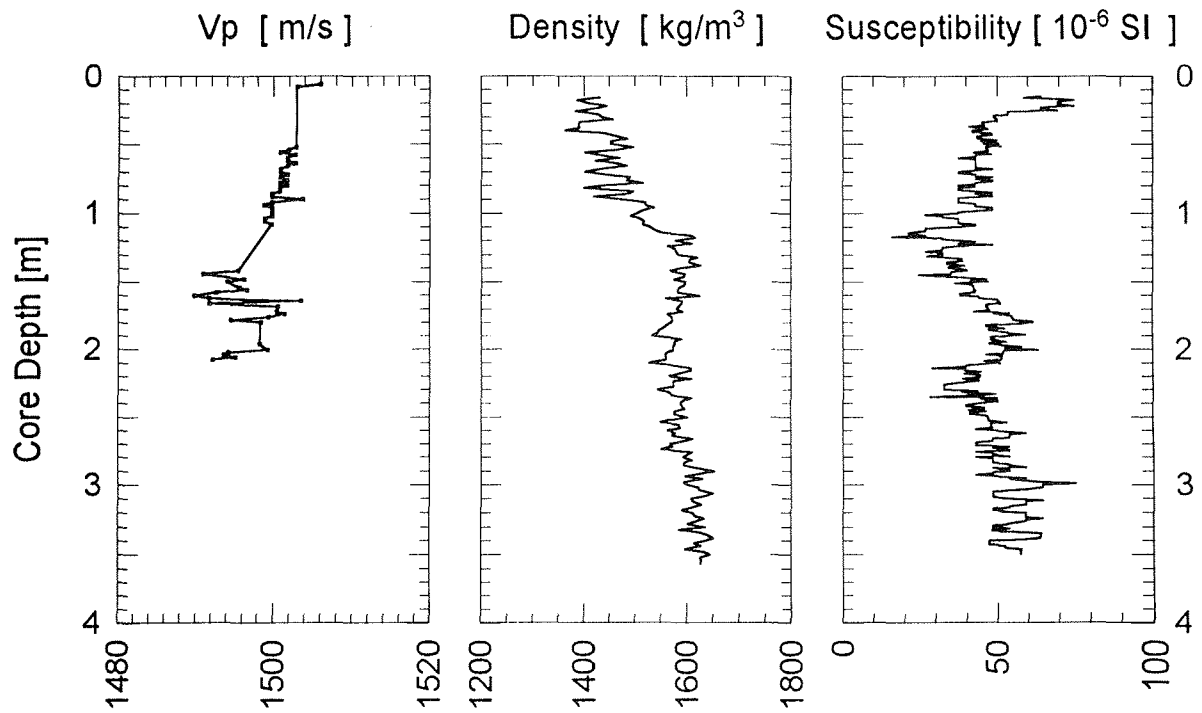
Date: 19.05.93 Pos: 11°55,3' S 13°23,0' E
Water Depth: 479 m Core Length: 358 cm

Figure 52 Gravity core GeoB 2306-2 (Angola Diapir Field area): Physical property logs.

GeoB 2307-02

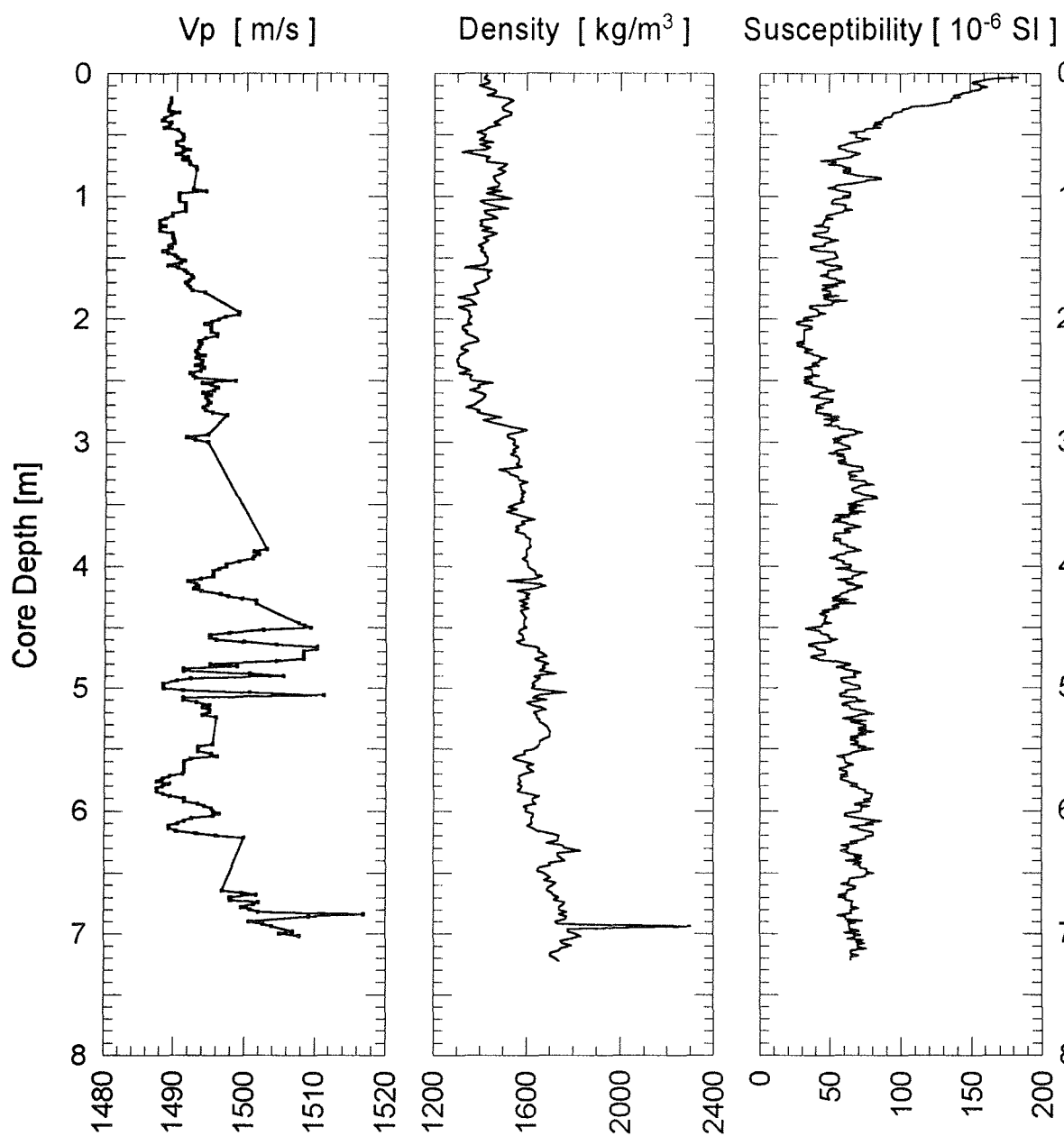
Date: 21.05.93 Pos: 14°13,9' S 11°31,1' E
Water Depth: 2892 m Core Length: 724 cm

Figure 53 Gravity core GeoB 2307-2 (Angola Benguela Front area): Physical property logs.

GeoB 2308-02

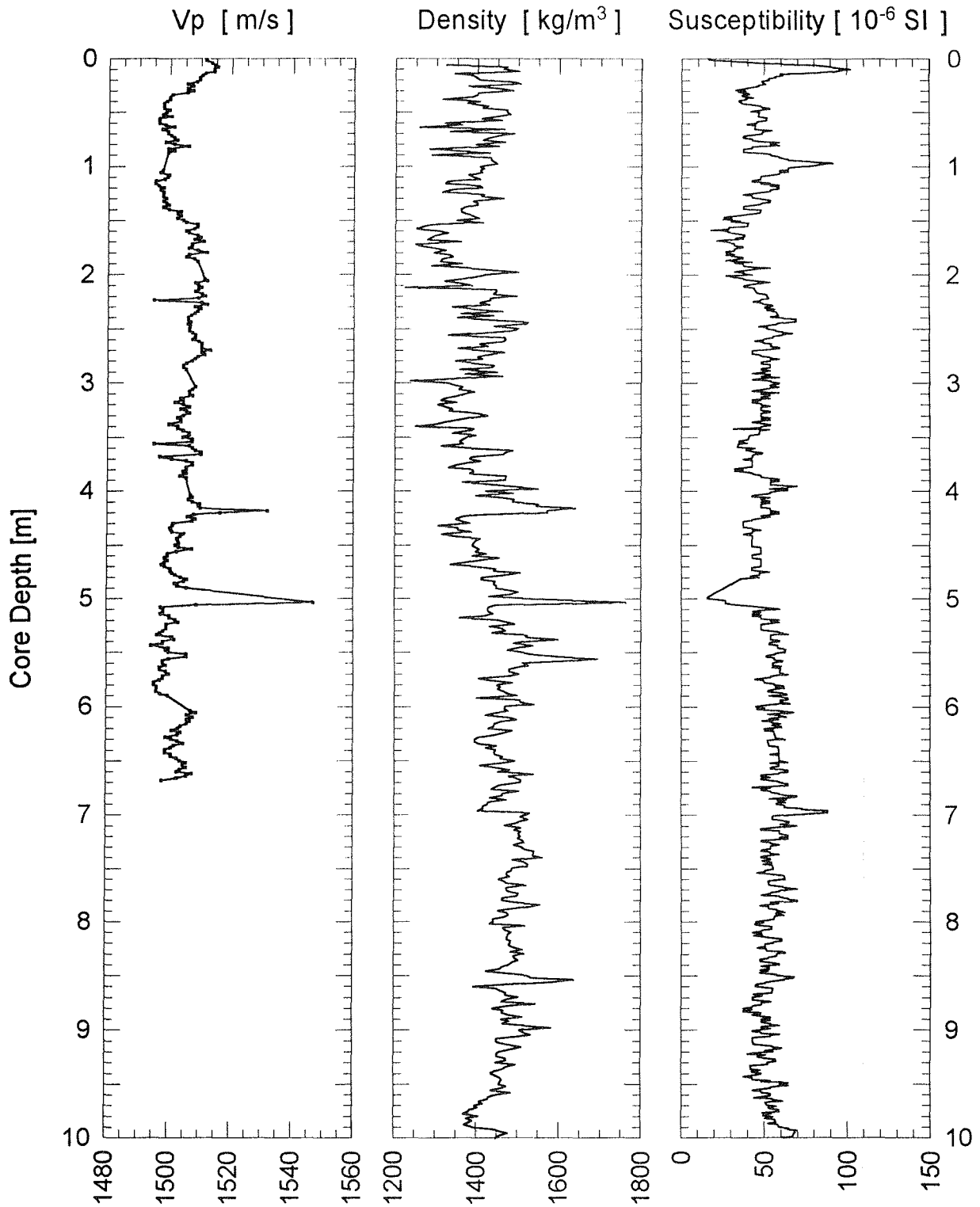
Date: 24.05.93 Pos: 16°43,7' S 11°02,3' E
Water Depth: 2114 m Core Length: 1133 cm

Figure 54 Gravity core GeoB 2308-2 (Angola Benguela Front area): Physical property logs.

GeoB 2308-02

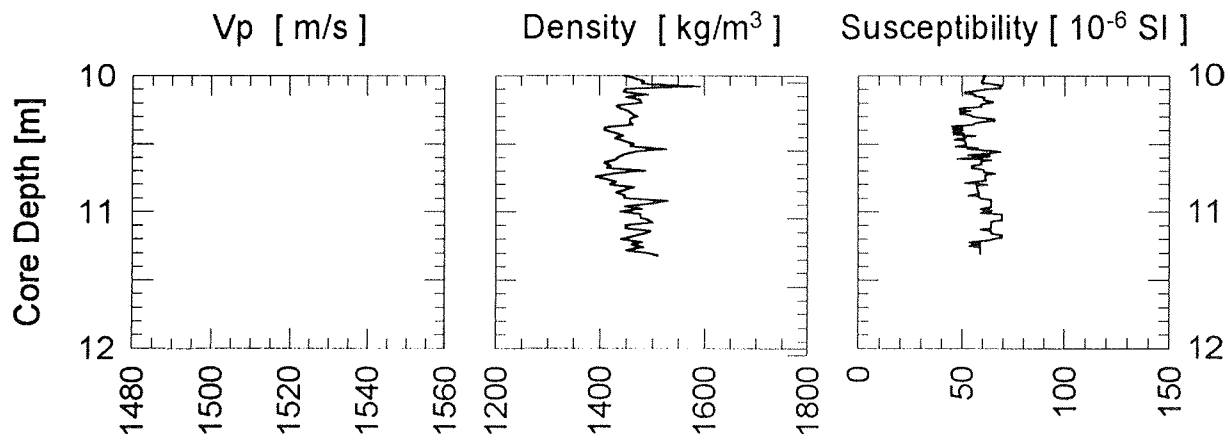
Date: 24.05.93 Pos: 16°43,7' S 11°02,3' E
Water Depth: 2114 m Core Length: 1133 cm

Figure 54 continued.

GeoB 2309-02

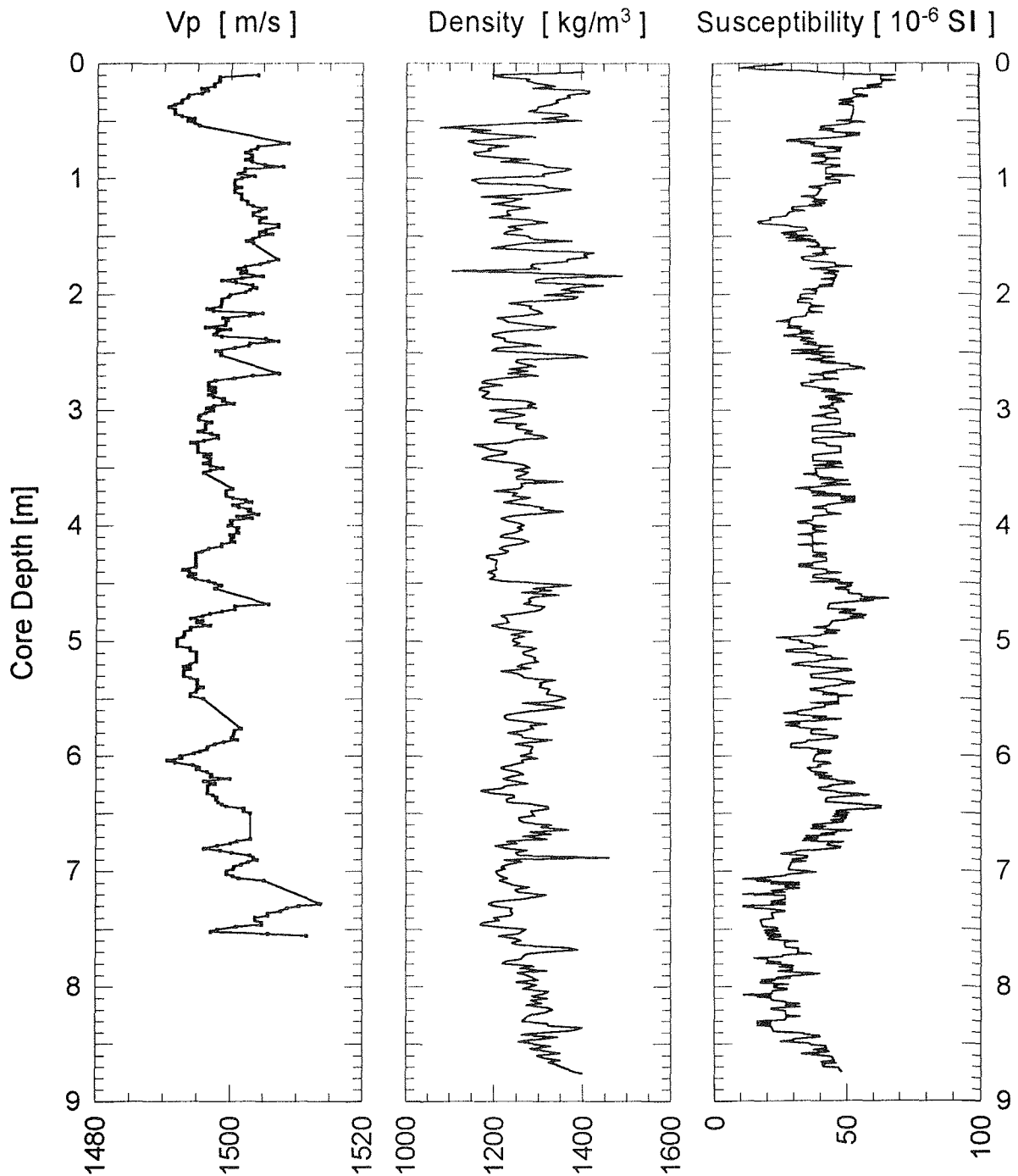
Date: 24.05.93 Pos: 16°34,7' S 10°50,5' E
Water Depth: 2675 m Core Length: 878 cm

Figure 55 Gravity core GeoB 2309-2 (Angola Benguela Front area): Physical property logs.

GeoB 2310-02

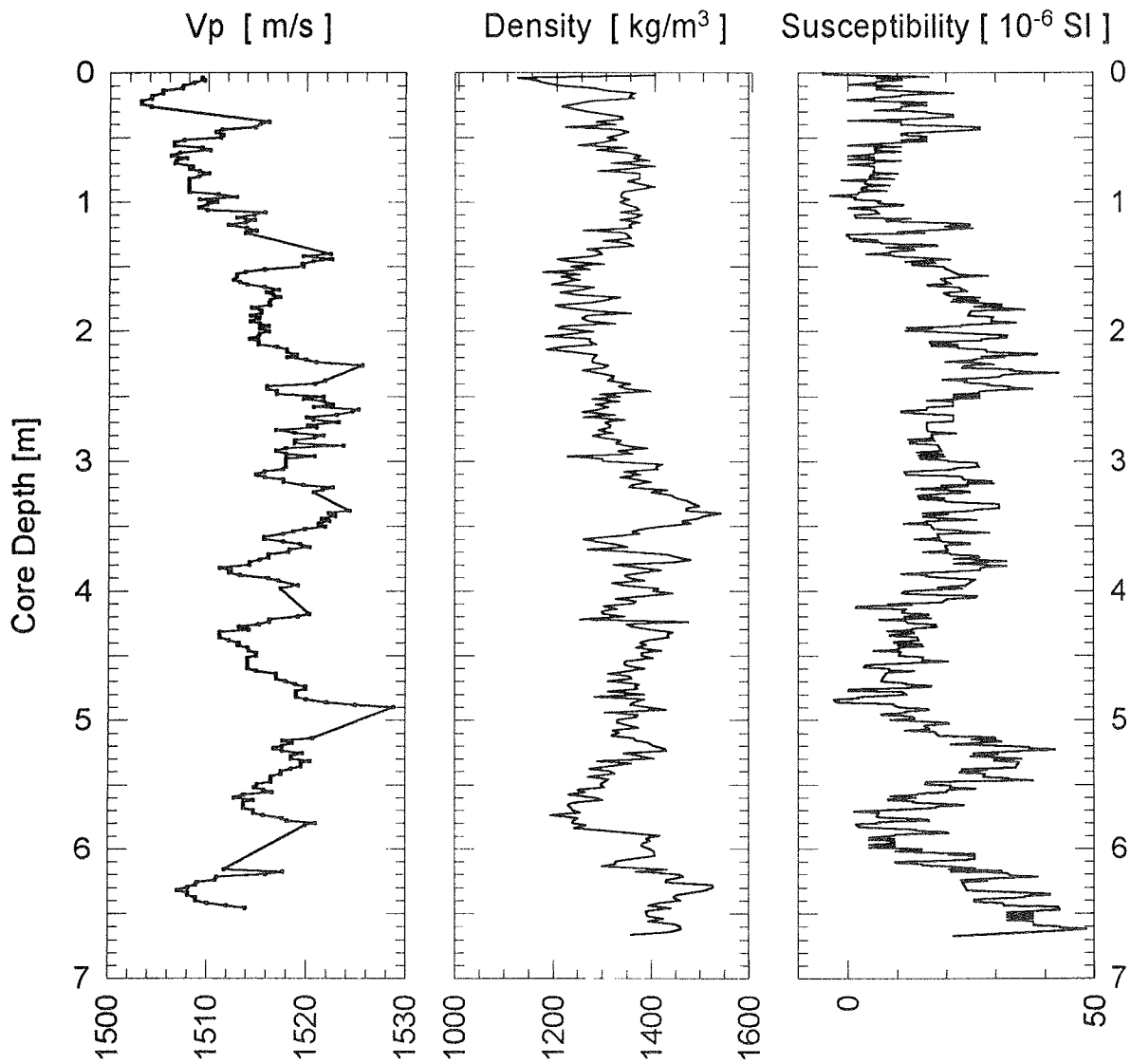
Date: 27.05.93 Pos: 22°16,0' S 12°32,3' E
Water Depth: 1024 m Core Length: 675 cm

Figure 56 Gravity core GeoB 2310-2 (northeastern Cape Basin): Physical property logs.

Magnetic susceptibilities decrease in the upper 0.5 m of core GeoB 2307-02 from $190 \cdot 10^{-6}$ to about $50 \cdot 10^{-6}$ SI. Smooth changes between $30 \cdot 10^{-6}$ and $80 \cdot 10^{-6}$ SI in the deeper parts to some extent appear to be positively correlated to density variations.

The magnetic susceptibilities logs of the two other cores show no pronounced variations, their mean values amount to $50 \cdot 10^{-6}$ (GeoB 2308-02) and $40 \cdot 10^{-6}$ SI (GeoB 2309-02), respectively.

Cape Basin (GeoB 2310-02)

P-wave velocities ranging between about 1505 and 1530 m/s reveal a series of cyclic variations and on average are significantly higher than those of the other cores recovered during this cruise.

Wet bulk densities essentially vary between 1200 and 1500 kg/m³. Corresponding porosities range between about 75 and 90%. Low-frequency density variations with minima at about 1.5 and 5.5 m and maxima at about 0.8, 3.4 and 6.3 m show no persistent correlation to changes in P-wave velocity.

Magnetic susceptibilities are very low reaching maximum values of only $50 \cdot 10^{-6}$ SI. Low-frequency variations in the upper parts are negatively, near the base of the core positively correlated to wet bulk densities.

5.5 Accelerator Monitored Coring

B. Heesemann and H. Villinger

5.5.1 Introduction

Gravity or piston coring is the standard method for obtaining long sediment cores from the bottom of the ocean. These cores provide the material to study the depositional processes of the past. One of the basic assumptions when interpreting the depth variations of sediment parameters is that the core is an undisturbed sample of the *in situ* sedimentary sequences. Investigations have shown, however, that the process of coring itself may result in a more or less severe disturbance of the core causing a compression of the core or even a selective sampling by which certain layers are omitted by the coring process. Such core disturbances have serious consequences on the calculation of sedimentation or accumulation rates as well as on the spectral analysis of cyclic variations in sediment parameters.

One possibility to reconstruct the total penetration of the core barrel into the sediment is to monitor the penetration process by measuring and recording the

acceleration. As the core barrel and core head move essentially only in a vertical direction, the system described below measures vertical accelerations and tilt (deviation from the vertical) during penetration.

5.5.2 Measuring System

The measuring system used during Cruise S0 86 consisted of a vertical accelerometer, a tilt sensor and a data logger. The electronics are housed in a pressure case which is designed for operation in water depth up to 6000 m. The signals of the accelerometer and the tilt sensor are digitized and stored after passing the anti-aliasing filter and the amplifier of a signal conditioning module. The range of the accelerometer is 3 g with a sensitivity of 0.001 g. The sensor can survive a maximal shock of 10000 g according to the specifications of the manufacturer. The tilt sensor covers a range of $\pm 20^\circ$ with a sensitivity of 0.5 seconds of an arc. The resolution of the A/D converter is 13 bits at a sample rate of 100 Hz. At this rate the data logger can record two channels of data for 22 minutes.

To house the pressure case in the weight stand of the gravity core, five of the usual lead disks were replaced by steel disks of identical dimensions, containing a hole slightly larger than the outside diameter of the pressure case. Lining up the holes of the individual steel disks creates an opening large enough to house the pressure case. Additional set screws press the pressure case against the steel disks to avoid relative movement between the two. This arrangement guarantees that the sensors in the pressure case records the true motion of the core head.

Two prototypes of the instrument were used during Cruise SO 86 with different triggering systems to start the recording of data. One simply used a shortening connector. This has the consequence that the sampling rate has to be reduced to 50 Hz in order to obtain a large enough recording window to monitor the penetration of the core. The other prototype contained a pressure sensor whose pressure is monitored continuously by the data logger. If the pressure exceeds a certain preset limit, the high-frequency sampling and recording of acceleration and tilt is initiated.

5.5.3 Shipboard Results

The system was successfully used at eight gravity core stations, GeoB 2301 and 2304 to 2310. Only one measurement failed because of a water leak at a damaged connector in 1000 m water depth.

Figure 57 shows the acceleration and tilt during penetration of the gravity core at station GeoB 2301. The time origin ($t = 0$) is arbitrary. Before penetration the gravity core is accelerated up and down due to the heave of the ship with periods of around

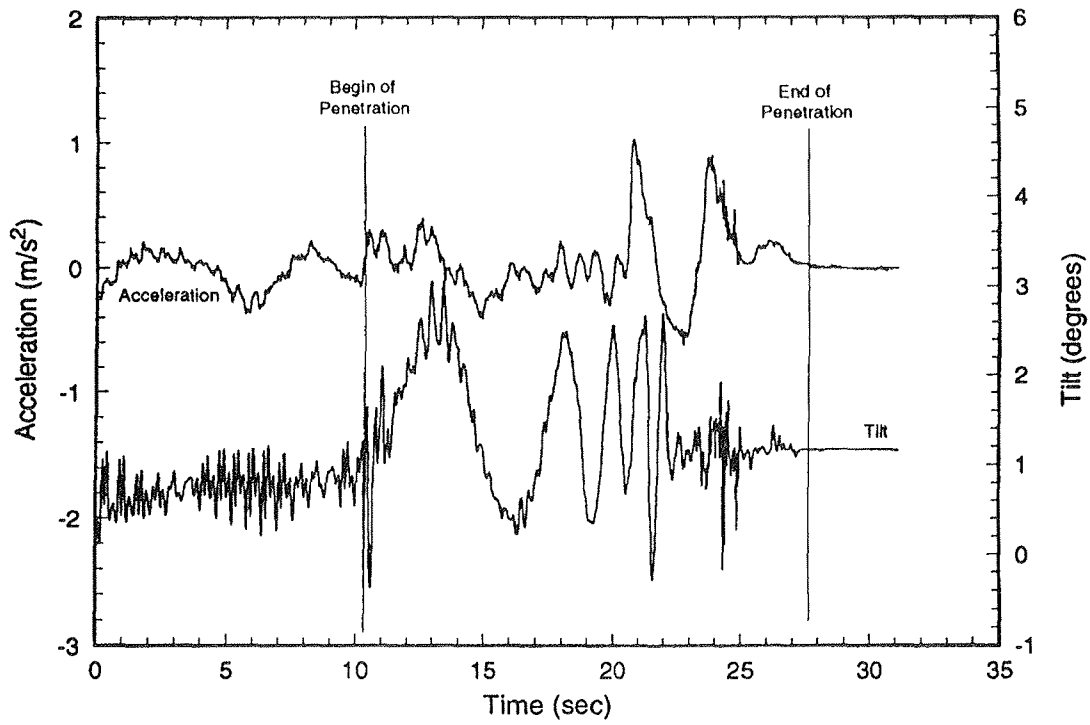


Figure 57 Acceleration and tilt versus time during penetration of gravity core GeoB 2301-3.

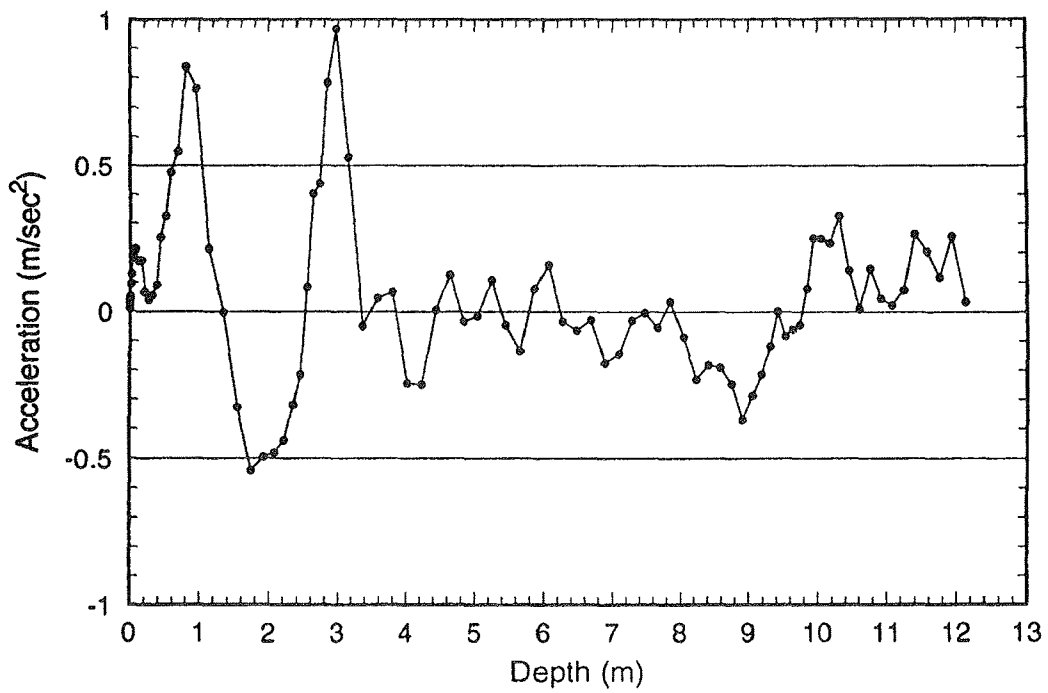


Figure 58 Acceleration versus penetration depth of gravity core GeoB 2301-3.

10 seconds and smaller accelerations in the range of $\pm 0.5 \text{ m/s}^2$. The magnitude of these accelerations mainly depends on the sea state while the core is taken. The pre-penetration tilt data show similar periodic variations as acceleration with amplitudes of $\pm 0.5^\circ$. On top of this signal are high-frequency changes which may be associated with the wire strum. Picking the exact instant when the core cutter hits the ocean floor is sometimes difficult, especially in case of very soft sediments without a sharp but a gradual change in physical properties like density or shear strength at the sediment/water boundary. In Figure 1 the moment of penetration is clearly identified by an obvious change in acceleration pattern as well as a clear shift in tilt signal characteristics. It is interesting to note how the frequency of the tilt signal changes from lower to higher values as the barrel penetrates deeper and deeper and the part of the barrel which still sticks out of the sediment becomes shorter and shorter. This specific behaviour was clearly observed at most coring stations. The tilt suddenly increases in the moment of penetration to values of up to $\pm 1^\circ$ and ends at a value of about 1° after the core has come to a stop in the sediment. Accelerations amount to maximal values of $\pm 1 \text{ m/s}^2$ about 12 sec after the beginning of the penetration which may be due to the decreasing porosity at the base of a section of hemipelagic mud as indicated in the sedimentological core description. The total penetration time is about 17.5 sec.

The result of the double integration of the acceleration is shown in Figure 58. Note that a reversed depth scale is used with the maximum penetration depth at the origin. According to this calculation the total penetration depth amounts to only about 12.5 m which falls considerably short of the core recovery of 15.34 m. The major acceleration peak near the bottom of the core is most likely related to the change in lithology from hemipelagic mud to foram-bearing hemipelagic mud (see Fig. 35).

At present the discrepancy between calculated penetration depth and recovered core length remains to be explained. A potential source of this problem could be the calibration of the acceleration sensor which will be inspected in further detailed experimental work. Nevertheless, the discussion of the data shows very clearly that altogether the new system performed very well and gives meaningful results.

6 Hydroacoustic System Development with the SEL-90 Echosounder

W.-D. Heinitz, J. Ewert, T. Merkel

The sediment echosounder SEL-90 was developed at the University of Rostock by the hydroacoustics working group in the Department of Electrical Engineering. Up to now it has predominantly been used in shallow water research. The main purpose of participating in R/V SONNE Cruise SO 86 was the continued technical modification of the instrument for deep sea applications initially begun during R/V SONNE Cruise SO 82 in October 1992.

The varying water depths and sedimentary deposits in the Angola Basin and at the African continental margin are an ideal area for the system testing with respect to structural resolution and frequency dependant signal penetration under deep water conditions. Also direct comparisons with the PARASOUND/PARADIGMA System as well as the GI-GUN high frequency seismic source could be carried out.

During the first week of the cruise, the SEL-90 system was completely set up and the transducer array installed with a new acoustical window which is reduced in thickness to lower sound attenuation for high signal frequencies. The comparison with earlier versions used on Cruise SO 82 showed a major improvement of the source level in particular for the most common signal frequency of 10 kHz.

In preparing the cruise, substantial modifications of the hardware and software were made to adapt the system for the longer sound travel times in deep waters. Specific algorithms for on-line and off-line signal processing were tested. The full computer control of the timing scheme allowed a very high repetition rate of the transmitted pulses. By manually adjusting the sounding trigger and the reception window to the actual water depth, both steps could be mixed to obtain an optimum spatial coverage of the sea floor. It is much higher than for other conventional echosounders including the PARASOUND system and can arbitrarily be chosen down to a few hundred milliseconds.

A new calibrated frequency compensation between the transducer array and the transmitter and receiver of SEL-90 was added to improve the sensitivity. The signal dynamic range was increased by a new controlled amplifier and filter in combination with a new data acquisition unit which were installed during the cruise and tested. The new interface boards include four special notch filters to reduce acoustic disturbances from other echosounders.

The notch filters were successful in eliminating the 15.5 kHz signal of the HYDROSWEEP system, but in the 5 kHz and 20 kHz operation mode of the SEL-90 the PARASOUND signals of 4, 18 and 22 kHz could not be completely erased. This was caused by the broader bandwidth of the standard one pulse PARASOUND signal at 4

kHz which cannot be covered by notch filters only. In the 10 kHz operation mode of the SEL-90 all noise signals were significantly reduced.

According to the original plans, the basic technical work could be finished with arrival in the working area at the Southwest African continental margin, and data were routinely recorded during geophysical surveying. For immediate use and later quantitative analyses the data were acquired as an on-line color printout of the echo amplitudes and digitally on a magneto-optical disc drive and a digital audio tape recorder.

For profiles of about 860 nm length color echoprints and digital data on MO discs were collected during the cruise. In addition, for about 240 nm the signals of the SEL-90 and the PARASOUND system were stored in parallel on digital audio tapes.

The direction of the sound emission beam significantly affects the signal quality and the imaging characteristics of an echosounder. The detection of the sea bottom and the vertical resolution can be improved by beam steering according to changes in the morphology and inclination of the sea bed. To test the influence of this parameter, the SEL-90 system was equipped with a computer controlled electronic beam steering module. Several experiments yielded a major improvement in particular for slope angles steeper than 4° . It turned out, however, that the present version of SEL-90 does not provide sufficiently small steering angle increments to allow an imaging of the observed topography with constant quality.

In addition to the main activities described above, several new features were built in the SEL-90 system during the cruise:

- integration of the ship's navigation data into the SEL-90 system and in each seismogram header;
- generation of a special digital data strings for analog recordings to improve subsequent laboratory tests with real analog signals;
- expanded data record structure for digital data recording to allow for an improved post processing;
- the printer driver was supplemented to work with both the color printer Mannesmann Tally MT92C and Hewlett Packard Paint Jet;
- a new online algorithm for high resolution echo signal detection was written and successfully tested.

Summarizing the results of the cruise, it can be stated that the sonar system SEL-90 has proved to be suitable for measurements under deep sea conditions. Signal penetration into the sea floor and the resolution of sediment structures was comparable to conventional sediment echosounder systems. Under optimum conditions a penetration depth of up to 100 m was reached. Special algorithms for on-line signal processing to optimize the graphical resolution were successfully tested.

The system design of the sonar system SEL-90 is based on full computer control of all boards, modules and system features and thereby provides extraordinary flexibility. Recording parameters can be easily changed, scales of the echodrawings arbitrarily selected for screen and printer according to the requirements of the survey. The version of SEL-90, which was successively modernized for a complete integration of high speed computers and digital electronic equipment, is a further step towards a fully adaptive echosounder system which optimizes signal transmission/reception by accounting for water depth, morphology of the sea floor, penetration depth or observed sediment structures.

7 Plankton Sampling

R. Schneider, L. Dittert, P. Helmke

Marine plankton has been collected from the surface waters during the entire cruise (Table 7). For this purpose the shipboard clean seawater pump system was used to filter some 2000 to 5000 l each day, mostly during daylight hours. The seawater was pumped through a net with a mesh size of 10 microns, the amount of water filtered was determined on basis of the plankton mass caught in the net. In case the water flow stopped due to material closing the net openings, the plankton was washed into plastic bottles and the sampling resumed with the cleaned net. For each day the wet plankton samples were combined into one bottle and frozen at -15 °C.

On the transit from Buenos Aires to the eastern Angola Basin only relatively low amounts of plankton were obtained. In contrast, the recovery was high within the freshwater plume of the Congo River and in the coastal upwelling areas north of the Congo and off Namibia. Intermediate amounts of plankton were caught off Angola between 8 and 15°S, and in those parts of the cruise track which crossed the coastal upwelling centers at distances greater than about 50 miles from the African continent.

The plankton material will be investigated for the bulk composition of the biogenic detritus in order to determine the ratios between opal, organic carbon and carbonate produced by near surface water plankton communities. In particular, the marine organic material will be investigated in more detail. Planned work includes analyses of stable isotopes and individual organic compounds which can be related to specific phytoplankton organisms. This type of data is required for a comparison of marine planktic production in the surface waters to fluxes of biogenic particles caught in sediment traps and found in the surface sediments beneath different productivity systems.

Table 7 Plankton Sampling, SONNE Cruise 86

Date	Time	Start Filtration				Stop Filtration					Liters pumped
		Latitude	Longitude	Salinity (‰)	Temperature (°C)	Time	Latitude	Longitude	Salinity (‰)	Temperature (°C)	
26.04.93	10:45	24°04,8'S	41°39,9'W	37.10	27.8	16:40	23°12,9'S	40°41,0'W	36.91	26.7	2360
28.04.93	10:35	19°27,1'S	36°44,7'W	37.26	28.2	17:16	19°05,5'S	35°21,5'W	37.35	28.0	2555
29.04.93	08:43	18°01,5'S	32°32,7'W	37.31	27.8	16:59	17°44,7'S	31°50,4'W	37.40	27.5	4126
30.04.93	08:30	16°37,7'S	29°02,9'W	37.33	27.0	16:41	16°01,9'S	37°33,6'W	37.30	27.0	4623
01.05.93	08:40	14°56,6'S	24°48,4'W	37.30	27.0	16:54	14°28,9'S	23°15,2'W	37.30	26.7	4249
02.05.93	08:30	13°42,5'S	20°12,9'W	36.90	25.9	16:43	13°29,9'S	18°36,0'W	36.80	26.0	4230
03.05.93	08:30	13°05,0'S	15°23,6'W	36.80	26.0	16:45	12°46,5'S	13°43,1'W	36.70	25.8	4391
04.05.93	08:15	12°10,8'S	10°40,1'W	36.70	25.7	16:43	11°50,2'S	09°04,4'W	36.50	26.1	4631
05.05.93	08:30	11°12,3'S	05°57,7'W	36.60	25.8	16:37	10°52,3'S	04°18,9'W	36.50	25.9	4230
06.05.93	08:45	10°13,1'S	01°05,6'W	36.40	26.1	16:40	09°46,1'S	00°27,9'E	36.20	26.6	4229
07.05.93	08:45	08°25,2'S	03°09,8'E	35.30	26.7	17:01	07°41,3'S	04°37,7'E	34.20	27.6	3579
08.05.93	08:50	06°06,8'S	07°25,7'E	33.10	27.8	18:30	05°27,3'S	08°45,3'E	34.60	26.4	4420
09.05.93	07:30	05°16,9'S	09°48,5'E	35.40	25.8	19:45	05°07,1'S	10°48,3'E	32.24	25.9	3496
10.05.93	08:45	04°42,2'S	11°02,6'E	34.35	25.7	20:05	04°46,9'S	10°07,6'E	34.03	26.5	3366
11.05.93	08:55	05°11,7'S	10°22,0'E	31.40	25.8	20:15	04°52,7'S	10°37,0'E	31.50	26.5	3400
12.05.93	07:45	05°04,1'S	11°06,7'E	29.85	25.4	20:05	05°11,5'S	10°22,0'E	28.20	26.5	4686
13.05.93	08:30	06°28,3'S	10°40,2'E	33.65	26.8	19:00	07°02,9'S	10°13,2'E	35.54	26.6	4196
14.05.93	08:30	07°04,5'S	11°10,7'E	35.63	26.8	20:10	06°44,6'S	11°10,5'E	34.38	27.3	4163
15.05.93	08:05	07°26,5'S	10°31,1'E	34.80	27.2	20:48	08°39,8'S	11°04,4'E	35.88	26.4	3638
16.05.93	08:10	10°27,3'S	12°14,9'E	35.80	26.5						
17.05.93						19:00	11°59,9'S	12°37,5'E	36.24	26.9	6864

Table 7 continued

Date	Time	Start Filtration				Stop Filtration					Liters pumped
		Latitude	Longitude	Salinity (‰)	Temperature (°C)	Time	Latitude	Longitude	Salinity (‰)	Temperature (°C)	
18.05.93	09:10	12°04,4'S	13°26,0'E	35.80	26.7	17:20	12°21,9'S	12°31,4'E	36.23	26.2	5461
19.05.93	06:00	12°00,2'S	13°08,9'E	35.78	27.0	19:00	11°55,4'S	13°19,0'E	35.80	27.0	4736
20.05.93	08:00	12°03,0'S	12°53,1'E	35.80	26.8	20:55	12°26,6'S	12°12,3'E	36.05	26.7	4604
21.05.93	08:30	13°05,7'S	11°28,9'E	36.00	24.8	21:30	14°41,0'S	11°17,5'E	36.24	22.3	3720
22.05.93	08:10	16°07,8'S	10°28,9'E	36.00	20.4	18:30	16°49,6'S	11°09,9'E	36.01	17.8	1921
22.05.93	18:40	16°50,1'S	11°10,5'E	35.89	17.6	0:00	17°06,7'S	11°24,9'E	35.66	15.7	717
23.05.93	08:30	17°06,3'S	10°43,3'E	35.82	17.2	20:15	16°37,6'S	10°37,3'E	35.97	19.8	2457
24.05.93	07:15	16°47,8'S	11°03,9'E	35.86	17.4	19:00	17°03,5'S	10°29,3'E	35.81	17.5	3427
25.05.93	08:45	19°12,1'S	09°22,8'E	35.68	20.5	21:30	19°30,5'S	10°01,9'E	35.77	18.9	4857
26.05.93	08:30	19°42,5'S	10°31,9'E	35.83	19.0	19:40	21°06,3'S	11°28,9'E	35.66	17.5	2506
27.05.93	03:30	22°11,2'S	12°27,9'E	35.50	16.6	20:40	24°41,6'S	13°55,2'E	35.20	13.2	3188
28.05.93	08:30	25°29,3'S	13°32,1'E	35.32	15.0	18:30	25°40,1'S	12°38,7'E	35.38	16.5	1687

8 References

- AUSTIN, Jr., J.A. and E. UCHUPI, 1982. Continental - oceanic crustal transition off Southwest Africa. *Am. Ass. Petr. Geol. Bull.* **66**, 1328-1347.
- BAUMGARTNER, T.R. and T.H. VAN ANDEL, 1971. Diapirs of the continental margin of Angola, Africa. *Geol. Soc. Am. Bull.* **82**, 793-802.
- BOLLI, H.M., W.B.F. RYAN et al., 1978. Initial Reports of the Deep Sea Drilling Project **40**, Washington, U.S. Govt. Printing Office, 1079 p.
- BOYCE, R.E., 1968. Electrical resistivity of modern marine sediments from the Bering sea. *J. Geophys. Res.* **73**, 4759-4766.
- BOYCE, R.E., 1976. Sound velocity-density parameters of sediment and rock from DSDP drill sites 315 - 318 on the Line Island Chain, Manihiki Plateau, and Tuamotu Ridge in the Pacific Ocean. In: S.O. Schlanger, E.D. Jackson et al. (Eds.), Initial Reports of the Deep Sea Drilling Project **33**, Washington, U.S. Govt. Printing Office, 695-728.
- BREITZKE, M. and V. SPIEB, 1993. An automated full waveform logging system for high-resolution P-wave profiles in marine sediments. *Mar. Geophys. Res.* **15**, 297-321.
- BRICE, S.E., M.D. COCHRAN, G. PARDO and A.D. EDWARDS, 1982. Tectonics and sedimentation of the South Atlantic Rift Sequence: Cabinda, Angola. In: J.S. Watkins and C.L. Drake (Eds.), *Studies in Continental Margin Geology*. *Am. Ass. Petr. Geol. Mem.* **34**, 5-18.
- CHERKIS, N.Z., H.S. FLEMING and J.M. BROZEAN, 1989. Bathymetry of the South Atlantic Ocean, Naval Research Laboratory, Map and Chart Series MCH-069, *Geol. Soc. Am.*
- EISMA, D. and A.J. VAN BENNEKOM, 1978. The Zaire River and Estuary and the Zaire outflow in the Atlantic Ocean. *Neth. J. Sea Res.* **12**, 255-272.
- EMBLEY, R.W. and J.J. MORLEY, 1980. Quaternary sedimentation and paleoenvironmental studies off Namibia (South-West Africa). *Mar. Geol.* **36**, 183-204.
- EMERY, K.O. and E. UCHUPI, 1984. *The Geology of the Atlantic Ocean*. New York, Springer, 925 p.

- EMERY, K.O., E. UCHUPI, C. BOWIN, J. PHILLIPS and E.S.W. SIMPSON, 1975a. Continental margin off western Africa: Cape St. Francis (South Africa) to Walvis Ridge (South-West Africa). *Am. Ass. Petr. Geol. Bull.* **59**, 3-59.
- EMERY, K.O., E. UCHUPI, J. PHILLIPS, C. BOWIN and J. MASCLE, 1975b, Continental margin off western Africa: Angola to Sierra Leone, *Am. Ass. Petr. Geol. Bull.* **59**, 2209-2265.
- HEEZEN, B.C., R.J. MENZIES, E.D. SCHNEIDER, W.M. EWING and N.C.L. GRANELLI, 1964. Congo submarine canyon. *Am. Ass. Petr. Geol. Bull.* **48**, 1126-1149.
- JANSEN, J.H.F., 1985. Middle and late Quaternary carbonate production and dissolution, and paleoceanography of the eastern Angola Basin, South Atlantic Ocean. In: K.J. Hsu and H.J. Weissert (Eds.), *South Atlantic Paleoceanography*, Cambridge, University Press, 25-46.
- JANSEN, J.H.F., T.C.E. VAN WEERING, R. GIELES and J. VAN IPEREN, 1984. Middle and late Quaternary oceanography and climatology of the Zaire-Congo Fan and the adjacent eastern Angola Basin. *Neth. J. Sea Res.* **17**, 201-249.
- KENNETT, J., 1982. *Marine Geology*, Englewood Cliffs, Prentice-Hall, 813 p.
- LEYDEN, R., G. BRYAN and M. EWING, 1972. Geophysical reconnaissance on African Shelf: 2. Margin sediments from Gulf of Guinea to Walvis Ridge. *Am. Ass. Petr. Geol. Bull.* **56**, 682-693.
- NELSON, G. and L. HUTCHINS, 1983. The Benguela upwelling area. *Prog. Oceanog.* **12**, 333-356.
- PETERS, J.J., 1978. Discharge and sand transport in the braided zone of the Zaire Estuary. *Neth. J. Sea Res.* **12**, 273-292.
- SHELL, I.I., 1970. Variability and persistence in the Benguela Current and upwelling off Southwest Africa. *J. Geophys. Res.* **75**, 5225-5241.
- SCHNEIDER, R., 1991. Spätquartäre Produktivitätsänderungen im östlichen Angola-Becken: Reaktion auf Variationen im Passat-Monsun-Windsystem und in der Advektion des Benguela-Küstenstroms. *Berichte Fachbereich Geowissenschaften, Universität Bremen* **21**, 198 p.
- SCHULTHEISS, P. J. and S.D. McPHAIL, 1989. An automated P-wave logger for recording fine-scale compressional wave velocity structures in sediments. In: W. Ruddiman, M. Sarnthein et al. (Eds.), *Proceedings of the Ocean Drilling*

Program, Scientific Results **108**, College Station, Ocean Drilling Program, 407-413.

SHEPARD, F.P. and K.O. EMERY, 1973. Congo submarine canyon and fan valley. *Am. Ass. Petr. Geol. Bull.* **57**, 1679-1691.

SIEDLER, G., and H. PETERS, 1986. Properties of sea water. In: K. H. Hellwege and O. Madelung (Eds.), *Landolt-Börnstein. Zahlenwerte und Funktionen aus Naturwissenschaften und Technik, Band V/3a*, Berlin, Springer, 233-264.

STRAMMA, L. and R.G. PETERSON, 1989. Geostrophic transport in the Benguela Current region. *J. Phys. Oceanography* **19**, 1440-1448.

VAN WEERING, T.C.E. and J. VAN IPEREN, 1984. Fine-grained sediments of the Zaire deep-sea fan, southern Atlantic Ocean. In: D.A.V. Stow and D.J.W. Piper (Eds.), *Fine-Grained Sediments, Deep Water Processes and Facies*. Oxford, Blackwell, 95-113.

9 Acknowledgements

The scientific party aboard R/V SONNE during Cruise No. 86 gratefully acknowledges the friendly cooperation and efficient technical assistance of Captain Bruns and his crew.

We also appreciate the most valuable help of ship's managing owners, the RF Reedereigemeinschaft Forschungsschiffahrt, Bremen and the German Embassies at Brasilia and Buenos Aires, in particular Drs. Matthes and Geipel, in the realization of the cruise.

The work was funded by the German Federal Ministry for Research and Technology (Bundesministerium für Forschung und Technologie, BMFT) under contract "PROBOSWA" (PROjektstudie für eine geplante Bohrkampagne des Ocean Drilling Program (ODP)).

Publications of this Series

- No. 1 Wefer, G., E. Suess und Fahrtteilnehmer, 1986. Bericht über die POLARSTERN-Fahrt ANT IV/2, Rio de Janeiro - Punta Arenas, 6.11. - 1.12.1985. 60 S.
- No. 2 Hoffmann, G., 1988. Holozänstratigraphie und Küstenlinienverlagerung an der andalusischen Mittelmeerküste. 173 S.
- No. 3 Wefer, G., U. Bleil, P.J. Müller, H.D. Schulz, W.H. Berger, U. Brathauer, L. Brück, A. Dahmke, K. Dehning, M.L. Duarte-Morais, F. Fürsich, S. Hinrichs, K. Klockgeter, A. Kölling, C. Kothe, J.F. Makaya, H. Oberhänsli, W. Oschmann, J. Posny, F. Rostek, H. Schmidt, R. Schneider, M. Segl, M. Sobiesiak, T. Soltwedel, V. Spieß, 1988. Bericht über die METEOR-Fahrt M 6/6, Libreville - Las Palmas, 18.2. - 23.3.1988. 97 S.
- No. 4 Wefer, G., G.F. Lutze, T.J. Müller, O. Pfannkuche, W. Schenke, G. Siedler, W. Zenk, 1988. Kurzbericht über die METEOR-Expedition Nr. 6, Hamburg - Hamburg, 28.10.1987 - 19.5.1988. 29 S.
- No. 5 Fischer, G., 1989. Stabile Kohlenstoff-Isotope in partikulärer organischer Substanz aus dem Südpolarmeer (Atlantischer Sektor). 161 S.
- No. 6 Berger, W.H. und G. Wefer, 1989. Partikelfluß und Kohlenstoffkreislauf im Ozean. Bericht und Kurzfassungen über den Workshop vom 3.-4. Juli 1989 in Bremen. 57 S.
- No. 7 Wefer, G., U. Bleil, H.D. Schulz, W.H. Berger, T. Bickert, L. Brück, U. Claussen, A. Dahmke, K. Dehning, Y.H. Djigo, S. Hinrichs, C. Kothe, M. Krämer, A. Lücke, S. Matthias, G. Meinecke, H. Oberhänsli, J. Pätzold, U. Pflaumann, U. Probst, A. Reimann, F. Rostek, H. Schmidt, R. Schneider, T. Soltwedel, V. Spieß, 1989. Bericht über die METEOR-Fahrt M 9/4, Dakar - Santa Cruz, 19.2. - 16.3.1989. 103 S.
- No. 8 Kölling, M., 1990. Modellierung geochemischer Prozesse im Sickerwasser und Grundwasser. 135 S.
- No. 9 Heinze, P.-M., 1990. Das Auftriebsgeschehen vor Peru im Spätquartär. 204 S.
- No. 10 Willems, H., G. Wefer, M. Rinski, B. Donner, H.-J. Bellmann, L. Eißmann, A. Müller, B.W. Flemming, H.-C. Höfle, J. Merkt, H. Streif, G. Hertweck, H. Kuntze, J. Schwaar, W. Schäfer, M.-G. Schulz, F. Grube, B. Menke, 1990. Beiträge zur Geologie und Paläontologie Norddeutschlands: Exkursionsführer. 202 S.
- No. 11 Wefer, G., N. Andersen, U. Bleil, M. Breitzke, K. Dehning, G. Fischer, C. Kothe, G. Meinecke, P.J. Müller, F. Rostek, J. Sagemann, M. Scholz, M. Segl, W. Thießen, 1990. Bericht über die METEOR-Fahrt M 12/1, Kapstadt - Funchal, 13.3.1990 - 14.4.1990. 66 S.
- No. 12 Dahmke, A., H.D. Schulz, A. Kölling, F. Kracht, A. Lücke, 1991. Schwermetallspuren und geochemische Gleichgewichte zwischen Porenlösung und Sediment im Wesermündungsgebiet. BMFT-Projekt MFU 0562, Abschlußbericht. 121 S.

- No. 13 Rostek, F., 1991. Physikalische Strukturen von Tiefseesedimenten des Südatlantiks und ihre Erfassung in Echolotregistrierungen. 209 S.
- No. 14 Baumann, M., 1991. Die Ablagerung von Tschernobyl-Radiocäsium in der Norwegischen See und in der Nordsee. 133 S.
- No. 15 Kölling, A., 1991. Frühdiagenetische Prozesse und Stoff-Flüsse in marinen und ästuarinen Sedimenten. 140 S.
- No. 16 SFB 261 (Hrsg.), 1991. 1. Kolloquium des Sonderforschungsbereichs 261 der Universität Bremen: Der Südatlantik im Spätquartär - Rekonstruktion von Stoffhaushalt und Stromsystemen. Kurzfassungen der Vorträge und Poster. 66 S.
- No. 17 Pätzold, J., T. Bickert, L. Brück, C. Gaedicke, K. Heidland, G. Meinecke, S. Mulitza, 1993. Bericht und erste Ergebnisse über die METEOR-Fahrt M 15/2, Rio de Janeiro - Vitória, 18.1. - 7.2.1991. 46 S.
- No. 18 Wefer, G., N. Andersen, W. Balzer, U. Bleil, L. Brück, D. Burda, A. Dahmke, B. Donner, T. Felis, G. Fischer, H. Gerlach, L. Gerullis, M. Hauf, R. Henning, S. Kemle, C. Kothe, R. Melyooni, F. Pototzki, H. Rode, J. Sagemann, M. Schlüter, M. Scholz, V. Spieß, U. Treppke, 1991. Bericht und erste Ergebnisse über die METEOR-Fahrt M 16/1, Pointe Noire - Recife, 27.3. - 25.4.1991. 120 S.
- No. 19 Schulz, H.D., N. Andersen, M. Breitzke, D. Burda, K. Dehning, V. Diekamp, T. Felis, H. Gerlach, R. Gumprecht, S. Hinrichs, H. Petermann, F. Pototzki, U. Probst, H. Rode, J. Sagemann, U. Schinzel, H. Schmidt, R. Schneider, M. Segl, B. Showers, M. Tegeler, W. Thießen, U. Treppke, 1991. Bericht und erste Ergebnisse über die METEOR-Fahrt M 16/2, Recife - Belem, 28.4. - 20.5.1991. 149 S.
- No. 20 Berner, H., 1991. Mechanismen der Sedimentbildung in der Fram-Straße, im Arktischen Ozean und in der Norwegischen See. 167 S.
- No. 21 Schneider, R., 1991. Spätquartäre Produktivitätsänderungen im östlichen Angola-Becken: Reaktion auf Variationen im Passat-Monsun-Windsystem und in der Advektion des Benguela-Küstenstroms. 198 S.
- No. 22 Hebbeln, D., 1991. Spätquartäre Stratigraphie und Paläozeanographie in der Fram-Straße. 174 S.
- No. 23 Lücke, A., 1991. Umsetzungsprozesse organischer Substanz während der Frühdiagenese in ästuarinen Sedimenten. 137 S.
- No. 24 Wefer, G., D. Beese, W.H. Berger, U. Bleil, H. Buschhoff, G. Fischer, M. Kalberer, S. Kemle-von Mücke, B. Kerntopf, C. Kothe, D. Lutter, B. Pioch, F. Pototzki, V. Ratmeyer, U. Rosiak, W. Schmidt, V. Spieß, D. Völker, 1992. Bericht und erste Ergebnisse der METEOR-Fahrt M 20/1, Bremen - Abidjan, 18.11.1991 - 22.12.1991. 74 S.

- No. 25 Schulz, H.D., D. Beese, M. Breitzke, L. Brück, B. Brügger, A. Dahmke, K. Dehning, V. Diekamp, B. Donner, I. Ehrhardt, H. Gerlach, M. Giese, R. Glud, R. Gumprecht, J. Gundersen, R. Henning, H. Petermann, M. Richter, J. Sagemann, W. Schmidt, R. Schneider, M. Segl, U. Werner, M. Zabel, 1992. Bericht und erste Ergebnisse der METEOR-Fahrt M 20/2, Abidjan - Dakar, 27.12.1991 - 3.2.1992. 173 S.
- No. 26 Gingele, F., 1992. Zur klimaabhängigen Bildung biogener und terrigener Sedimente und ihrer Veränderung durch die Frühdiagenese im zentralen und östlichen Südatlantik. 202 S.
- No. 27 Bickert, T., 1992. Rekonstruktion der spätquartären Bodenwasserzirkulation im östlichen Südatlantik über stabile Isotope benthischer Foraminiferen. 205 S.
- No. 28 Schmidt, H., 1992. Der Benguela-Strom im Bereich des Walfisch-Rückens im Spätquartär. 172 S.
- No. 29 Meinecke, G., 1992. Spätquartäre Oberflächenwassertemperaturen im östlichen äquatorialen Atlantik. 181 S.
- No. 30 Bathmann, U., U. Bleil, A. Dahmke, P. Müller, A. Nehr Korn, E.-M. Nöthig, M. Olesch, J. Pätzold, H.D. Schulz, V. Smetacek, V. Spieß, G. Wefer, H. Willems, 1992. Bericht des Graduierten Kollegs "Stoff-Flüsse in marinen Geosystemen". Berichtszeitraum Oktober 1990 - Dezember 1992. 396 S.
- No. 31 Damm, E., 1992. Frühdiagenetische Verteilung von Schwermetallen in Schlicksedimenten der westlichen Ostsee. 115 S.
- No. 32 Antia, E.E., 1993. Sedimentology, Morphodynamics and Facies Association of a Mesotidal Barrier Island Shoreface (Spiekeroog, Southern North Sea). 370 p.
- No. 33 Duinker, J. und G. Wefer (Hrsg.), 1993. Bericht über den 1. JGOFS-Workshop. 1./2. Dezember 1992 in Bremen. 83 S.
- No. 34 Kasten, S., 1993. Die Verteilung von Schwermetallen in den Sedimenten eines stadtbremischen Hafenbeckens. 103 S.
- No. 35 Spieß, V., 1993. Digitale Sedimentographie. Neue Wege zu einer hochauflösenden Akustostratigraphie. 199 S.
- No. 36 Schinzel, U., 1993. Laborversuche zu frühdiagenetischen Reaktionen von Eisen (III) - Oxidhydraten in marinen Sedimenten. 189 S.
- No. 37 Sieger, R., 1993. CoTAM - ein Modell zur Modellierung des Schwermetalltransports in Grundwasserleitern. 56 S.
- No. 38 Willems, H. (ed.) 1993. Geoscientific Investigations in the Tethyan Himalayas. in prep.

- No. 39 Hamer, K., 1993. Entwicklung von Laborversuchen als Grundlage für die Modellierung des Transportverhaltens von Arsenat, Blei, Cadmium und Kupfer in wassergesättigten Säulen. 147 S.
- No. 40 Sieger, R., 1993. Modellierung des Stofftransports in porösen Medien unter Anknüpfung kinetisch gesteuerter Sorptions- und Redoxprozesse sowie thermischer Gleichgewichte. 158 S.
- No. 41 Thießen, W., 1993. Magnetische Eigenschaften von Sedimenten des östlichen Südatlantiks und ihre paläozeanographische Relevanz. 170 S.
- No. 42 Spieß, V., A. Abelman, T. Bickert, I. Brehme, A. Cavalcanti de C. Laier, R. Cordes, K. Dehning, T. v. Dobeneck, B. Donner, I. Ehrhardt, M. Giese, J. Grigel, W. Hale, R. Haese, S. Hinrichs, S. Kasten, H. Petermann, R. Rapp, J. Rogers, M. Richter, A. Schmidt, M. Scholz, F. Skowronek, M. Teixeira de Oliveira, M. Zabel, 1994. Report and Preliminary Results of METEOR-Cruise M 23/1, Capetown - Rio de Janeiro, 4.2.1993 - 25.2.1993. 139 p.
- No. 43 Bleil, U., A. Ayres Neto, D. Beese, M. Breitzke, K. Dehning, V. Diekamp, T. v. Dobeneck, A. Figueiredo, M. Pimentel Esteves, M. Giese, R. Glud, J. Grigel, J. Gundersen, R. Haese, S. Hinrichs, S. Kasten, G. Meinecke, S. Mulitza, H. Petermann, R. Petschik, R. Rapp, M. Richter, C. Rühlemann, M. Scholz, K. Wallmann, M. Zabel, 1994. M 23/2, Rio de Janeiro - Recife, 27.2.1993 - 19.3.1993. 133 p.
- No. 44 Wefer, G., D. Beese, W.H. Berger, K. Buhlmann, H. Buschhoff, M. Cepek, V. Diekamp, G. Fischer, E. Holmes, S. Kemle-von Mücke, B. Kerntopf, C.B. Lange, S. Mulitza, W.-T. Ochsenhirt, R. Plugge, V. Ratmeyer, C. Rühlemann, W. Schmidt, M. Schwarze, C. Wallmann, M. Zabel, 1994. Report and Preliminary Results of METEOR-Cruise M 23/3, Recife - Las Palmas, 21.3.1993 - 12.4.1993. 71 p.
- No. 45 Giese, M. und G. Wefer (Hrsg.), 1994. Bericht über den 2. JGOFS-Workshop. 18./19. November 1993 in Bremen. 93 S.
- No. 46 Balzer, W., M. Bleckwehl, H. Buschhoff, G. Fischer, F.G. Palma, M. Kalberer, U. Kuller, V. Ratmeyer, U. Rosiak, D. Schneider, A. Zimmermann, 1994. Report and Preliminary Results of METEOR-Cruise M 22/1, Hamburg - Recife, 22.9. - 21.10.1992. 24 p.
- No. 47 Stax, R., 1994. Zyklische Sedimentation von organischem Kohlenstoff in der Japan See: Anzeiger für Änderungen von Paläozeanographie und Paläoklima im Spätkänozoikum. 150 S.
- No. 48 Skowronek, F., 1994. Frühdiagenetische Stoff-Flüsse gelöster Schwermetalle an der Oberfläche von Sedimenten des Weser Ästuars. 107 S.
- No. 49 Dersch-Hansmann, M., 1994. Zur Klimaentwicklung in Ostasien während der letzten 5 Millionen Jahre: Terrigener Sedimenteintrag in die Japan See (ODP Ausfahrt 128). 149 S.

No. 50 Zabel, M., 1994. Frühdiagenetische Stoff-Flüsse in Oberflächen-Sedimenten des äquatorialen und östlichen Südatlantik. 129 S.

